INFORMATION TO USERS

This manuscript has been reproduced from the microfilm master. UMI films the text directly from the original or copy submitted. Thus, some thesis and dissertation copies are in typewriter face, while others may be from any type of computer printer.

The quality of this reproduction is dependent upon the quality of the copy submitted. Broken or indistinct print, colored or poor quality illustrations and photographs, print bleedthrough, substandard margins, and improper alignment can adversely affect reproduction.

In the unlikely event that the author did not send UMI a complete manuscript and there are missing pages, these will be noted. Also, if unauthorized copyright material had to be removed, a note will indicate the deletion.

Oversize materials (e.g., maps, drawings, charts) are reproduced by sectioning the original, beginning at the upper left-hand corner and continuing from left to right in equal sections with small overlaps. Each original is also photographed in one exposure and is included in reduced form at the back of the book.

Photographs included in the original manuscript have been reproduced xerographically in this copy. Higher quality 6" x 9" black and white photographic prints are available for any photographs or illustrations appearing in this copy for an additional charge. Contact UMI directly to order.

UMI

A Bell & Howell Information Company
300 North Zeeb Road, Ann Arbor MI 48106-1346 USA
313/761-4700 800/521-0600

UNIVERSITY OF ALBERTA

Proteolytic Cleavage and Sequencing Studies of Rat Monoclonal Antibodies, and the Synthesis of 3,6-Dideoxyhexose Disaccharide Analogues of the *Trichinella spiralis* Epitope

by

Yue Zheng 

A thesis submitted to the Faculty of Graduate Studies and Research in partial fulfillment of the requirements for the degree of

Master of Science

Department of Chemistry

Edmonton, Alberta

Spring 1998

UNIVERSITY OF ALBERTA

Faculty of Graduate Studies and Research

The undersigned certify that they have read, and recommended to the Faculty of Graduate Studies and Research for acceptance, a thesis entitled **Proteolytic Cleavage and Sequencing Studies of Rat Monoclonal Antibodies, and the Synthesis of 3,6-Dideoxyhexose Disaccharide Analogues of the *Trichinella spiralis* Epitope**

submitted by **Yue Zheng** in partial fulfillment of the requirements for the degree of **Master of Science**.

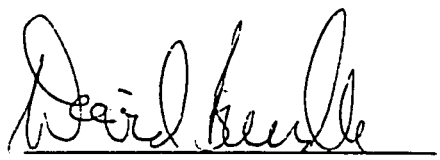

David R. Bundle, Supervisor

Ole Hindsgaul, Examiner

Randy Read, Examiner

Date: January 13th, 1998.

Dedicated to the Memory of my

Maternal Grandmother:

WEI-CHENG ZHAO

(1918-1994)

ABSTRACT

Three rat monoclonal antibodies that are protective against the parasite *Trichinella spiralis*, have been purified from ascites fluid and subjected to proteolytic cleavage to yield antigen binding Fab fragments. One of these antibodies, designated 18H, preferentially binds a linear epitope Tyv-GalNAc-GlcNAc, which lacks a branching fucose present on the major fraction of *N*-linked glycans produced by parasite larvae. This antibody was separated into heavy and light chains and preliminary amino acid sequence studies were performed by mass spectrometry. A substantial portion of the light chain variable domain and most of the constant domain sequences of the heavy and light chains were established.

Synthetic studies were undertaken to obtain 3,6-dideoxyhexose epimers of the native *Trichinella spiralis* disaccharide epitope, Tyv-GalNAc. Thus disaccharides that contain paratose and abequose, the C-2 and C-4 epimers of 3,6-dideoxy-D-*arabino*-hexose, methyl 2-acetamido-2-deoxy-3-*O*-(3,6-dideoxy-β-D-*ribo*-hexopyranosyl)-β-D-galactopyranoside **1** and methyl 2-acetamido-2-deoxy-3-*O*-(3,6-dideoxy-β-D-*xylo*-hexopyranosyl)-β-D-galactopyranoside **2** were synthesized in good yield.

ACKNOWLEDGMENTS

First and foremost, I would like to thank my supervisor Dr. D. R. Bundle for giving me the opportunity to carry out this work in his laboratories and for his continuous support throughout my studies. I would also like to thank the very kind Dr. Pierre Thibault of NRC, Ottawa for helping me to do the amino acid sequencing work in his laboratory and Mr. David Watson (NRC, Ottawa) for performing gas phase sequencing on the N-termini of the heavy and light chains. I am grateful to the Department of Chemistry at the University of Alberta for their financial support.

Many thanks to the members of the Bundle group, past and present. In particular, Dr. Pavel Kitov, Dr. Ping Zhang, Lina Setti, Joanna Sadowska and Dr. Jian Zhang for their helpful discussions and inputs during my studies. I would like to extend my thanks to the members of the spectral and analytical services of this department, especially to Dr. Albin Otter.

I would like to thank my parents Yu-Zhen Tong and Bao-Shan Zheng and my sister Yao Zheng for their support and encouragement. Last of all, but certainly not least, I would like to thank Myrl Tanton for driving up from Calgary every weekend to visit me and to keep me sane.

TABLE OF CONTENTS

LIST OF TABLES

LIST OF FIGURES

LIST OF ABREVIATIONS

[α]	specific rotation
Abe	abequose
Ac	acetyl
ATZ	anilinothiazolinone
Bn	benzyl
BSA	bovine serum albumin
Bz	benzoyl
C	constant region
CAN	cerium ammonium nitrate
CDR	complementarity determining regions
DBU	1,8-Diazabicyclo[5,4]undec-7-ene
DEAE	diethylaminoethyl
DMAP	dimethylamino pyridine
DTT	dithiothreitol
EDTA	ethylenediamine tetraacetic acid
EIA	enzyme immuno assay
ESMS	electrospray mass spectrometry
ES	excretory/secretory
ESA	excretory/secretory antigen
Et	ethyl
Fab	antibody binding fragment
Fc	constant fragment
Fd	peptide composed of the V_H and C_H1 domains that results from papain cleavage of the heavy chain of the IgG molecule
FPLC	fast protein liquid chromatography
Fuc	fucose
Gal	galactose
GalNAc	*N*-acetyl galactosamine
Glc	glucose

GlcNAc	*N*-acetyl glucosamine
GC/MS	gas chromatography/mass spectrometry
H-chain	heavy chain
HPLC	high performance chromatography
Ig	immunoglobulin
J	Coupling constant
KDa	kilodalton
KeV	kilo electron volt
lacdiNAc	β-D-Gal*p*NAc(1$\rightarrow$4)-β-D-Glc*p*NAc
L-chain	light chain
LC-MS	liquid chromatography-mass spectrometry
L1	first stage muscle larva
LTBH	lithium tributyl borohydride (super hydride)
m	multiplet
Man	mannose
Me	methyl
MHC	major histocompatibility complex
MHz	megahertz
NBS	*N*-bromosuccinimide
NHAc	acetamido
NIS	*N*-iodosuccinimide
NMR	nuclear magnetic resonance
Par	paratose
PITC	phenylisothiocyanate
Piv	pivaloyl
PNGase	*N*-glycosidase
ppm	parts per million
PTH	phenyl thiohydantoin
Pyr	pyridine
R_f	retention factor

SDS-PAGE	sodium dodecyl sulphate polyacrylamide gel electrophoresis
TFA	trifluoroacetic acid
TLC	thin layer chromatography
TMB	3,3',5,5'-tetramethylbenzidine
TMSOTf	trimethylsilyl trifluoromethanesulfonate
Ts	toluenesulfonyl
TSL-1	*Trichinella spiralis* antigen group 1
Tyv	tyvelose
V	variable region

LIST OF ABREVIATIONS OF AMINO ACIDS

3 letter code	1 letter code	Name of amino acid
Ala	A	Alanine
Arg	R	Arginine
Asn	N	Asparagine
Asp	D	Aspartic acid
Cys	C	Cysteine
Gln	Q	Glutamine
Glu	E	Glutamic acid
Gly	G	Glycine
His	H	Histidine
Ile	I	Isoleucine
Lys	K	Lysine
Leu	L	Leucine
Met	M	Methionine
Phe	F	Phenylalanine
Pro	P	Proline
Ser	S	Serine
Thr	T	Threonine
Trp	W	Tryptophan
Tyr	Y	Tyrosine
Val	V	Valine

Chapter I Introduction

1.1 General Introduction

Carbohydrates have traditionally been considered as energy storage agents, and as a major part of non-food consumer products and industrial raw materials. However, one of the most significant functions of carbohydrates is their role as recognition factors in cellular process. These include the recognition of specific mammalian cell surface structures by bacteria and viruses; recognition of changes in cell-surface carbohydrates on tumor cells by mammalian lectins and antibodies[1-3] as well as immune system recognition of foreign polysaccharides or glycoconjugate antigens present on the surface of bacteria and viruses[4,5]. The role of carbohydrates as antigens in the immune response has promoted the design of tumor specific vaccines for cancer therapy[6-8] and the development of vaccines against pathogenic bacteria[9,10].

1.2 Structure of Glycoproteins

Cell surface carbohydrates are commonly found linked to either membrane associated proteins (glycoproteins) or lipids (glycolipids). Glycoproteins are classified in two basic groups, the *O*-linked and the *N*-linked sugar chains. An *O*-linked glycan chain contains a 2-acetamido-2-deoxy galactose residue at its reducing end, which is attached via the anomeric carbon atom to the hydroxyl groups of serine or threonine constituents of the protein. In contrast, the *N*- or asparagine-linked glycan has a 2-acetamido-2-deoxy-D glucose unit at its reducing end which is linked via a *N*-glycosidic bond to the amide nitrogen side chain of an asparagine residue in the sequence Asn-X-Thr (or Ser) in the polypeptide backbone, where X could be any

amino acid other than proline. Other glycosyl amino acids such as β-xylosylserine, β-galactosyl-hydroxylysine, and β-L-arabinosyl-hydoxyproline are found in proteoglycans, collagens, plant and algal glycoproteins, respectively[11].

N-linked oligosaccharides are further classified into three subclasses: high mannose type, complex type and hybrid type. All three types contain a common pentasaccharide trimannosyl core structure: Manα1→6[Manα1→3]Manβ1→4 GlcNAcβ1→4 GlcNAc (Fig 1).

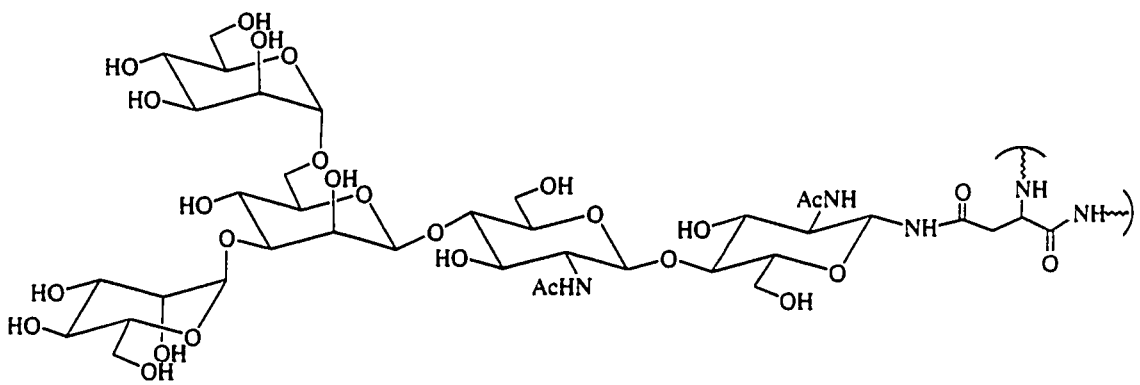

Fig 1. Pentasaccharide core of *N*-linked glycoproteins.

High mannose type glycans contain only α-mannosyl residues in addition to the pentasaccharide core[12] (Fig 2), whereas the complex type has no additional mannose residues other than those present in the core pentasaccharide structure. *N*-acetylglucosamine residues at the reducing termini of the outer chains are linked to the 2 α-mannosyl residues on the core of glycans of the complex variety (Fig 3). Often an α-fucosyl residue linked to the C-6 position of the proximal *N*-acetylglucosamine unit, and a β-*N*-acetylglucosamine residue linked to the C-4 position of the β-mannosyl unit of the trimannosyl core are present as well. In

addition, there is a large amount of structural variation associated with the complex type glycans. One to five outer chains can be linked to the trimannosyl core, resulting in mono-, bi-, tri-, tetra- and penta-antennary sugar chains (Fig 4).

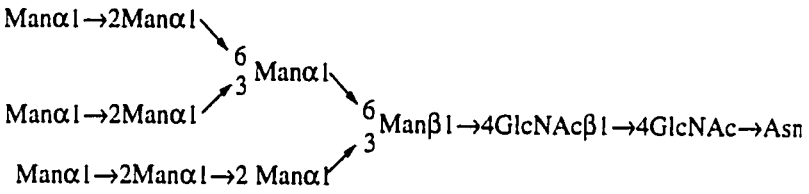

Fig 2. High mannose type of *N*-linked glycoproteins.

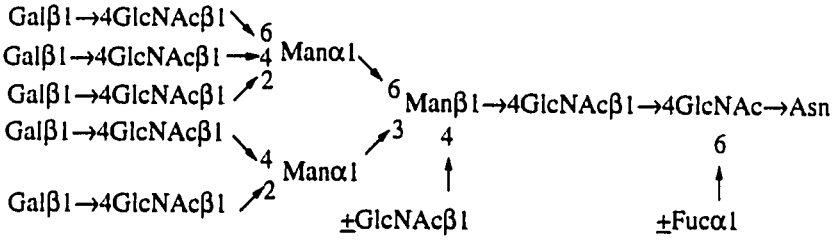

Fig 3. Complex type of *N*-linked glycoproteins.

The third hybrid type *N*-glycans are named for their characteristic features that combine the structural elements of both high mannose and complex sugar chains (Fig 5). The outer oligosaccharide chains found on complex type glycans are linked to the Manα1→3 arm of the trimannosyl core and one or two α-mannosyl residues are linked to the Manα1→6 arm of the core. Fucosylation and insertion of a branching *N*-acetylglucosamine residue on the pentasaccharide core may also occurs in the hybrid type.

O-linked glycans have at least six core classes of the serine (threonine)-*N*-acetylgalactosamine type of linkage[13-16], but since they are not relevant to the work of

this thesis, their structures are not discussed.

Monoantennary

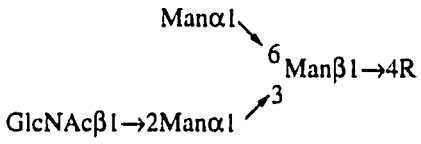

Biantennary

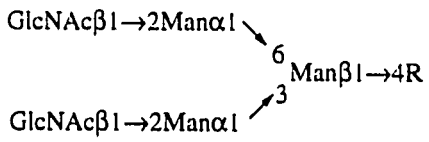

Triantennary

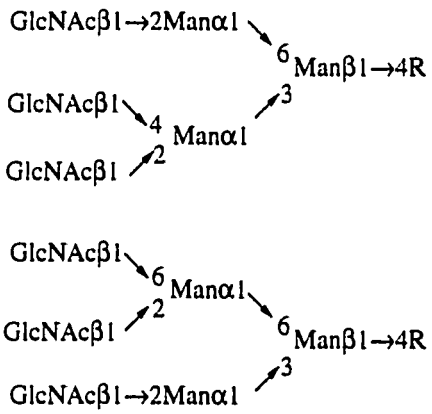

Tetraantennary

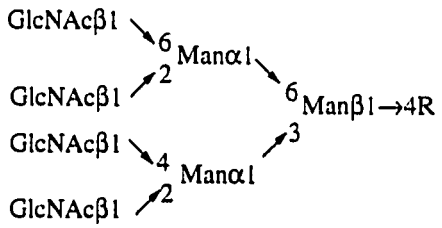

Pentaantennary

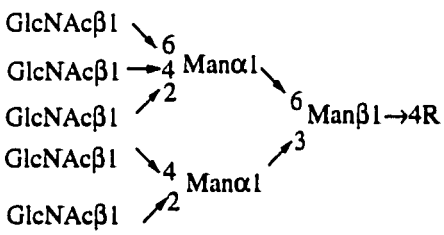

R=GlcNAcβ1→4GlcNAc→Asn

Fig 4. Branching of complex type *N*-linked glycans.

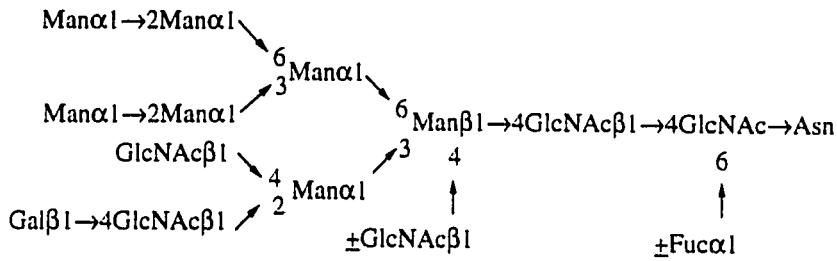

Fig 5. Hybrid type of *N*-linked glycoproteins.

1.3 Immune Response

The immune system in vertebrates provides a defense mechanism against foreign organisms such as bacteria, parasites and viruses via two recognition proteins, antibodies and the T-cell receptors. Antibodies are produced from B-cells that originate in the bone marrow, while T-cell receptors are present on the surface of cooperating "helper" T-cells originating from the thymus.

In thymus-dependent responses, a change in the major histocompatibility complex (MHC) on the surface of antigen presenting cells or infected cells initiates recognition and binding by the T-cell receptors. The MHC is classified into two major categories, MHC type I and MHC type II. MHC type I molecules respond to viruses and self antigens, and consist of a single polypeptide chain that is associated with a β_2-microglobulin molecule on the surfaces of most nucleated cells. MHC type II molecules respond to foreign antigens and consist of two polypeptide chains and have a more limited cellular distribution. Different T-cell receptors recognize and respond to foreign antigens only when they are associated with a specific class of MHC molecules. A precise set of MHC molecule is present on the cell surfaces of each individual. When a cell is invaded, MHC molecules bind to degraded fragments of the antigen, generated from within the cell (Fig 6). The T-cell receptor recognizes the

peptide presented as a complex with the MHC molecule and forms a tertiary complex, which is destroyed. Cytokines released as a result of T-cell activation stimulate B-cells and program the secondary response (for example the IgM to IgG class switch).

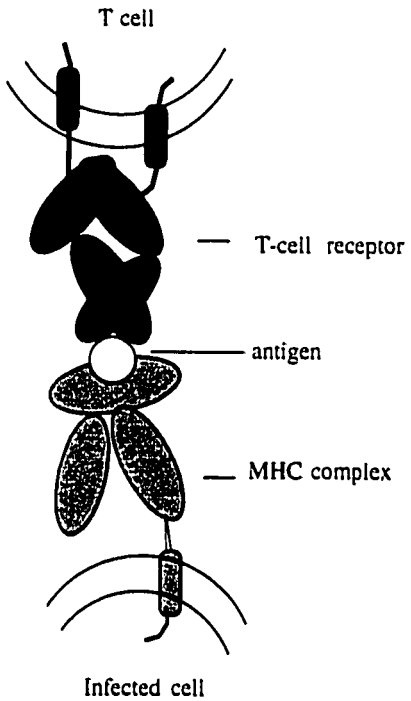

Fig 6. T-cell receptor recognition of antigens via MHC.

Antibodies, also known as immunoglobulins, on the surface of B-cells, recognize and bind to specific foreign antigen, present on the cell surface of invading microorganisms, independently of the T-cells (Fig 7). This binding together with a concurrent T-cell response accompanied by the release of cytokines stimulates B-cells to expand clones of identical cells that secrete soluble antigen binding immunoglobulins into the blood stream. The antibodies then form binding complexes with cognate antigens, which are destroyed by macrophages.

The T- and B-cells may respond to different epitopes on the antigen, but in

order for cell cooperation to occur, the epitopes have to be on the same molecule. Certain antigens, such as polysaccharides however, can trigger B-cells without significant help from T-cells, to give a so-called T-independent response, which involves predominantly the production of IgM, and does not include the development of immunologic memory.

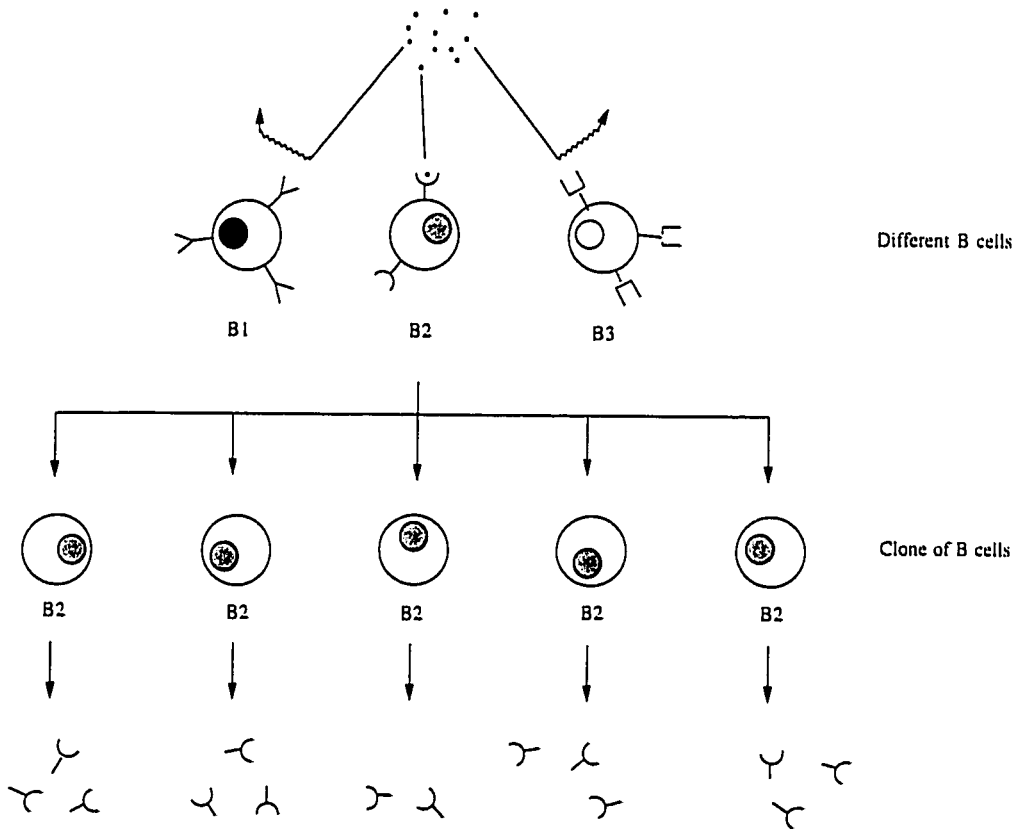

Fig 7. Recognition of foreign molecules by antibodies.

1.3.1 Structure of Immunoglobulins

The basic structure of immunoglobulin (Ig) molecules is composed of two large polypeptide chains (H, heavy) and two small chains (L, light), held together by disulfide bonds. The heavy chains are isotyped into five different functional classes,

IgG, IgD, IgE, IgM and IgA. The light chain can be either λ or κ type, with no known functional differences.

IgG, one of the biomolecules of central interest to this thesis, is the major immunoglobulin present in normal human serum. It is composed of a monomer of the basic Y-shaped IgG motif. Each light chain is attached to a heavy chain and each heavy chain pairs with another heavy chain via covalent and noncovalent interactions to produce a symmetrical molecule consisting of four polypeptide chains (Fig 8). The covalent interactions refer to the formation of inter-chain disulfide bonds between cysteine residues and noncovalent interactions arise mainly from hydrophobic interactions. Both the heavy and light chains contain homologous repeating units, each of about 110 amino acid residues in length, which fold independently into similar globular motifs called immunoglobulin domains. The heavy chains have four such domains and the light chains have two.

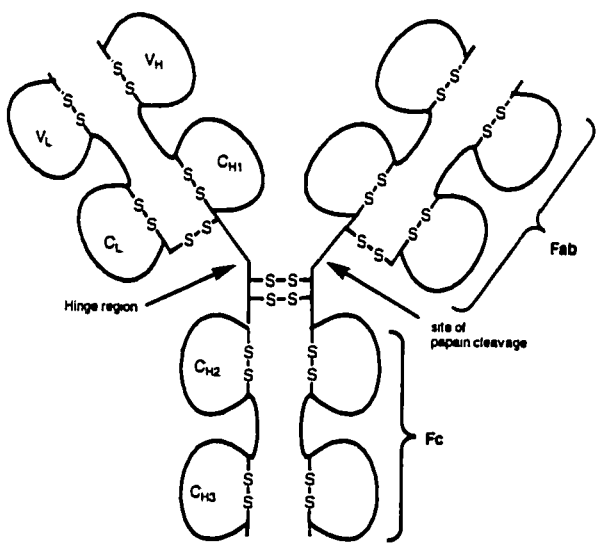

Fig 8. Detailed structure of the IgG molecule.

The light chains and the N-terminal half of the heavy chains contain the antigen binding region (Fab) and the C-terminal half of the H-chains contain the crystallizable region (Fc). Papain digestion cleaves the IgG molecule at the hinge region, which results in the liberation of a Fc fragment and two Fab fragments. It is these 50K Dalton Fab fragments that are commonly used to grow crystals for protein crystallography with and without the corresponding antigen. When crystals are obtained and the X-ray structure is solved, a clear picture of the binding site and interactions between the amino acid residues of the binding site and antigen can be developed.

The amino acid sequences of the amino terminal domains called the variable regions consist of H-chain V_H and L-chain V_L. These domains are distinguished from the more conserved sequences on the rest of the chain which are called the constant regions, C_{H1}, C_{H2}, C_{H3} for the H-chain and C_L for the L-chain.

The major portion of the variable domain, called framework regions, have high homology between classes. Small regions where great variability occurs are called the hypervariable or complementarity determining regions (CDR1, CDR2 and CDR3). These are the regions that are involved in the determination of specificity of the antibody-antigen interaction. The three CDR regions are commonly found between amino acids 31-35, 50-65 and 95-102 on the heavy chains and between 24-34, 50-56 and 89-97 on the light chains. These amino acids form the binding site and selected amino acids make contact with antigen.

1.3.2 Three Dimensional Structure of Immunoglobulins

The three dimensional structures of immunoglobulin domains are constructed from β-sheets. The constant regions, built from seven antiparallel β strands arranged in a Greek key barrel-like motif, are connected by short loops and joined together by a disulfide bridge from β strand 6 to 2 (Fig 9). Most invariant residues are found in the sheet framework. The sizes of the loops vary between immunoglobulin classes, but are constant within each class.

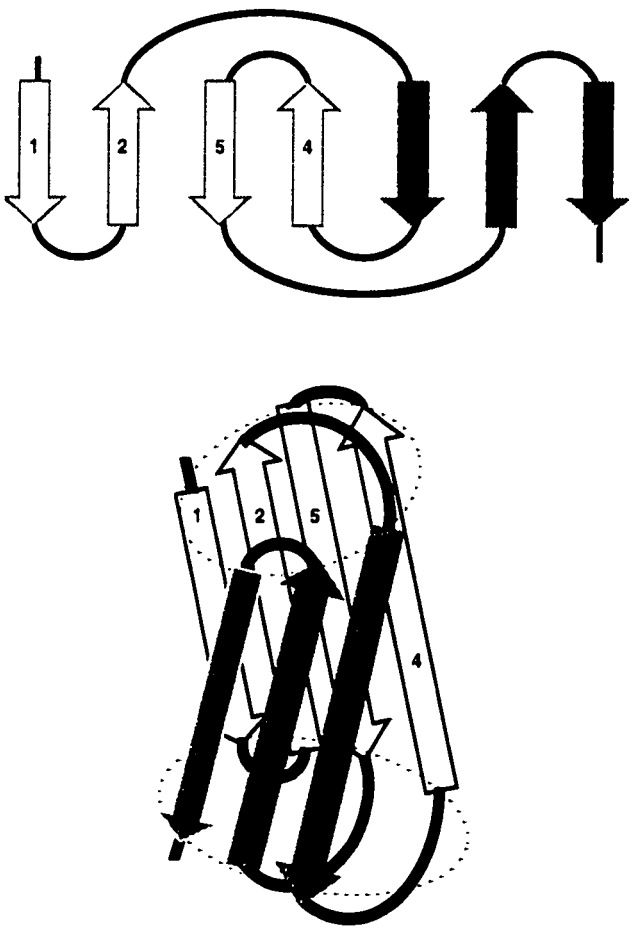

Fig 9. Three dimensional folding of the constant region.

The variable domain has a similar structure, with the exception of two extra β-strands (3b and 3c) that are inserted between strand 3 and 4 (Fig 10). The loop connecting these two strands contains CDR2. The CDR2 loop is folded in such a way that it is close to the other two loops of the hypervariable regions, the loop connecting strands 2 and 3 (CDR1) and the loop connecting strands 6 and 7 (CDR3). The CDR loops from both the heavy and light chains form the antigen binding region of the immunoglobulin molecule.

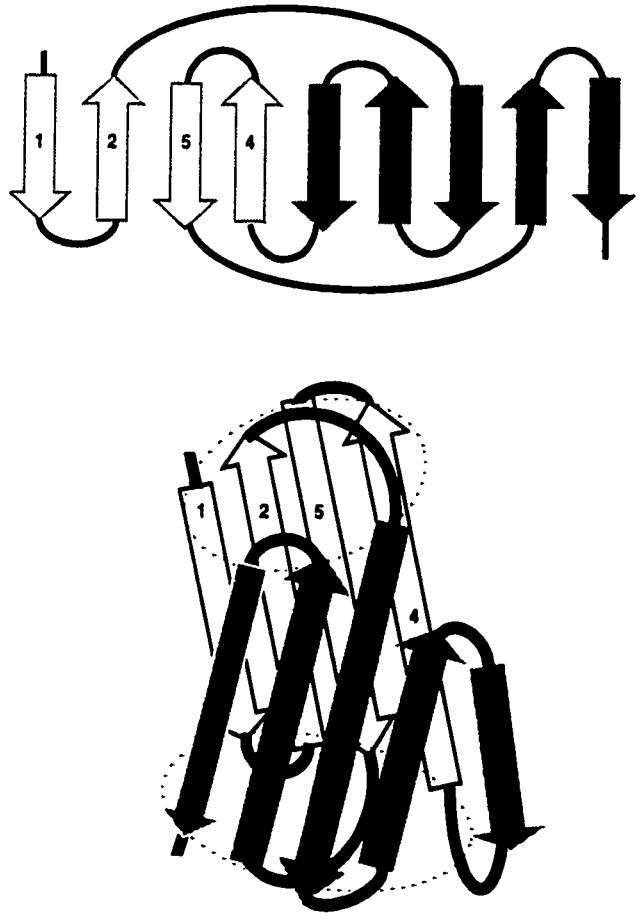

Fig 10. Three dimensional folding of the variable region.

1.4 Carbohydrate-Protein Binding Studies

Antibodies, lectins and enzymes are able to differentiate between closely related carbohydrate structures and this exquisite molecular recognition has intrigued chemists. In order to understand the specifics of molecular recognition, various carbohydrate-protein systems have been studied by chemists, immunologists and biologists. Monoclonal antibodies generated to natural antigens present on bacteria or cancer cells have been studied by several approaches[17-20]. One chemical approach is the mapping of sequential single site modifications on the epitope, also called an antigenic determinant. A precise and potentially unambiguous approach is crystallographic studies of the complex between low molecular weight ligand and antibody. Both methods have identified a small number of crucial hydroxyl groups in the carbohydrate molecule that are involved in essential hydrogen bonds with the protein. Chemical mapping studies help to elucidate this hydrogen bonding scheme and to delineate the topology of the combining site[21]. By replacing the hydroxyl group with a hydrogen or a fluorine, the change in binding affinity of the protein-carbohydrate system reveals the specific involvement of that group[22,23]. Replacement of a hydroxyl group by an *O*-methyl group provides information not only about the hydrogen-bonding relationships at that position but also about the stringency of the combining site to steric demands for complex formation[24]. Binding studies using other synthetic derivatives, such as epimeric, amino or *C*-methyl analogues, can provide additional insights into the hydrogen-bonding and steric requirements, as well as information on the distribution of polar and non-polar regions within the combining site[21]. The conclusions of chemical mapping studies are compared with

data from crystal structures, allowing the evaluation of the analogues as probes of the molecular and stereochemical requirements of binding and providing a more detailed appreciation of the atomic features of the interaction[21]. Possible point mutations on the ligand can sometimes be achieved synthetically to give a tighter binding complex.

Other tools are also used to study carbohydrate-protein recognition systems. NMR studies can provide details of oligosaccharide conformation in the bounded state[25]; microcalorimetry provides a thermodynamic description of the energetics of association[26]; and amino acid sequencing is essential to interpret X-ray diffraction data and to understand antibody gene usage[18,27].

1.5 *Trichinella spiralis*

Trichinella spiralis is a parasitic nematode that infects the skeletal muscle cell in an infection called trichinosis. A wide variety of mammals worldwide are susceptible to infection by the parasite[27]. In man it is mainly transmitted by ingesting raw or poorly cooked meat. Once *Trichinella* enters the digestive system, it multiplies and then its larvae are transported via the lymphatic system to the muscle cells where they reside until the next round of replication/infection. The host experiences severe muscle pains, diarrhea, fever and other unpleasant symptoms of food poisoning. In serious cases, fatality results[28-30].

Although *Trichinella spiralis* was discovered in the 1800's, it has been involved in the life of mankind for much longer. The earliest known case (retrospectively) of its infection in man occurred in about 1200 BC in an Egyptian weaver[31]; an intercostal muscle of his mummified body was found to contain a *T.*

spiralis cyst. Since its discovery, trichinosis has been an actively pursued topic for over a century. The number of outbreaks have decreased dramatically in recent years compared to when it was first discovered. There are also many drugs, such as benzimidazoles, available to treat the symptoms and to speed recovery. Serological testing of *Trichinella* oligosaccharide specific antibodies is one method currently in the developmental stage. However, it is a difficult disease to diagnose and in severe cases, death is still inevitable. Further exploration in its treatment and in prevention by vaccination is still much needed. *T. spiralis* is also an attractive model for the study of immunity and pathogenicity[32].

1.6 Tyvelose Involvement

Since the early 1920's, there has been evidence that rats infected with *Trichinella spiralis* become markedly immune to subsequent infection[33]. Rat pups suckling *T. spiralis*-infected dams are found to acquire a protective immunity, which eliminates up to 99% of an oral challenge dose of infective larvae[34]. This dramatic and specific response, called rapid expulsion, is mediated by maternal antibodies that force larvae from their intestinal epithelial niche[35]. The antigens recognized by the protective antibodies are stage specific[36], originate in the L1 stichosome[37,38], and are abundant both in excretory/secretory (ES) products and on the larval cuticular surface[36].

Rat monoclonal antibodies have been generated from rats infected with *T. spiralis*[39]. Eight antibodies belonging to the IgG class have been studied in detail (Table 1)[39], and several of these have been made available to our laboratory for

chemical mapping studies. Among the hybridoma antibodies, 6D, 9D, 9E and 18H have relatively high affinity for the EIA plates coated with muscle larvae. Several of the monoclonal antibodies also provide a significant level of protection against infection when injected into rats. In contrast, antibodies 18H and 10G bind well to the larvae, but afford little protection *in vivo*. Monoclonal antibodies 18B and 16H have low affinity for the EIA plates coated with larvae, and provide poor *in vivo* protection against the parasite[39].

Table 1. Summery of EIA and protective activity of monoclonal antibodies specific for *T. spiralis* ESA (taken from ref. 39).

Antibody subclass	Monoclonal antibody	Binding activity to Larvae in EIA (A_{495})	Mean % *in vivo* protection
IgG1	6D	1.5	72
	9D	1.5	78
	16H	0.12	9
	18B	0.12	8
IgG2a	18H	1.47	18
IgG2b	10G	0.90	29
IgG2c	9E	0.55	88
	18D	1.20	71

The hybridoma antibodies have been used to identify the target antigen of the parasite[40]. Preliminary studies have shown that the antigens recognized by the protective antibodies, named TSL-1 (*Trichinella spiralis* antigen group 1), are

glycoproteins that contain *N*-glycans, the carbohydrate portion of which turned out to be the immunodominant epitope in mice and rabbits[36,38]. One of the rat antibodies (9D), has been shown to compete with a glycan specific mouse antibody for binding to *T. Spiralis* antigens[41]. Total monosaccharide compositions of the larval homogenate, TSL-1 antigens, and ES antigens were determined by GC/MS of both the trimethylsilyl ethers of methyl glycosides and of the alditol acetate derivatives[42]. The glycosyl composition of the TSL-1 fraction was remarkable in 2 respects: (1) fucose accounted for 36% of the total hexose residues; and (2) a 3,6-dideoxyhexose, tyvelose (Fig 11), previously only found in certain gram-negative bacterial lipopolysaccharides[43], was identified, accounting for at least 24% of the hexose residues (Table 2)[42].

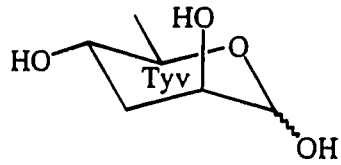

Fig 11. Tyvelose.

Further studies using peptide *N*-glycosidase PNGase F digestion and fast atom bombardment mass spectrometry of the oligosaccharide products have concluded that the *T. Spiralis* glycan exists as tri- and tetra-antennary glycans (Fig 12)[43]. The terminal sugar is tyvelose, which is glycosidically linked to a GalNAc residue of a fucosylated LacdiNAc structure, similar to that of Lewis X, except for the presence of a β-GalNAc residue instead of β-Gal. This tetrasaccharide epitope is attached to a trimannosyl core. The linkage between GalNAc and GlcNAc is β, and between Fuc

and GlcNAc is α. The tri- antennary glycans carry fully fucosylated GlcNAc residues on both the antennae and the chitobiose core. The tetra-antennary glycans contain a total of four fucoses. This gives rise to two possibilities; either the core GlcNAc and three antenary GlcNAc residues are fucosylated or all four branching residues are fucosylated leaving the core GlcNAc unsubstituted.

Table 2. Glycosyl composition of *T. spiralis* muscle larval antigens from GC/MS (taken from ref. 42).

	TSL-1 antigens	ES antigens	Larval homogenate
Tyvelose	24	21	8
Fucose	36	19	12
Xylose	0	1	1
Mannose	22	17	19
Galactose	0.5	2	2
Glucose	1	4	19
GalNAc	9	15	13
GlcNAc	7	21	25
Myo-inositol	0.5	0	1
Sialic acid	0	0	0

The anomeric configuration of tyvelose was deduced using immunochemical methods by performing inhibition and direct binding studies of a panel of synthetic mono-, di-, tri- and tetrasaccharide epitopes and glycoconjugates containing both α

Tetraantennary glycans

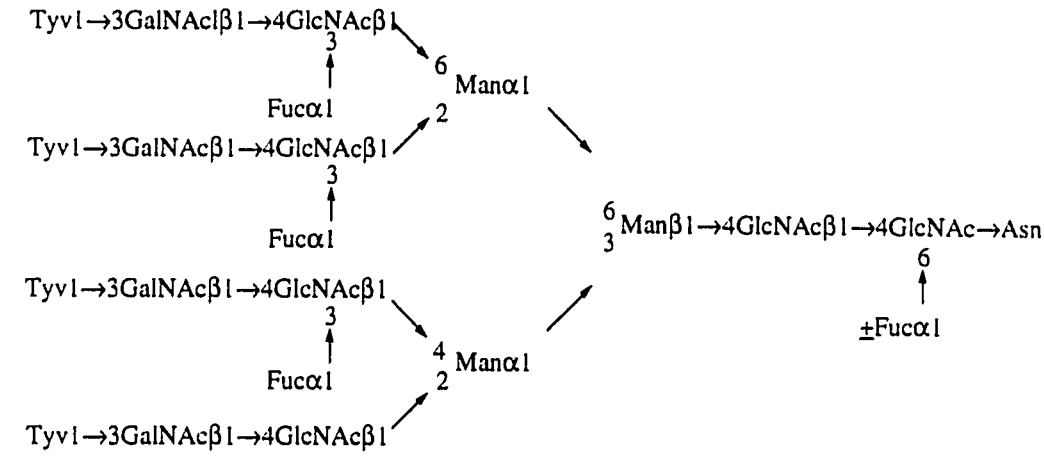

Triantennary glycans

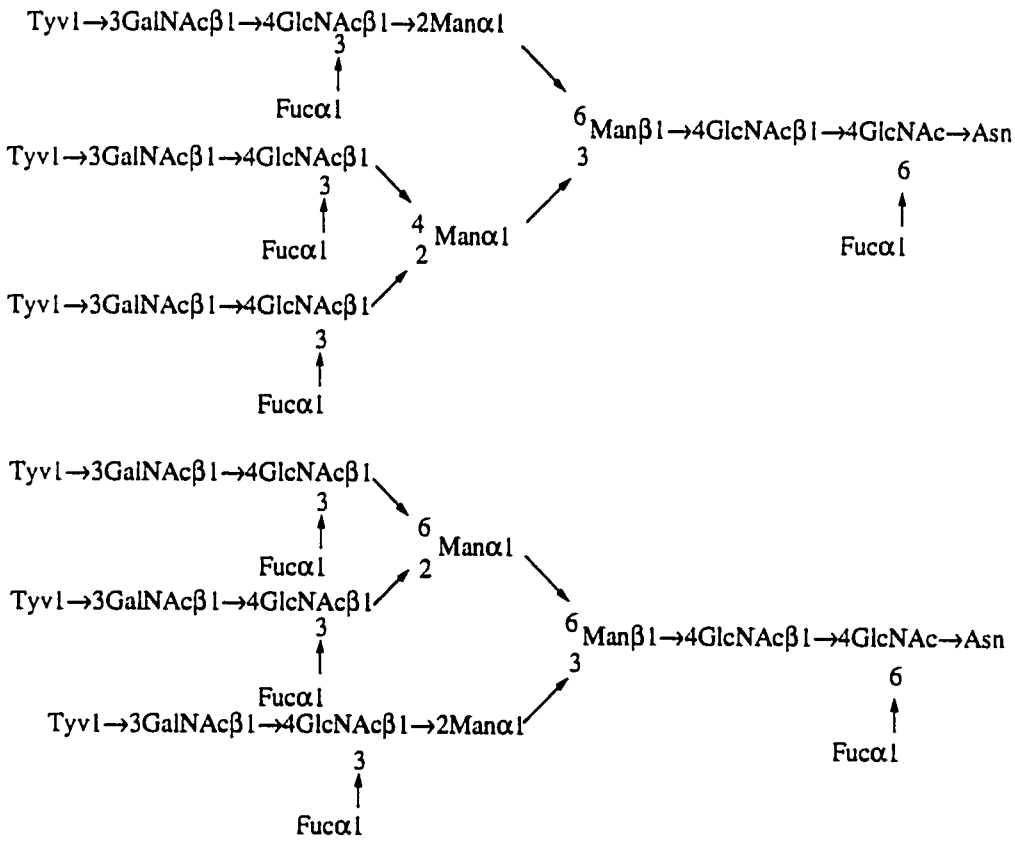

Fig 12. Proposed structures of major N-glycans present on *T. spiralis* antigens.

and β forms of tyvelose (Fig 13)[44,45]. This indirect method of structural elucidation was necessary due both to a lack of endo- or exo- glycosidases that hydrolyze unusual terminal sugars like the 3,6-dideoxyhexoses[46,47], and to the minute quantities of glycan available for NMR studies[48,49].

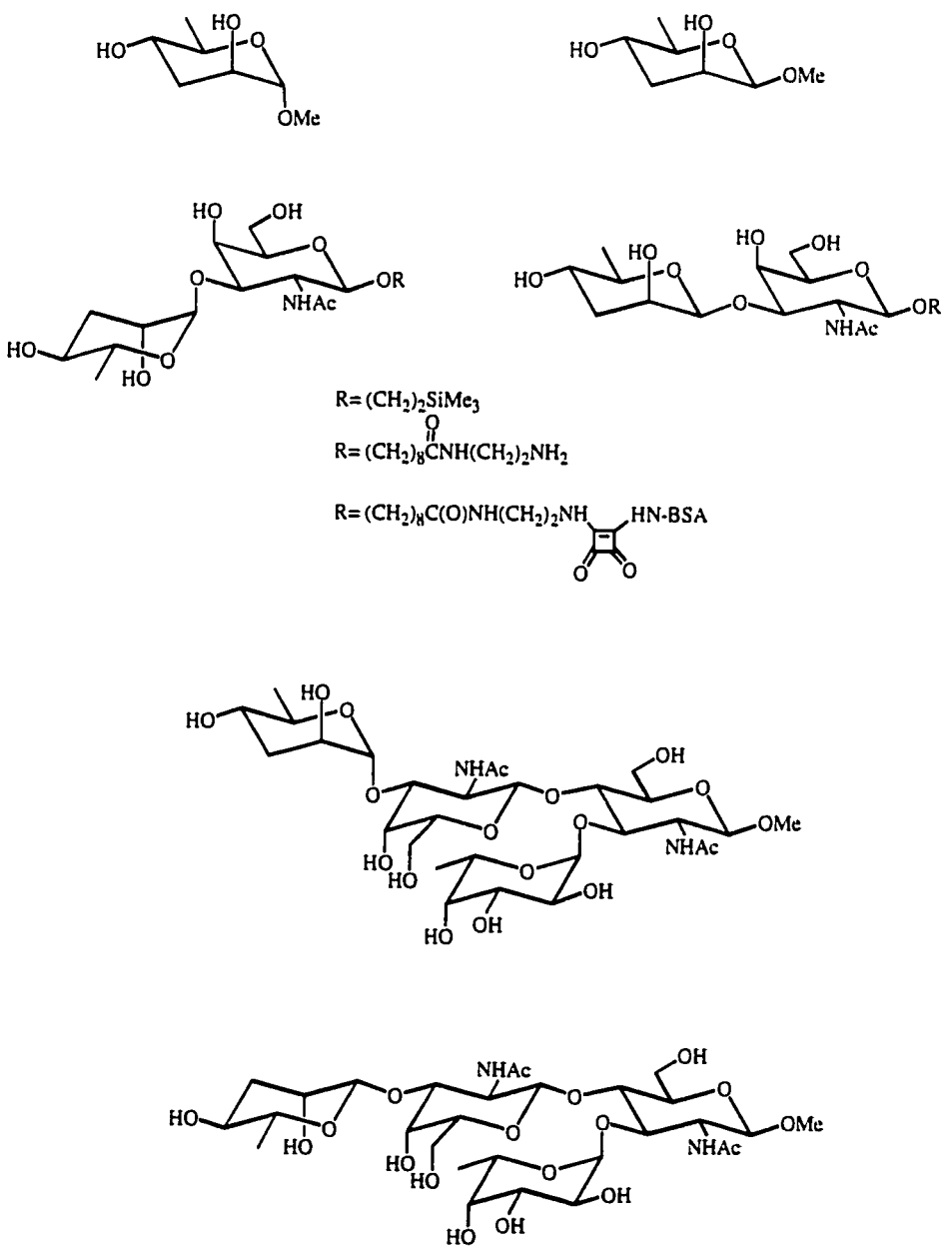

Fig 13. Structures of synthetic oligosaccharide inhibitors and glycoconjugates.

Studies with protective monoclonal antibodies 6D, 9D, 9E, 18D, 18H and 305 have found that none of them bind to the EIA plate coated with the disaccharide-BSA conjugate, α-D-Tyv*p*(1→3)-β-D-Gal*p*NAc-linker-BSA (Fig 13). The β-linked glyco-conjugate, β-D-Tyv*p*(1→3)-β-D-GalNAc*p*-linker-BSA, however was found to bind well to the mAbs, especially 18H. Further inhibition studies with the α/β mono- and disaccharides have shown that none of the α anomers have any affinity towards the antibodies and β anomers exhibit partial to full inhibition. These results lead to the surprising conclusion that β tyvelose is the terminal sugar on the *T. Spiralis* antennary glycans. To date, observation of 3,6-dideoxyhexoses in biopolymers have been confined to the α-pyranose form only[50]. The *Trichinella* antigens are the first instance of a naturally occurring 3,6-β-dideoxyhexoside[44].

The higher binding affinity of 18H towards the linear disaccharide in comparison to the tetrasaccharide confirms the tentative GC-MS results that pointed to the possibility of non-fucosylated outer chains on the tetra-antennary glycans[50] (see tetraantenary structure in Fig 12).

1.7 Scope of Project

The focus of the work in this thesis involves the purification of the Fab fragments of *T. spiralis* monoclonal antibodies 18H, 9D, and 9E; partial amino acid sequencing of the heavy and light chains of the 18H IgG molecule; and the synthesis of two disaccharide analogues.

1.7.1 Fab Purification

The antibodies generated by Dr. Judith Appleton's laboratory that exhibit high affinity for the parasite larvae coated on the EIA plates were chosen for Fab studies. An experimental protocol was developed for the purification of mAbs 9E, 9D and 18H, and their Fab components.

1.7.2 Amino Acid Sequencing

The monoclonal antibody 18H was used for amino acid sequencing. The pure IgG molecules were subjected to denaturation and alkylation to give heavy and light chains. These chains were then fragmented with trypsin and subjected to analysis by electrospray mass spectrometry in collaboration with Dr. Pierre Thibault (NRC, Ottawa) to give the partial sequence of the heavy and light chains.

1.7.3 Synthesis of disaccharide analogues

The surprising discovery of the presence of β-tyvelose in the *T. spiralis* glycoprotein antigen has raised the question as to whether the monoclonal antibodies will bind to other 3,6-deoxyhexoses. Paratose has equatorial hydroxyl groups at the C-2 and C-4 positions, while abequose has an equatorial OH at C-2 and an axial OH at C-4 to give a *galacto*-like configuration. Together with tyvelose all three occur in the A, B and D *Salmonella* serogroups. This invites speculation that the parasites may also possess the biosynthetic machinery to express such antigens. It is also of interest to establish the fine specifics of *T. spiralis* antibodies for these dideoxyhexoses.

It has been shown by Ellis *et al*[50] that the smallest fragment of the antigen

required for efficient binding by EIA is a disaccharide (Fig 14). Therefore, the synthesis of the analogues β-D-Par*p*(1→3)-β-D-Gal*p*NAc→OMe **1** and β-D-Abe*p*(1→3)-β-D-Gal*p*NAc→OMe **2** are reported in the part of the thesis dealing with oligosaccharide synthesis.

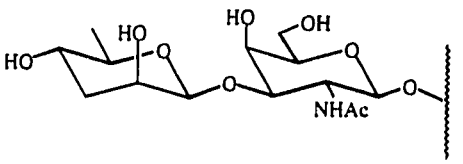

Tyv-GalNAc

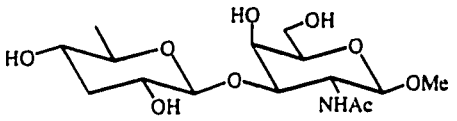

1

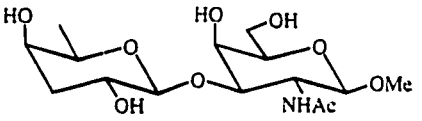

2

Fig 14. Smallest antibody binding fragment Tyv-GalNAc and its analogues.

Chapter II Purification, Heavy and Light Chain Separation and Papain Digestion of Rat IgG

2.1 Introduction

With the exception of antibody fragments created by protein engineering the smallest antigen binding fragment of an antibody is the 50K Dalton Fab. Since they can be liberated from whole IgG in good yield by proteolysis with papain, Fabs are of a suitable molecular weight for crystal structure studies. Crystallographic studies also require that the sequence of the L and Fd (H) chains be known, so that electron density can be used to position the peptide backbone and amino acid side chains. Therefore, in order to obtain the crystal structure of an oligosaccharide complex, high purity IgG and the Fab must be prepared. Once crystals of Fab are shown to yield usable X-ray diffraction data, the sequence of the amino acid side chains has to be determined. This requires the cleavage of the IgG molecule into L and H chains, or the separation of the L and Fd chains of Fab.

Antibodies may be purified by a wide range of chromatographic techniques, the choice of which is governed by the quantity antibody to be purified. For each technique, ion exchange, gel exclusion and affinity chromatography, there are advantages and disadvantages. For the separation of reduced and alkylated L and H chains gel exclusion chromatography is used.

2.1.1 Ion exchange chromatography

Ion exchange chromatography is one of the simplest and most useful methods of immunoglobulin purification. The principle of operation involves two main events, 1) the binding of the protein to the fixed charges on the matrix and 2) the elution of the protein from the matrix. The matrix commonly consists of cellulose or agarose, to which is attached an ionizable diethylaminoethyl (DEAE) group, known as the anion exchanger[51]. At pH 8, the matrix is strongly positively charged, attracting negative anions or charged side chains of proteins. Therefore, retention is achieved via electrostatic interactions. With increased concentration of anions such as chloride ions, and/or the decrease of pH, which protonates the amino acid side chains, the protein is released from the matrix. Immunoglobulins, one of the most basic serum proteins, with isoelectric points in the range 6-8, are the first ones to be eluted.

At pH 8, a large volume of a protein mixture can be loaded onto the column without sacrificing the resolution. A simple linear salt gradient can then be applied to elute the protein of interest, thus making ion exchange a very popular chromatographic tool.

2.1.2 Gel filtration chromatography

When a very pure sample is needed, a gel filtration or size exclusion column is required. The column is packed using porous beads as chromatographic support to occupy about 70% of its volume. Small molecules can enter into the beads, while large molecules are excluded from the beads, hence they will pass right through the column. Unlike other methods, such as ion exchange chromatography, which may

require harsh elution conditions to break the electrostatic interactions between the sample and the chromatographic support, the unique ability of protein separation based on relative size utilizes one gentle running buffer to avoid damage during chromatography. However, because of the absence of such interactions, the resolution is limited. Therefore, only a small volume of the protein mixture can be injected into the column for each run and unlike an ion exchange column which can actually concentrate the protein being purified, great dilution occurs when a gel filtration column is used.

2.1.3 Affinity chromatography

Affinity chromatography, one of the most powerful procedures in protein purification, is based on the irreversible immobilization of one component of a system on a solid-phase matrix and the subsequent binding and elution of a complementary ligand in free solution. Monoclonal antibodies can be purified from a column with immobilized specific antigen or with immobilized anti-immunoglobulin antibodies (Protein A).

When a large amount (50-100 mg) of antigen is available for the specific monoclonal antibody of interest, it can be coupled to agarose beads and used for antibody isolation. The antibody binds to the column at neutral pH and physiological salt concentration. Elution may be accomplished by changes in pH or ionic strength[52]. Similar to the ion exchange column, a large volume of mixture can be loaded onto the column without affecting the resolution of separation. However, denaturation and aggregation could result during purification due to harsh elution condition that are

sometimes required.

A Protein A column is a much more general method of antibody purification. Certain classes of monoclonal antibodies are recognized by Protein A, a protein produced by most strains of *Staphylococcus aureus*. It binds to IgG via the Fc portion of the molecule. Commercially available Protein A-sepharose columns have unlimited usage provided that it binds the antibody of interest.

2.1.4 Purification of rat IgG

The synthesis of the Tyv-GalNAc disaccharide (Fig 14) was complicated by the difficulty of controlled formation of a β-mannoside type 1,2-*cis* linkage on tyvelose. Consequently, no attempts were made to prepare and employ an affinity chromatographic column. A protein A column is also unsuitable for the purification of our antibodies, since rat IgG has low affinity for protein A. As a result, after experimenting with various columns and conditions, a combination of gel filtration column followed by an ion exchange column was selected to carry out the purification of the rat IgG molecule.

2.1.5 Heavy and light chain separation

In order to perform amino acid sequencing, the heavy and light chains have to be separated. Under denaturing and reducing conditions the IgG molecule can be separated into H and L chains by breaking the inter-chain and intra-chain disulfide bonds. Subsequent alkylation of the thiol groups keeps the chains from folding back into their original shape. The denatured heavy and light chains are then separated

using chromatographic techniques. In the case of antibody 18H, a gel filtration column in the presence of guanidine HCl was used for this purpose.

2.1.6 Papain digestion

The hinge region of an IgG molecule can be cleaved using a thiol protease, papain, to give two Fab and one Fc fragments. In order for papain to be active, the SH group in the active site has to be in its reduced form. A common reducing agent used is dithiothreitol, which also has the potential to cleave the labile inter-chain disulfide bonds of the IgG. EDTA is also part of the digestion solution to chelate any heavy metals present and prevent them from inactivating the papain by forming a complex with its sulphydryl group. The digestion may be terminated by alkylating the enzyme's thiol group with iodoacetamide. The L and Fd inter-chain disulfide bond is also broken and alkylated in this step. The rat Fc and Fab fragments were separated on a gel filtration column.

2.2 Results

2.2.1 IgG purification from ascites fluid

T. spiralis monoclonal antibodies 9E, 18H, and 9D were first concentrated from ascites fluid by salt fractionation with ammonium sulfate[53]. They were then passed through a Superdex 200 (Pharmacia, Uppsala, Sweden) FPLC column[54]. Concentration of different fractions using acetone precipitation and SDS polyacrylamide gel electrophoresis, determined that the major peak that appears at the 30 minute mark contained the IgG molecules (Fig 15). After the first column, the 9E

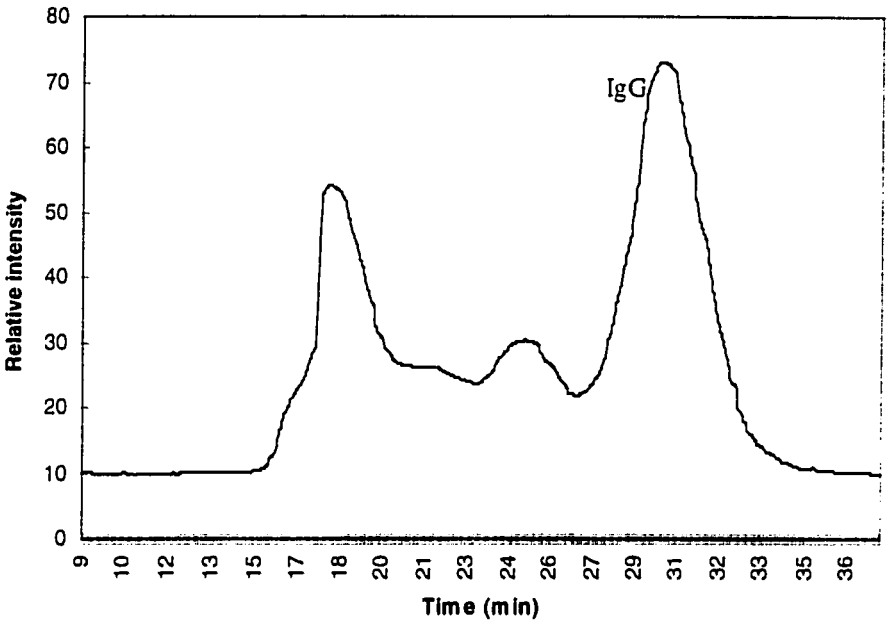

Fig 15. Gel filtration Chromatograph of 9E IgG from a Superdex 200 column.

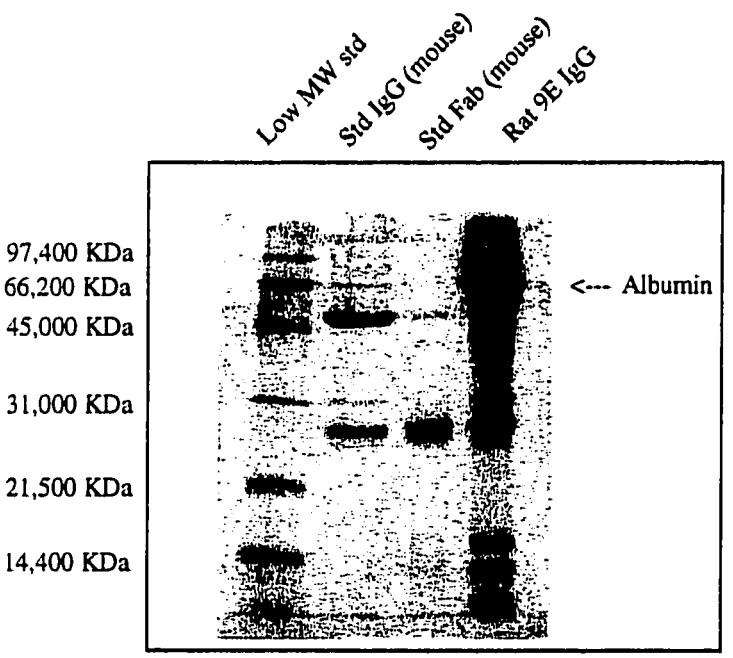

Fig 16. SDS gel of 9E IgG after gel filtration.

and 9D IgGs, still contained a large amount of a ~66K Dalton molecular weight

protein, likely serum albumin (Fig 16). They were then further purified on a DEAE-5PW column (Waters, Mississauga, ON, Canada) (Fig 17).

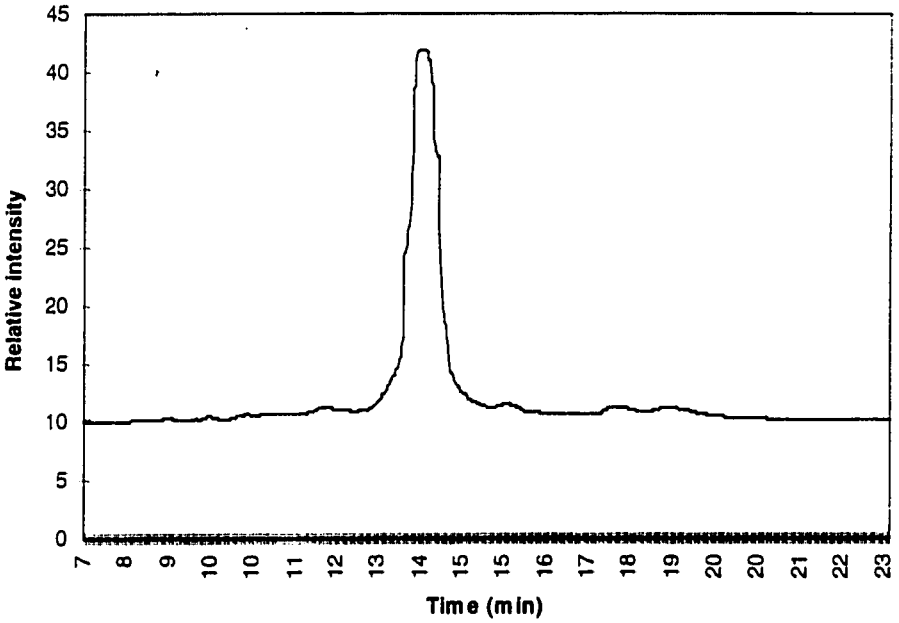

Fig 17. Chromatograph of 9E after further purification with DEAE column.

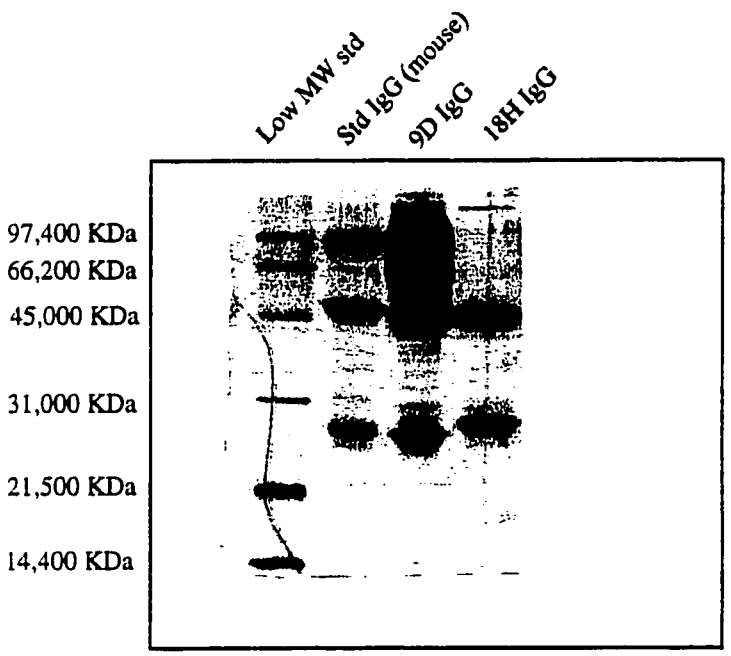

Fig 18. SDS gel of 9D and 18H IgG after gel filtration.

Good separation of the 18H IgG and serum albumin was obtained on a Superdex 200 gel filtration column (Fig 18). Therefore, the 18H IgG was subjected to digestion without further purification on the DEAE column.

2.2.2 Rat heavy and light chain separation

Heavy and light chain separation was performed according to the method of Aebersold[55]. Purified 18H IgG was subjected to denaturation by guanidine HCl and DTT was used to break the 16 inter-chain and intra-chain disulfide bonds. Iodoacetamide was added to alkylate the cysteine residues. The alkylated chains were then separated by gel filtration Superdex 200 column (Fig 19), before they were freeze dried. Isotyping of the IgG was performed using an Amersham mouse

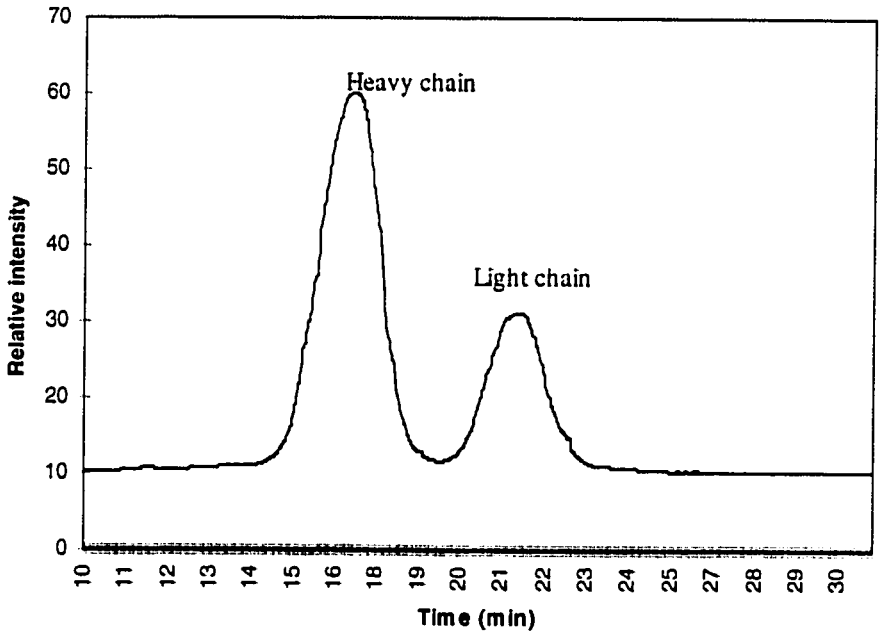

Fig 19. Separation of 18H heavy and light chain.

monoclonal antibody isotyping kit (Amersham, UK) (a rat isotyping kit was not available at the time). It confirmed the results obtained by Appleton *et al*[39], that the

heavy chain is an IgG2a. The light chain was found to belong to the κ isotype. The Kabat data base of Ig sequences was searched to find the amino acid sequences that have already been determined in the literature for rat κ chain and H chain of IgG2a isotype. These sequences were used as a guide for the mass spectra interpretation.

2.2.3 Proteolytic digestion of rat IgG using papain

The proteolytic digestion was performed with papain in the presence of DTT in a well-buffered Tris solution containing EDTA and terminated with iodoacetamide. The Fc and Fab fragments were separated on a Superdex 75 (Pharmacia, Uppsala, Sweden) gel filtration column (Fig 20) to give pure Fab (Fig 21).

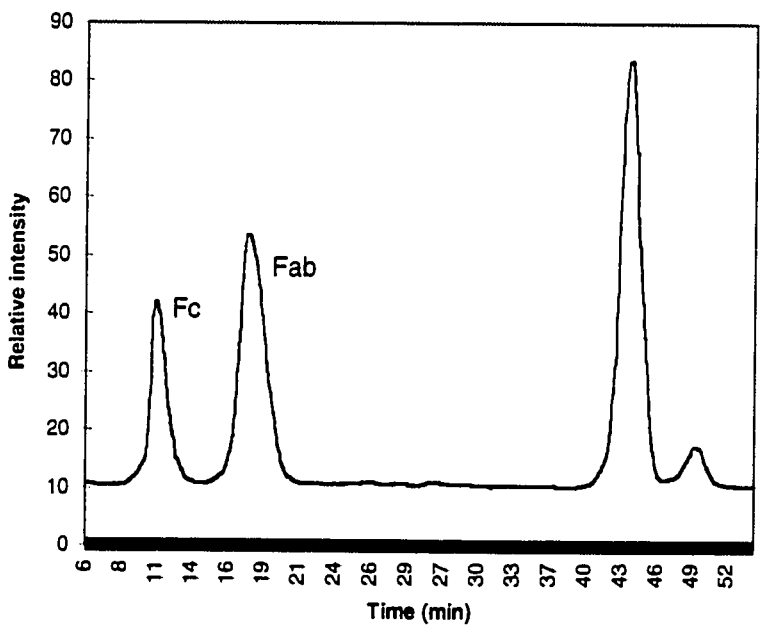

Fig 20. Separation of 18H Fab and Fc on a Superdex 75gel filtration column.

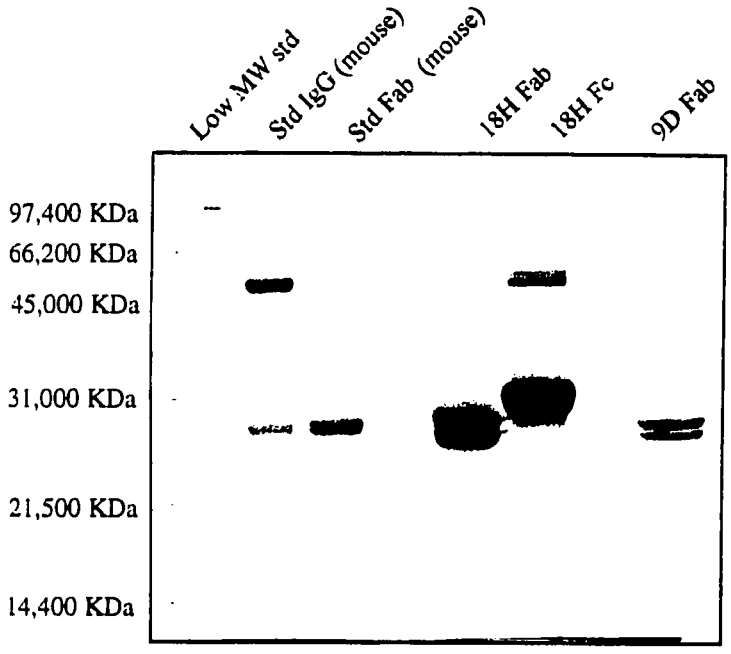

Fig 21. SDS gel of pure 9D and 18H Fab.

2. 3 Experimental procedure

2.3.1 General methods

The HPLC used was a Waters 626 LC system (Mississauga, ON, Canada), with a Waters 600S controller, Waters 486 Tunable Absorbance Detector and Waters 626 pump. Waters fraction collector and NGI Servogor 120 (Neudorf, Osterreich, Austria) plotter were used for fraction and data collection. All injections to the HPLC were first filtered through a Millex-GV 0.22 μM filter (Bedford, MA, USA) and all solvents were passed through Millipore 0.22 μM filters prior to use.

Gel electrophoresis was performed with BioRad mini gels (Hercules, CA, USA). Amicon Centricon 10 (Beverly, MA, USA) was used for IgG and Fab concentration. Spectra/Por tubing (Houston, Texas, USA) was used for dialysis.

Deionized water from a Millipore Milli-Q plus apparatus was used in the preparation of all solutions. PBS buffer refers to a 0.01 M solution of monobasic sodium phosphate and dibasic sodium phosphate with a pH of 7.0 containing 0.15 M NaCl.

2.3.2 Detailed procedures

Ammonium sulfate precipitation

Rat ascites (purchased from Dr. Judith Appleton's laboratory) (1 ml) was spun in an eppendorf centrifuge for 30 minutes at 6000 rpm to get rid of large debris. An equal volume of saturated ammonium sulfate solution was added dropwise to the supernatant while stirring. Mixing was continued for 2 more hours at room temperature, and then 1 hour at 4 °C. The precipitate was pelleted at 7500 rpm for 30

min and suspended in 50% ammonium sulfate solution (1 ml) before spinning at 12000 rpm for another 30 minutes. The pellet was then dissolved in PBS (300 µl) solution.

Purification of IgG antibodies on gel filtration column.

A Superdex 200 HPLC gel filtration column (HR 10/30) was equilibrated with 2 bed volumes of PBS solution. The purified ascites was filtered through a 0.22 µm filter, and 250 µl portions were injected into the column followed by elution at a flow rate of 0.5 ml/min. The major peak containing IgG was collected. All IgG fractions were pooled together, and concentrated using a Centricon concentrator (Amicon).

Further purification of IgG on a DEAE column.

Concentrated IgG from the gel filtration column in PBS was diluted with the start buffer, 20 mM Tris-HCl, pH 8.5 buffer, and concentrated again to give the required pH and salt concentration. The IgG solution (10 ml) was loaded onto the DEAE column, which had been equilibrated with the same start buffer. The protein was eluted with the eluting buffer, 20 mM Tris-HCl, 0.30 M NaCl, pH 7, using a linear gradient from 100% start buffer to 100% eluting buffer in 1 hour at a flow rate of 0.5 ml/min.

Acetone precipitation for SDS-PAGE

Cold acetone (1 ml) was added to protein fractions (200 µl) eluted from the gel filtration column. The mixture was incubated at –20 °C for 1 hr after vortex. The

fractions were then centrifuged in an eppendorf centrifuge for 5 minutes, before the supernatant was removed and the pellets were air dried. The dried pellets were resuspended in PBS buffer (10 μl) and were then ready to be used for electrophoresis.

Sodium dodecyl sulphate-polyacrylamide gel

SDS-PAGE was carried out using the Mini-Protean gel system and low molecular-mass protein standards (for 12.5% gels under reducing conditions) from Bio-Rad. The buffer system introduced by Laemmli[56] was used. Alternatively, SDS-PAGE was carried out using the Pharmacia Phast system employing Phast gels following the manufacturer's instruction.

Heavy and light chain separation

Purified 18H IgG from a Superdex 200 column was dialyzed in water overnight, before it was freeze dried. The lyophilized powder IgG (4.5 mg, $3x10^{-5}$ mmol) was then dissolved in buffer (1 ml) containing 0.5 M Tris HCl, 2 mM EDTA, 5 M guanidine HCl, pH 8.5. The mixture was left in a 50 °C water bath for 30 minutes before dithiothreitol (3.7 mg, 0.024 mmol, *ie* 50 molar excess disulfide bonds) was added. Incubation was continued for 4 hours. Iodoacetamide (10 mg, 0.058 mmol) was added to alkylate the denatured thiols by incubating the mixture at room temperature for 40 minutes. Injection onto a Superdex 200 HPLC column with a running buffer of 1 M acetic acid, 3 M guanidine HCl, gave the H and L chain peaks. The combined fractions of each chain were dialyzed against water 3x before lyophilization to give pure H and L chains.

IgG Digestion and Fab/Fc Separation

IgG, dissolved in equal volumes of 0.2 M Tris buffer pH 8 and 4 mM EDTA, was reduced with 10 mM dithiothreitol and digested with papain at an enzyme to substrate ratio of 1:100, 37 °C for 3 hours. The enzyme was inactivated by the addition of iodoacetamide (10 x enzyme concentration). The Fab and Fc products were separated on a Superdex 75 (HR 10/30) column following the same chromatographic procedure as that for Superdex 200.

Chapter III Preliminary Amino Acid Sequencing of the Heavy and Light Chains of Monoclonal Antibody 18H

3. 1 Introduction to protein sequencing

3.1.1 Edman degradation

The general methodology for protein sequencing using Edman degradation has changed very little since its introduction by Pehr Edman in the 1950s. Automated instruments, known as sequenators are used nowadays to eliminate the labour-intensive sample manipulation, and optimization of conditions has allowed the sequencing of low abundance proteins (picomole range). This highly accurate micro sequencing technique is widely used in the primary structural determination of protein.

The Edman reagent phenylisothiocyanate (PITC) is used in the three step peptide sequencing: coupling, cleavage, and conversion (Fig 22). The charged terminal amino group of the peptide is modified by the formation of a phenyl thiocarbamoyl derivative with PITC. Under mild acid hydrolysis, this terminal amino acid is removed as an unstable cyclic anilinothiazolinone (ATZ) derivative, leaving the peptide shortened by one amino acid. The ATZ is then converted to a stable phenyl thiohydantoin (PTH) amino acid that can be identified by chromatographic procedures. The peptide chain then enters a second cycle and the above procedure is repeated. Up to 40-60 successive N-terminal amino acid residues can be identified using the Edman degradation. However, anything longer than that becomes difficult

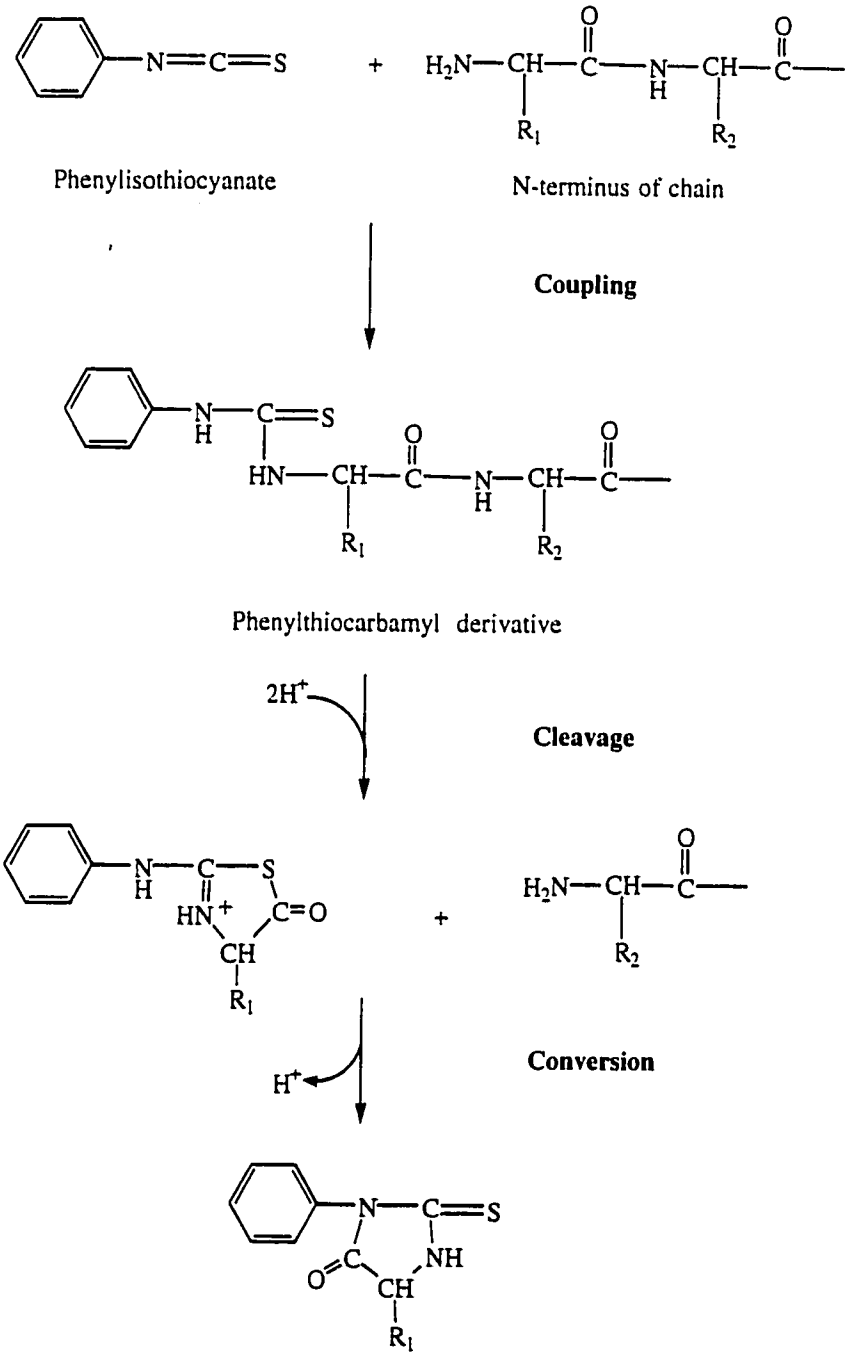

Fig 22. Edman degradation.

due to the contamination from accumulated impurities and incomplete reactions. For a much larger protein, enzymatic digestion is required first to cleave the protein into

smaller peptides and these fragments can then be sequenced individually after separation by chromatography.

In automated Edman sequencing, a variety of instruments can be used to separate the cleaved amino acids and the rest of the peptide. Gas-phase sequencing is based on the idea that the reactants and products are gaseous, therefore, they will be eluted off the column after each cycle. This variant of the solid-phase technique allows easier handling and less contamination in comparison to some of the older methods.

The most common problem encountered in Edman sequencing is the modification and N-terminal cyclization of the amino acids which prevents the attachment of PITC. Chemical and enzymatic cleavage can eliminate some of the blocking mechanisms; however, routine removal of certain groups is not possible.

3.1.2 Mass spectrometry

With the rise of new ionization and computer technologies in mass spectrometry in the last decade, the analytical tool that was once limited to only small molecules has become a popular choice for primary structure determination of proteins. Mass determination can indicate the presence of posttranslational modifications and provide information about blocked peptides and novel covalent cross-links within proteins[57,58]. Mass spectrometric sequencing also has the advantage of speed, high sensitivity and the ability to work from unseparated peptide mixtures[59]. Amongst the new developments, electrospray ionization has emerged as a method of choice for analyzing proteins up to 75 kDa[60].

Electrospray is based on the ability to generate multiply protonated, and therefore multiply charged, molecules by generating a spray of very small droplets of a solution of the protein emerging from the tip of a needle held a few keV above the entrance aperture of a quadrupole mass spectrometer[61] (Fig 23). The solvent surrounding the proteins provides protection to allow them to stay intact during the transition from the liquid to the gas phase, and sometimes the proteins can even maintain their tertiary structures.

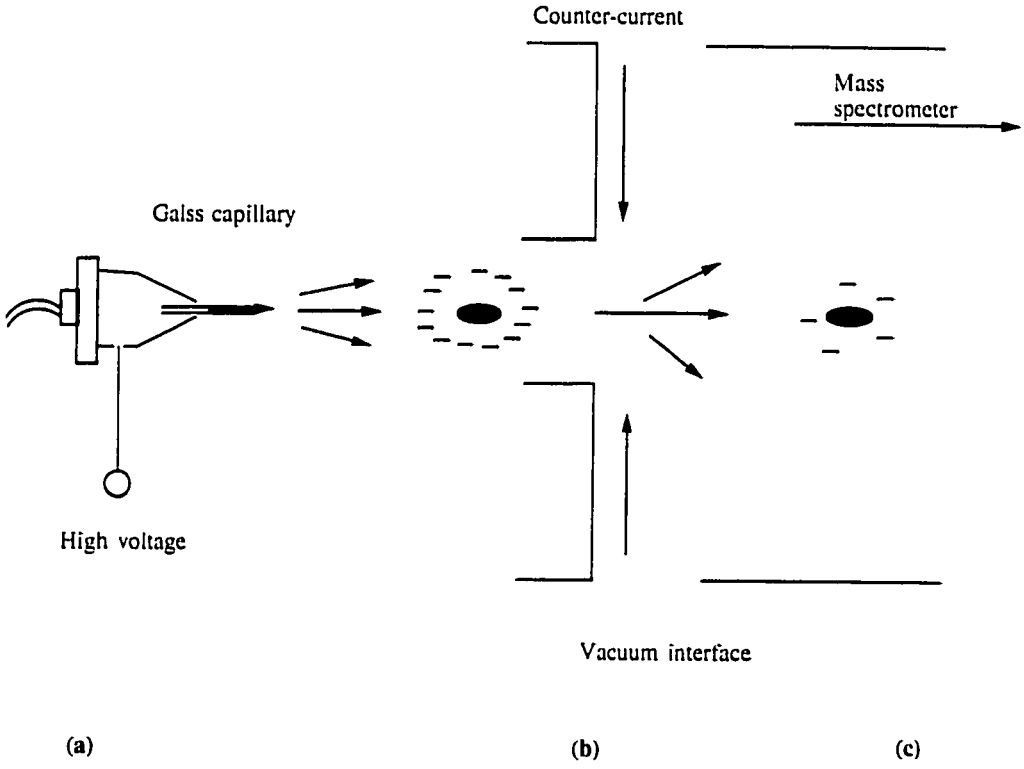

Fig 23. Three principal steps of ESMS. **(a)** Formation of highly charged droplets. **(b)** Desorption of protein ions from droplets into gas phase. **(c)** Mass analysis of the ions in a mass spectrometer.

The mass-to-charge ratios of a particular protein are measured, instead of the direct mass, allowing the measured peaks to fall within the mass range of normal instruments. Therefore, the molecular weight of a very large protein that is far in

excess of the mass range of the analyzer can be accurately measured.

A simple formula, $m_n = (M + z_n) / z_n$, is used to calculate the actual molecular weight of that protein. In this formula, m is the mass-to-charge ratio measured by the spectrometer, M is the actual molecular weight of the protein, z is the charge on the protein and n represents a particular ion peak. z can be determined using the formula $z_{n+1} = (m_n - 1) / (m_{n+1} - m_n)$. Algorithms have been developed to convert the molecular ions into a single peak corresponding to the neutral molecule[62,63] (Fig 24).

A small protein being sequenced can be injected into the mass spectrometer directly, whereas large proteins are usually subjected to protease digestion to give a mixture of peptide fragments first. These fragments are injected onto a HPLC column prior to being analyzed by the mass spectrometer. Unlike the Edman degradation, complete separation of the peptide fragments by the HPLC column is not necessary. The masses of these peptides can be used to map a known structure.

In order to obtain detailed sequencing of these peptides, tandem MS or MS-MS is often used. The peptide mixture is separated by the first mass spectrometer and the species of interest is fragmented, usually by collision with a certain pressure of "collision gas". The second mass spectrometer then separates and measures the masses of fragments produced from the peptide ion. Fragmentation occurs through bond cleavage resulting in different classes of fragment ions (Fig 25). The a_n, b_n and c_n types are generated, if the charge is retained on the N-terminus of the peptide, and the x_n, y_n and z_n ions are formed when the charge is retained on the C-terminus. The most common fragmentation is at the amide bonds of the peptide backbone, resulting in a nested set of peaks differing by amino acid residue masses[64].

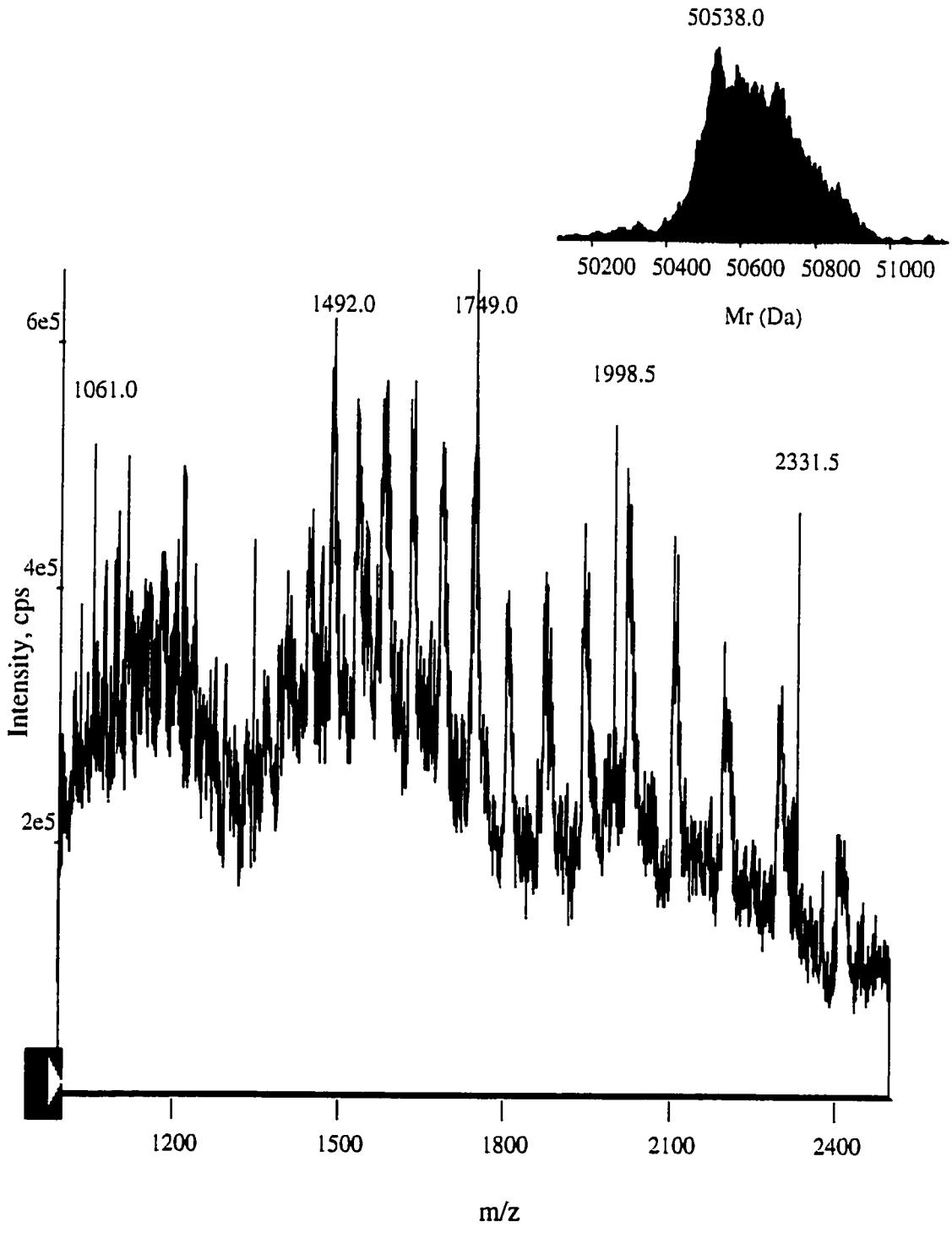

Fig 24. **(a)** Molecular ion peaks generated from a single peptide.
(b) Calculated actual molecular weight of the protein.

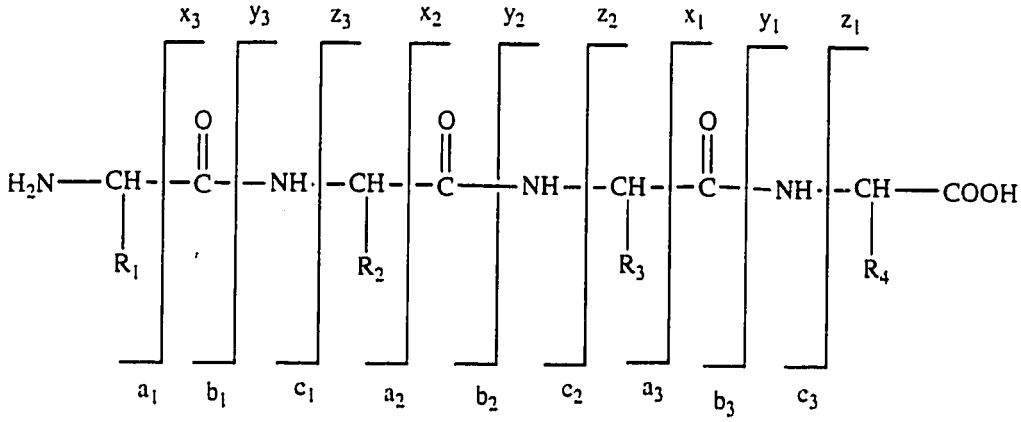

Fig 25. Fragmentation of the peptide in MS/MS.

Mass spectrometry provides an exciting alternative for protein sequencing by giving rapid results with minimal amounts of sample. However, factors such as instrument complexity, interpretation ambiguity and high cost are limiting its wider use. Based on entirely different chemical and physical principles, Edman degradation and mass spectrometry are highly complementary to each other. In this chapter, preliminary amino acid sequencing studies performed on the heavy and light chains of the 18H monoclonal antibodies are presented.

3. 2 Results

3.2.1 LC-MS analysis of the heavy and light chains

The mass spectrometry work was performed during a visit to Dr. Pierre Thibault's laboratory at NRC, Ottawa.

The heavy and light chains, prepared and purified at the University of Alberta, were digested with trypsin to give fractions of peptide chains that ended in either Lys or Arg. The mixture was separated on a reverse phase C-18 HPLC column while

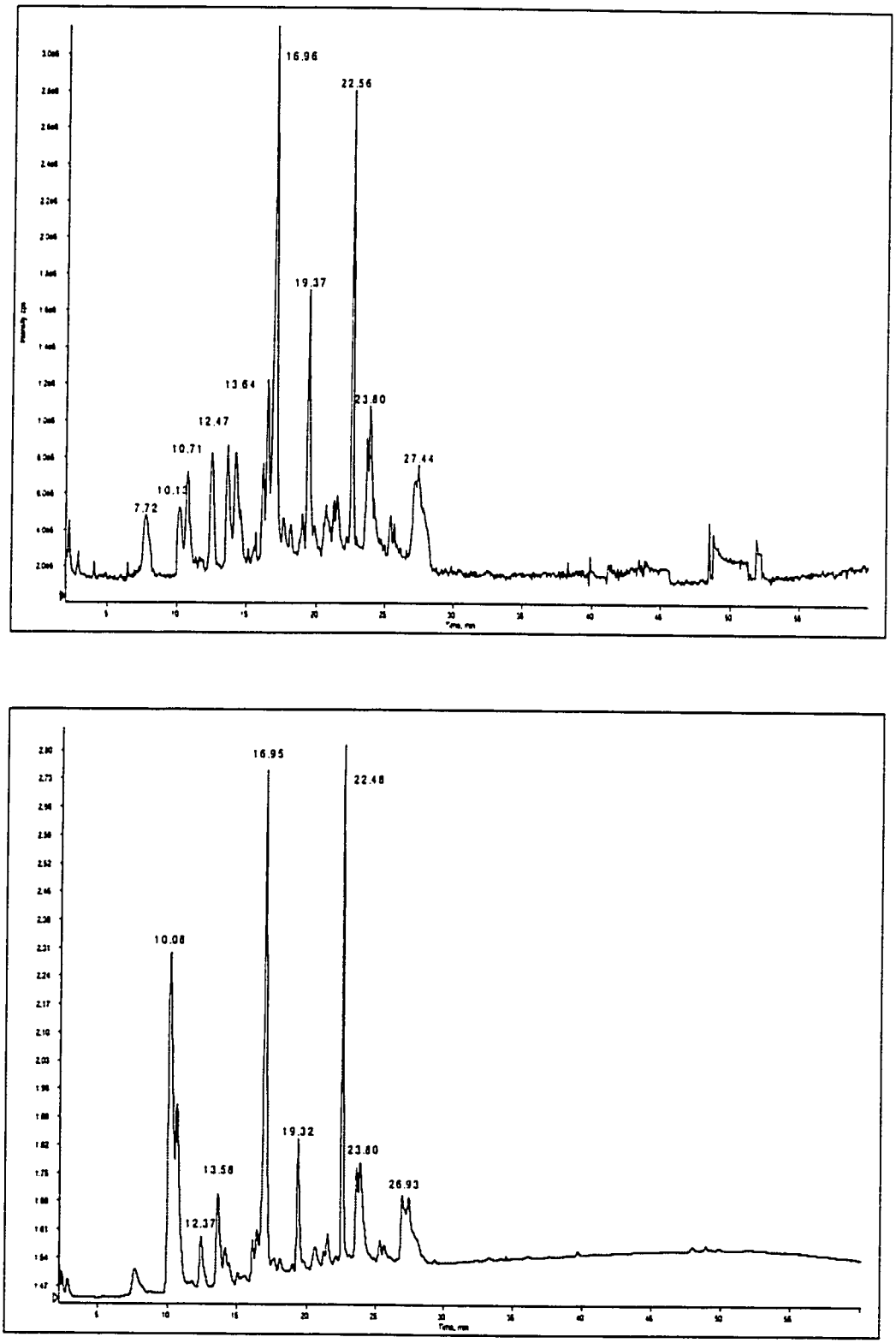

Fig 26. (**a**) Analysis of 18H L-chain digestion under full mass scan acquisition (m/z 40-4000), and (**b**) under LC-UV at 280 nm.

performing LC-MS measurements (Fig 26). No attempts were made to separate the fragments.

An initial amino acid sequence assignment of some of the fractions was made (Fig 27). The peptide from the L-chain that appeared 7.72 minutes after injection has a $[M+ H]^+$ ion of m/z 690. Searching for the literature data for possible tryptic digested fragments of light chains gave a match for the sequence "IDGTER". Similarly, the peptide that was eluted at 10.06 minute, with a m/z of 524 ($[M + H]^+$) was tentatively assigned the sequence "SFNR". The peptide eluted at 10.78 minute has a major peak at 805. It is the doubly protonated, $[M+ 2H]^{2+}$ ion of the fragment "TSSSPVVK".

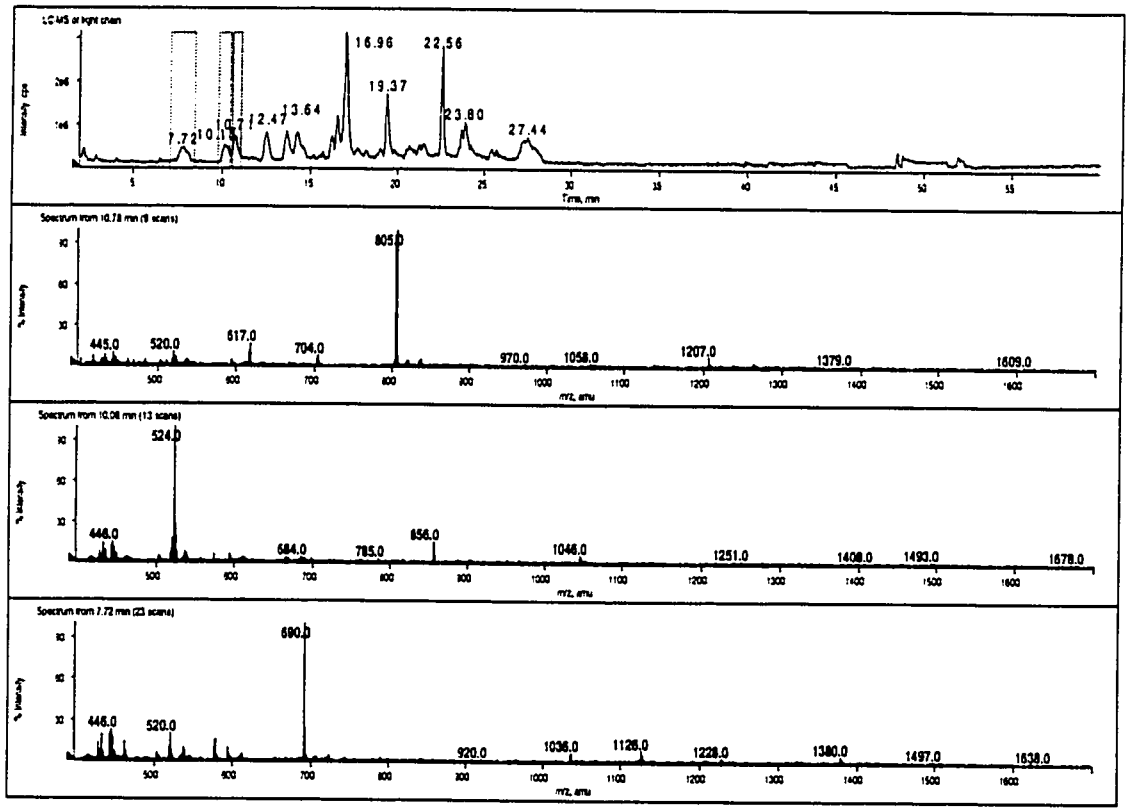

Fig 27. Extracted mass spectra for L-chain peaks eluted at **(a)** 10.78, **(b)** 10.06, and **(c)** 7.72 min.

3.2.2 LC-MS-MS and tandem MS characterization of H and L chains

The assignments for the majority of m/z peaks of the peptides, however were, not possible. Tandem mass spectrometry analysis was called upon to give a clearer MS picture. A LC-MS-MS analysis was first carried out, by injecting the digestion mixture into a HPLC column connected to the MS-MS spectrometer. Later, the fractions collected from the initial LC-MS experiment were injected individually to give MS-MS data. As a result, new fragments were sequenced and many of the previously determined sequences were confirmed.

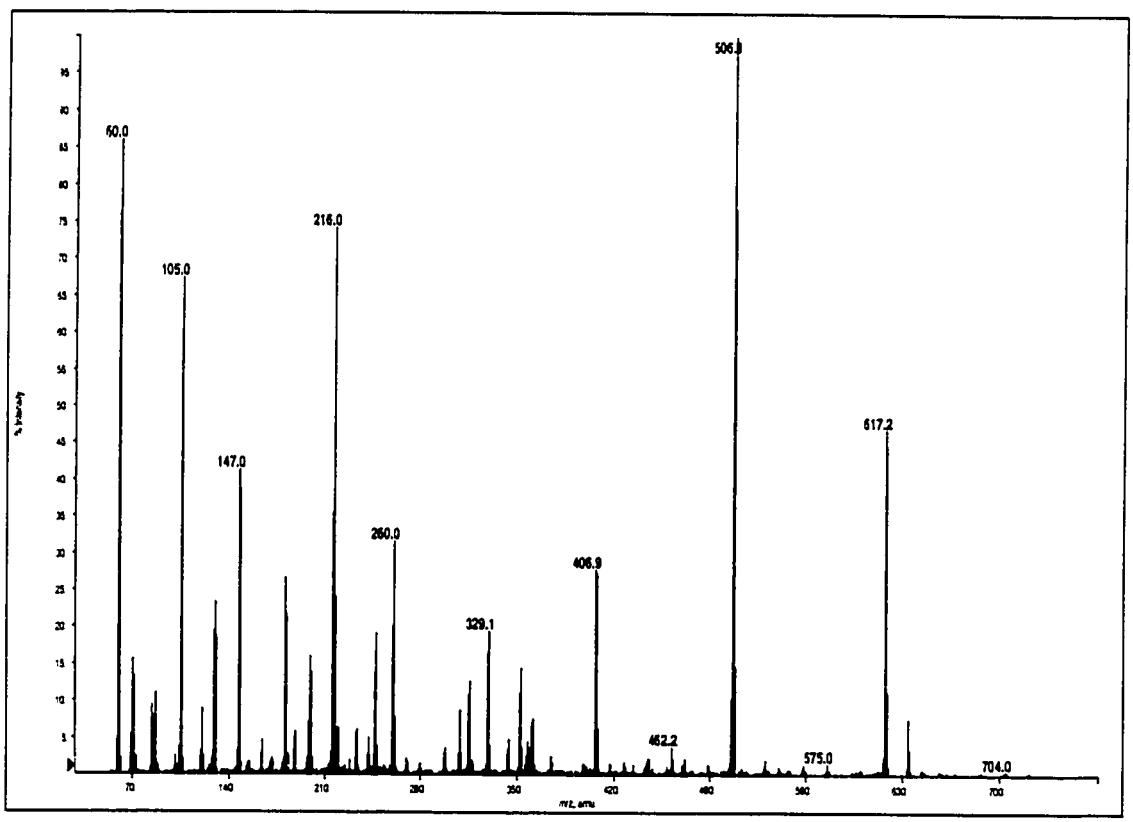

Fig 28. MS-MS spectrum of H-chain fraction 8.

The doubly charged $[M + 2H]^{2+}$ ion (m/z 361.5) for the heavy chain (Fig 28)

gave fragmented y" ions at 634.5, 506.1, 406.9, 260 and 147 suggesting the sequence "S-Q/K-V-F-L/I-K". The second amino acid is probably a Gln (Q), since a Lys (K) at that position would likely result in a cleavage. The assignment of Leu (L) and Ile (I) would have been ambiguous; however, literature data for the heavy chain contains a sequence of "SQVFLK", which is likely the same for the 18H strain.

The tandem mass spectrum for the m/z 805 ion (Fig 29) verifies the assignment described above. The y ions (804.5, 703.6, 616.4) clearly indicate the presence of T-S-S as the first three amino acids. By feeding the sequence "TSSSPVVK" into the computer, a simulated mass spectrum was generated (Fig 30b). The majority of the predicted fragmentation ions coincided with the experimental results.

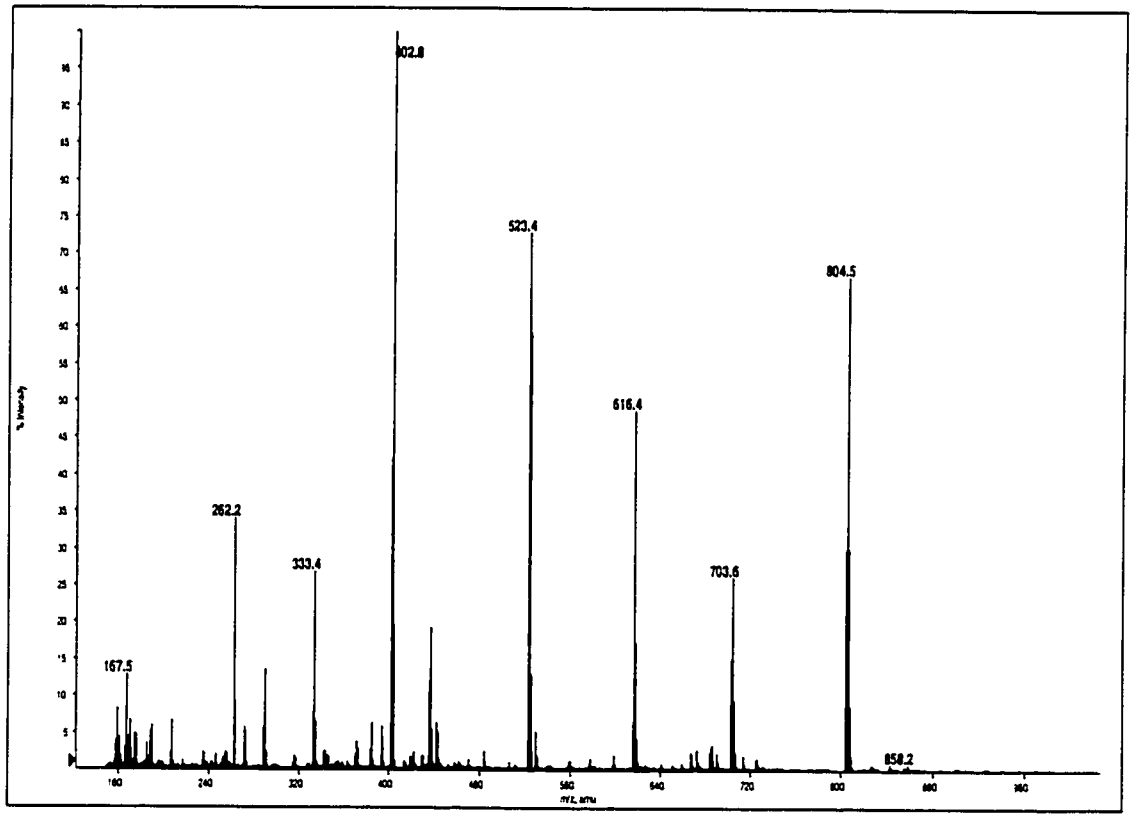

Fig 29. MS-MS spectrum of L-chain ion m/z 805.

Peptide 3 (num hits = 40)

TSSSPVVK

Symbol	Mass	a	a-17	b	b-17	y	y-17
T, Thr	101.11	**74.11**	**57.11**	**102.11**	**85.11**	804.90	787.90
S, Ser	87.08	**161.19**	**144.19**	**189.19**	**172.19**	**703.80**	**686.80**
S, Ser	87.08	**248.27**	**231.27**	**276.27**	**259.27**	**616.72**	**599.72**
S, Ser	87.08	**335.35**	**318.35**	**363.35**	**346.35**	**529.64**	**512.64**
P, Pro	97.12	432.46	**415.46**	**460.46**	**443.46**	**442.56**	**425.56**
V, Val	99.13	**531.60**	**514.60**	**559.60**	**542.60**	**345.45**	**328.45**
V, Va	99.13	**630.73**	**613.73**	658.73	**641.73**	**246.31**	**229.31**
K, Lys	128.17	758.90	741.90	786.90	769.90	**147.18**	**130.18**

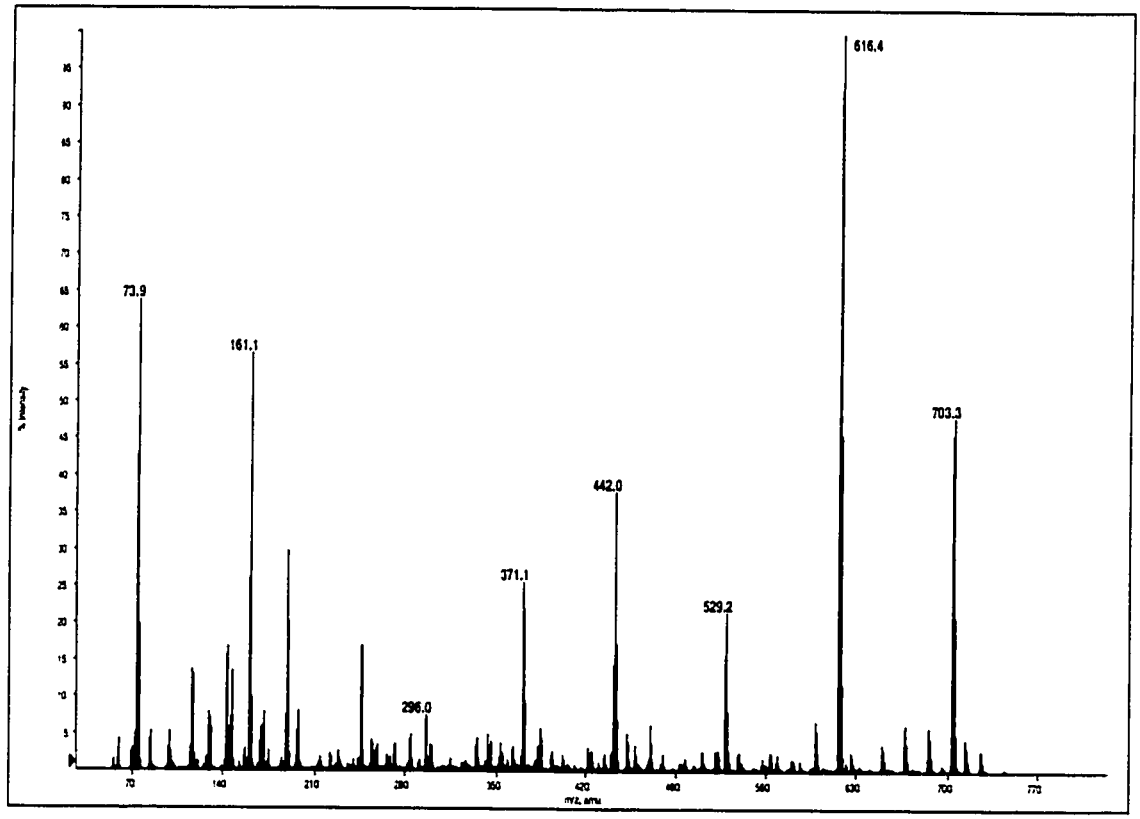

Fig 30. Computer verification of the deduced sequence for ion m/z 805. **(a)**Expected fragmentations from TSSSPVVK, where the expected and actual ions in agreement are shown in bold.**(b)** Simulated mass spectrum.

The sequences for some of the later fractions were still not determined because of the large size or heavy contamination of the fragments. Regretfully, due to time limitations, these large fragments were not investigated further.

Both the heavy and light chains were submitted to gas-phase sequencing of the N-termini. The first 40 residues of the N-terminus of the light chain was deduced successfully. The heavy chain, however, did not give good results by GC-MS.

Combining all of the sequencing data, partial sequences of 18H light and heavy chains were determined. (Discrete or overlapping sequences determined for 18H are shown in different lines.)

Table 3. **Heavy chain variable domain** (Shaded—a literature V_H sequence[65] for Rat H-chain V_H domain with possible homology to 18H V_H domain sequence—unshaded)

1-10	11-20	21-30	31-40	41-50
PGLVQPSQTL	SLTCTVSGLS	LTSNSVSWIR	QPPGKGLEWM	GVIWSSGGTD
51-60	**61-70**	**71-80**	**81-90**	**91-100**
YNSAIKSRLS	ISRDTSKSQV	FLKMNSLQTE	DTAMYFCARG	AYGYKYWGQG
LS	ISR	SQV	FLK	
101-107				
TLVTVSS				

Table 4. **Heavy chain constant domain** (Shaded—a literature C_H sequence[66] for Rat H-chain C_H domains with possible homology to 18H C_H domains sequence—unshaded)

108-117	118-127	128-137	138-147	148-157
AETTAPSVYP	LAPGTALKSN	SMVTLGCLVK	GYFPEPVTVT	WNSGALSSGV
		SN	SMVTLGCLVK	
			GYFPEPVTVT	WNSGALSSGV

158-167	168-177	178-187	188-197	198-207
HTFPAVLQSG	LYTLTSSVTV	PSSTWSSQAV	TCNVAHPASS	TKVDKKIVPR
				IVPR
HTFPAVLQSG	LYTLTSSVTV	P		

208-217	218-227	228-237	238-247	248-257
ECNPCGCTGS	EVSSVFIFPP	KTKDVLTITL	TPKVTCVVVD	ISQNDPEVRF
		TKDVLTITL	TPK	F
ECNPCGCTGS	EVSSVFIFPP	K DVLTITL	TPK	
			VTCVVVD	ISQNDPEVR

258-267	268-277	278-287	288-297	298-307
SWFIDDVEVH	TAQTHAPEKQ	SNSTLRSVSE	LPIVHRDWLN	GKTFKCKVNS
SWFIDDVEVH	TAQTHAPEKQ	SNSTLR SE	LPIVHR	VNS
		SVSE	LPIVHR	
			DWLN	GK

308-317	318-327	328-337	338-347	348-357
GAFPAPIEKS	ISKPEGTPRG	PQVYTMAPPK	EEMTQSQVSI	TCMVKGFYPP
GAFPAPIEK	PEGTPR		EEMTQSQVSI	TCMVK
S	ISK G	PQVYTMAPPK		GFYPP
S	ISKPEGTPR			

258-367	368-377	378-387	388-397	398-407
DIYTEWKMNG	QPQENYKNTP	PTMDTDGSYF	LYSKLNVKKE	TWQQGNTFTC
MNG	QPQENYK		LNVK	
DIYTEWK	NTP	PTMDTDGSYF	LYSK	

408-417	418-427	428-429
SVLHEGLHNH	HTEKSLSHSP	GK

Table 5. **Light chain variable domain** (Shaded—a literature V sequence[67] for Rat L-chain V_L domain with possible homology to 18H V_L domain sequence—unshaded. Bold letters indicate sequence differences)

1-10	11-20	21-30	31-40	41-50
DFVMTQSPSS	LAVSAGETVT	INCKSSQSLF	YSGNQKNYLA	WYQQKPGQSP
DVVMTQSPSS	LAVSAGETVT	INCQSSQSLL	YSGTQNNYLA	

51-60	61-70	71-80	81-90	91-100
KLLIYWASTR	QSGVPDRFIG	SGSGTDFTLT	ISSVQAEDLA	IYYCLQYYET
LLISWASTR				
	ESGVPDR			

101-110	111-115
PYTFGAGTKL	ELKRA
L	ELK

Table 6. **Light chain constant domain** (Shaded—a literature C_H sequence[68] for Rat L-chain C_L domains with possible homology to 18H C_L domains sequence—unshaded)

116-125	126-135	136-145	146-155	156-165
ADAAPTVSIF	PPSTEQLATG	GASVVCLMNN	EYPRDISVKW	KIDGTERRDG
			DISVK	RDG
			W	KIDGTER
				IDGTER

166-175	176-185	186-195	196-205	206-215
VLDSVTDQDS	KDSTYSMSST	LSLTKADYES	HNLYTCEVVH	KTSSSPVVKS
VLDSVTDQDS	K	ADYES	HNLYTCEVVH	K S
	DSTYSMSST	LSLTK		TSSSPVVK

216-221
FNRNEC
FNR

3. 3 Experimental

3. 3. 1 Mass spectrometry

Equipment

Mass spectra were obtained using a Perkin-Elmer SCIEX API III triple quadrupole mass spectrometer (Thornhill, ON, Canada) equipped with an atmospheric pressure ionization source and a Sciex IonSpray interface. A Macintosh Quadra 950 computer was used for instrument control, acquisition and processing. The computer program MacBioSpec (Sciex, Thornhill, ON, Canada) was used to support interpretation of the mass spectra[69]. The HPLC has a Hewlett-Packard (Palo Alto, CA, USA) HP1090 Series II liquid chromatograph equipped with a ternary DR5 solvent delivery system, an HP1040A diode-array detector, and an HP7994A data system[70]. LC-ESMS analysis was performed using a flow splitter connected after the column with only a quarter of the fractions going to the mass spectrometer.

LC-MS

Tryptic digestions were performed separately on the heavy (2 mg/ml) and light (2 mg/ml) chains in 0.1% trifluoroacetic acid at 37 °C overnight. The major fractions were separated on a C18 Zorbax reverse phase column with a linear gradient of 5-95% acetonitrile (0.1% TFA) in 60 minutes at a flow rate of 20 µl per min.

LC-MS-MS

Digestion mixture (25 µl) was injected into the C18 column without the splitter connecting the HPLC and the mass spectrometer with a gradient of 5-60%

acetonitrile (0.1% TFA) in 60 minutes.

MS-MS

Each individual fraction was injected into the mass analyzer for tandem ms studies.

Chapter IV Synthesis of Disaccharide Analogues

4.1 Introduction

The polyhydroxylated structure of carbohydrates endows a distinct character for forming linear and branched sequences, and thereby generates biopolymers that are much more complicated than nucleic acids and peptides. While three different amino acids are able to form only six tripeptides, 1056 unique trisaccharides are possible from the joining of three different monosaccharide residues[71]. Furthermore, each glycosidic linkage may have the α or β stereochemistry making the chemical synthesis of oligosaccharides very complicated.

Chemical glycosylation is achieved by bond formation between the anomeric centre of a fully protected glycosyl donor bearing a leaving group and the free hydroxyl group of a selectively protected glycosyl acceptor. Anomeric bromides and chlorides have traditionally been used as glycosyl donors utilizing many suitable catalysts in a wide variety of glycoside linking methods[72]. However, their popularity has dramatically decreased as other glycosyl donors such as anomeric fluorides[73], trichloroacetimidates[74-78] and thioglycosides[79,80] have been introduced. Glycosyl bromides and chlorides require harsh preparative conditions and they are of an unstable nature. The newer alternatives are generated under milder conditions and can be purified and stored for a much longer time. As well, these often lead to better stereocontrol of anomeric configuration.

The biggest concern in glycosylation reactions is the stereochemistry of the newly formed bond. The different configurations at C-1 and C-2 can be used to describe the types of anomeric linkages, for example, 1,2-*cis* (α) and 1, 2-*trans* (β) of

the *gluco*- and *galacto*-series and 1,2-*cis* (β) and 1, 2-*trans* (α) of the *manno*-series (Fig 31). Miscellaneous glycosidic linkages such as 2-deoxyglycosides and 3-deoxy-2-keto-ulo(pyranosylic) acids are found in biopolymers as well, but this will not be discussed here. Factors influencing this most challenging aspect of oligosaccharide synthesis include: the leaving group at the anomeric centre, type of saccharides involved, the solvent, promoter and temperature used and, most of all, the nature of the protecting group at C-2 of the glycosyl donor. A 2-*O*-acyl protecting group allows it to participate during glycosylation to give 1,2 *trans* glycosidic linkages. With a neighbouring non-participating group such as a benzyl ether, *trans* and *cis* bonds can be formed depending on the reaction conditions.

1. *Gluco-/Galacto*-series

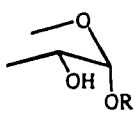

α 1,2-cis

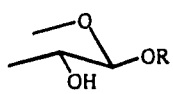

β 1,2-trans

2. *Manno*-series

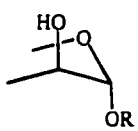

α 1,2-trans

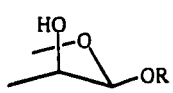

β 1,2-cis

Fig 31. Types of glycosyl linkages.

Neighbour group participation reaction

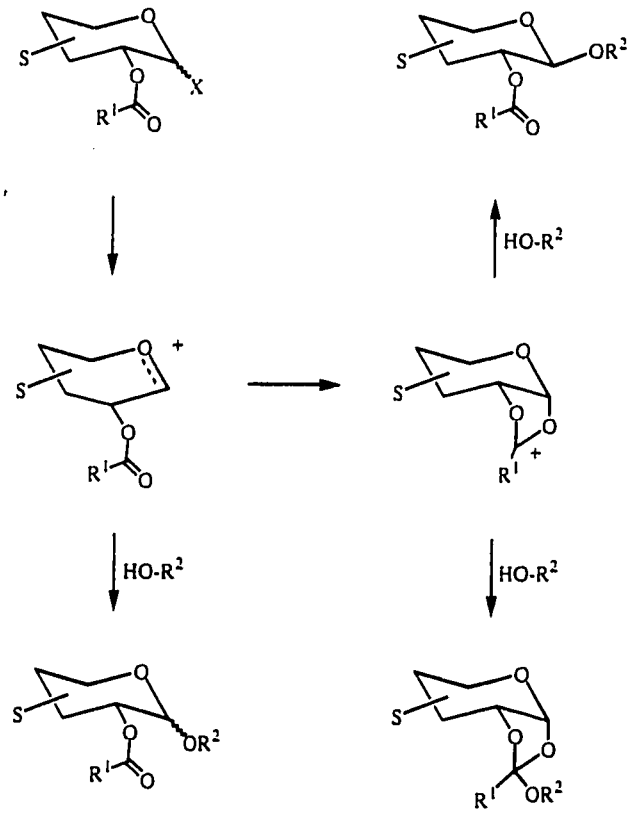

Fig 32. Neighbouring group participation reactions.

Various groups can be used for neighbouring group participation reactions. Using a *gluco-/galacto*-type donor (where S = substituents on the ring) as an example with a C-2 acyl group (Fig 32), the activated anomeric centre forms an oxonium ion, before the acyl protecting group at C-2 participates to form the acyloxonium ion. Attack by the alcohol at the anomeric centre results in the formation of the 1,2-*trans* product. In the case of mannose, a 1,2-*cis* glycoside will be obtained. These reactions usually give the desired products; however, sometimes the alcohol attacks via the oxonium ion to give a α/β mixture. Steric hindrance may play a role in preventing the formation of the acetoxonium ion. An orthoester can sometimes be formed as well,

from the attack of the dioxolane ring by the alcohol. In order to avoid the formation of orthoesters, a bulkier benzoyl or pivaloyl protecting group can be used to discourage the attack on the electrophilic carbon and to enhance the attack at the anomeric centre.

Formation of a *gluco*-like 1,2-*cis* glycosidic bond is usually achieved in the presence of a non-participating substituent at C-2 by inversion of configuration at the anomeric centre or via *in-situ* anomerization. A relatively stable β-leaving group is required to form a partial bond with a heterogeneous catalyst, allowing the alcohol to attack with inversion in an S_N2 manner (Fig 33).

Inversion of Configuration via S_N2

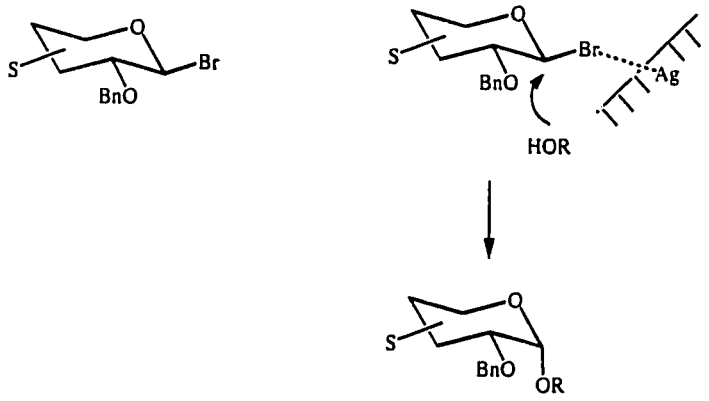

Fig 33. Formation of 1,2-*cis* bond via S_N2 attack of alcohol.

The *in-situ* anomerization method was first introduced by Lemieux and co-workers[81,82]. They reacted a bromide (Fig 34) with a glycosyl acceptor in the presence of tetrabutylammonium bromide to give an α-anomer as the major product. The tetrabutylammonium bromide catalyses the equilibration between the α- and β-halide with the equilibrium shifted strongly towards the α-halide as a result of the anomeric

effect. The transition energy required for the formation of the α-glycoside is lower than that of the β-glycoside; therefore, the β-halide is used up faster than its α counterpart, causing a shift in equilibrium towards the β-halide. When the rate of equilibration is much faster than that of glycosylation, α-glycosides can be obtained in high yield.

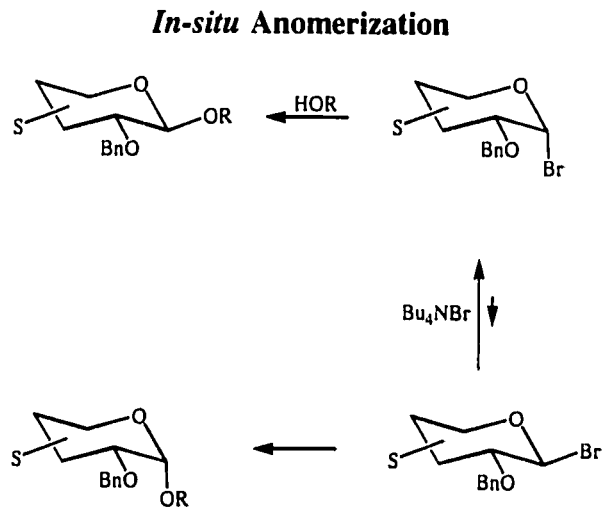

Fig 34. Formation of 1,2-*cis gluco*-like glycosidic linkage using *in-situ* anomerization.

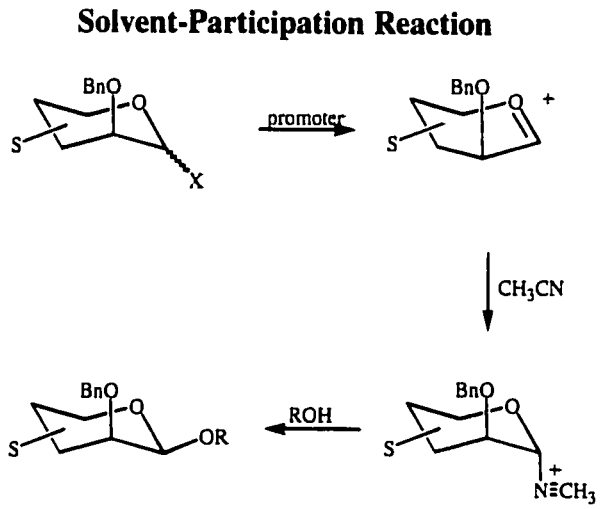

Fig 35. Formation of β-mannoside via inversion of configuration.

Intramolecular Aglycon Delivery

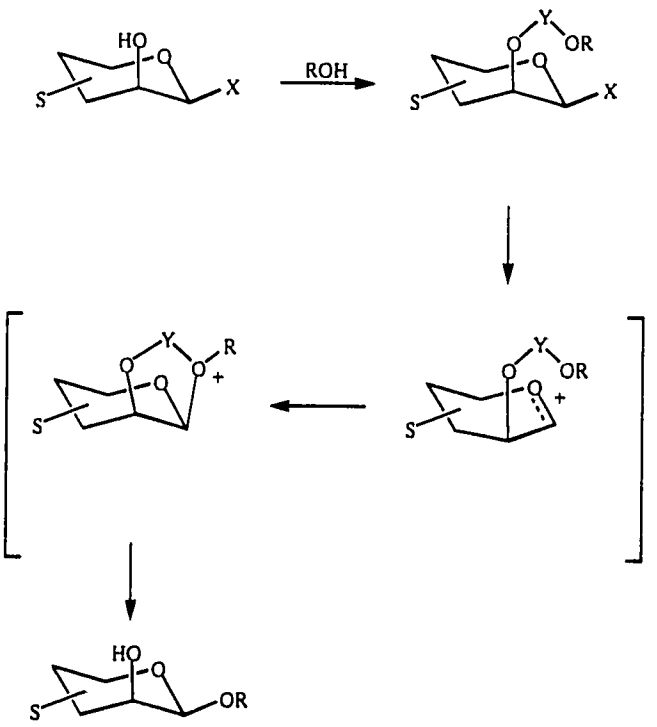

Fig 36. Intramolecular aglycon delivery.

β-Mannoside synthesis is one of the most challenging glycosidic bond formations in carbohydrate chemistry. Inversion of configuration with silver silicate[83] or silver zeolite[84] as catalysts has traditionally been used to form the β-linkage, which cannot be prepared by *in-situ* anomerization. A participating solvent such as acetonitrile is sometimes used to encourage the formation of an equatorial bond (Fig 35). Recently, Hindsgaul[85-87] and Stork[88] have independently reported the intramolecular aglycon delivery approach. The alcohol (acceptor) is linked to an acetal or silicon tether (Y=CH_2 or $SiMe_2$, respectively) to the C-2 position of a mannosyl donor and subsequent activation of the anomeric centre forces the aglycon to be delivered from the β-face of the glycosyl donor (Fig 36). However, the yield

obtained from either method is seldom high.

4.2 Synthesis of the 3,6-dideoxy analogues

In order to study the binding profile of protective antibodies that recognize the oligosaccharide epitope of *Trichinella spiralis* glycans, analogues with related structures were synthesized. The approach may be divided into phases that deal with the functionality that is essential for the recognition of the crucial component sugar 3,6-dideoxyhexose, the 2-amino-2-deoxy galactose, the 2-amino-2-deoxy glucose and the α-fucose residues. This work deals with 3,6-dideoxyhexose analogues.

Initial studies are aimed at establishing the stereochemical features of the 3,6-dideoxyhexose moiety. While the synthesis of the disaccharide epitope of *Trichinella spiralis* (Fig 14) has been very difficult due to the β-mannoside configuration, the isomers **1** and **2** (Fig 37), possess a 1,2-*trans* glycosidic configuration in their linkage to the GalNAc acceptor. This has made their syntheses much easier as the neighbouring participating group can be used to aid in the formation of the β linkage.

1 **2**

Fig 37. The target disaccharides, Par-GalNAc **1** and Abe-GalNAc **2**.

4.3 Results

4.3.1 Glycosyl acceptor

The choice of glycosyl acceptor is governed by considerations for extended syntheses that are beyond the scope of this thesis. However, these requirements are based on the need for a protecting group at C-2 that is capable of leading to higher oligosaccharides through the activation of C-1 of the galactosamine residue. Consequently, while an acetamido group at C-2 would yield the target disaccharides in the most direct way, further elaboration of the oligosaccharide would then be difficult, since the NHAc group is not compatible with either C-1 activation schemes

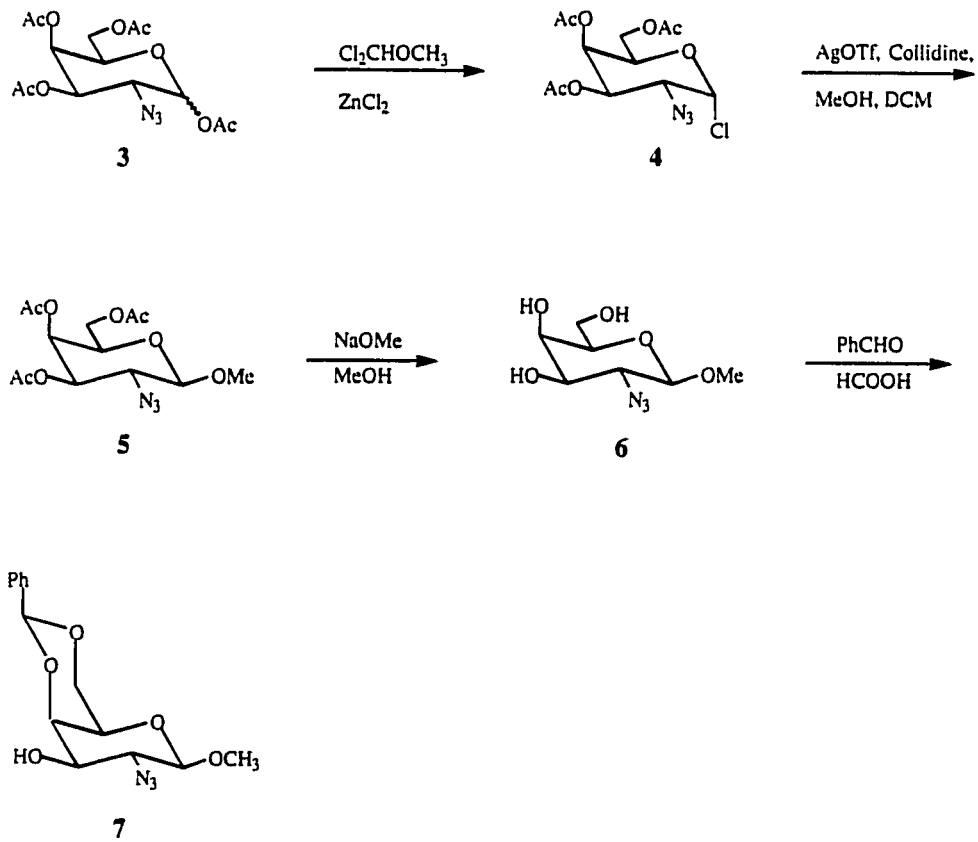

Fig 38. Synthesis of the glycosyl acceptor **7**.

or subsequent glycosylation reactions. The 2-azido-2-deoxy-galactose derivatives were selected as the most flexible way to carry a latent amino group and preserve potential reactivity at the anomeric centre.

The glycosyl acceptor was synthesized (Fig 38) using the commercially available tetraacetate **3** by treatment with dichloromethyl methyl ether[89] at reflux to give the glycosyl chloride in 92% yield. Silver triflate was used to promote the formation of the methyl 2-azido-2-deoxy-galactoside **5** in 80% yield, using collidine as the acid scavenger. Deprotection using sodium methoxide followed by the formation of the 4,6 benzylidene acetal in benzaldehyde and formic acid gave the methyl 2-azido-2-deoxy-4,6-*O*-benzylidene galactoside **7** in 89% yield, leaving the hydroxyl group on C-3 as the only OH available for glycosylation reactions.

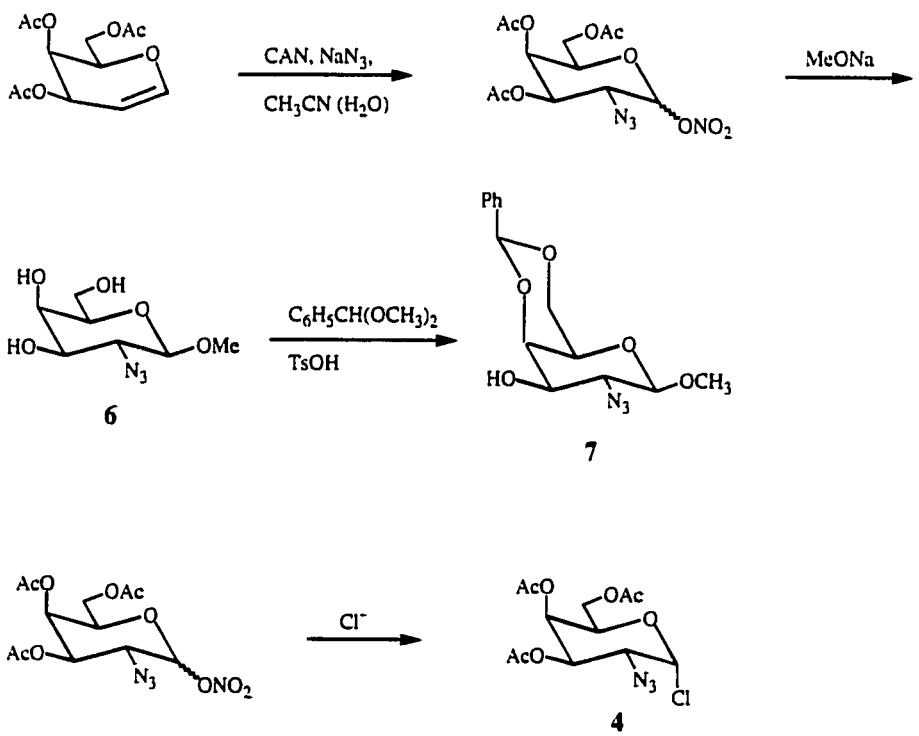

Fig 39. Alternative synthetic route for the formation of **7**.

Paulsen and Paal[90] have synthesized **7** using Lemieux's azidonitration method[91,92] (Fig 39) by converting 3,4,6-tri-*O*-acetyl-2-azido-2-deoxy galacto-pyranosyl nitrate to the deprotected methyl 2-azido-2-deoxy galactoside **6** in sodium methoxide. Subsequent protection with dimethoxytoluene and *p*-toluenesulfonic acid gives the desired glycosyl acceptor **7**. The triacetyl chloride **4** can also be synthesized from the galactopyranosyl nitrate using halide displacement[92].

4.3.2 Abe-GalNAc disaccharide

Abequose was synthesized according to a combination of the methods reported by Siewert and Westphal[93,94] and Baer and Astles[95]. This approach develops a 3,4-epoxide via the use of a 4-*O*-tosylate leaving group and leads to a 6-*O*-tosyl 3,4-epoxide that can be reduced to give a 3,6-dideoxy-D-*xylo*hexopyranoside in a single reaction (Fig 40). Methyl α-D-glucopyranoside **8** was first treated with benzaldehyde and zinc chloride to form the acetal, methyl 4,6-*O*-benzylidene glucopyranoside **9** (69%). Benzoylation with benzoyl chloride in pyridine gave the 2,3-dibenzoate **10** (96%). Acid hydrolysis of **10** in 80% acetic acid removes the benzylidene acetal to give **11** in 90% yield. The toluenesulfonyl groups were then introduced to the 4 and 6 hydroxy groups using toluenesulfonyl chloride in pyridine and dichloromethane with a catalytic amount of 4-dimethylaminopyridine (DMAP) to give the 2,3-dibenzoyl-4,6-*O*-ditosylate, **12** in 65%. Without DMAP, as reported in the original reference, the reaction takes days to complete as compared to hours.

Transesterification with sodium methoxide removes the benzoates and initiates an intra-molecular attack at the 4-position by a sugar alkoxide to give the 3,4

epoxide **13** in 54% yield. Super hydride was then used to reductively open the epoxide and reduce the 6-*O*-tosylate in a one pot reaction to give the methyl abequoside **14** in 88% yield.

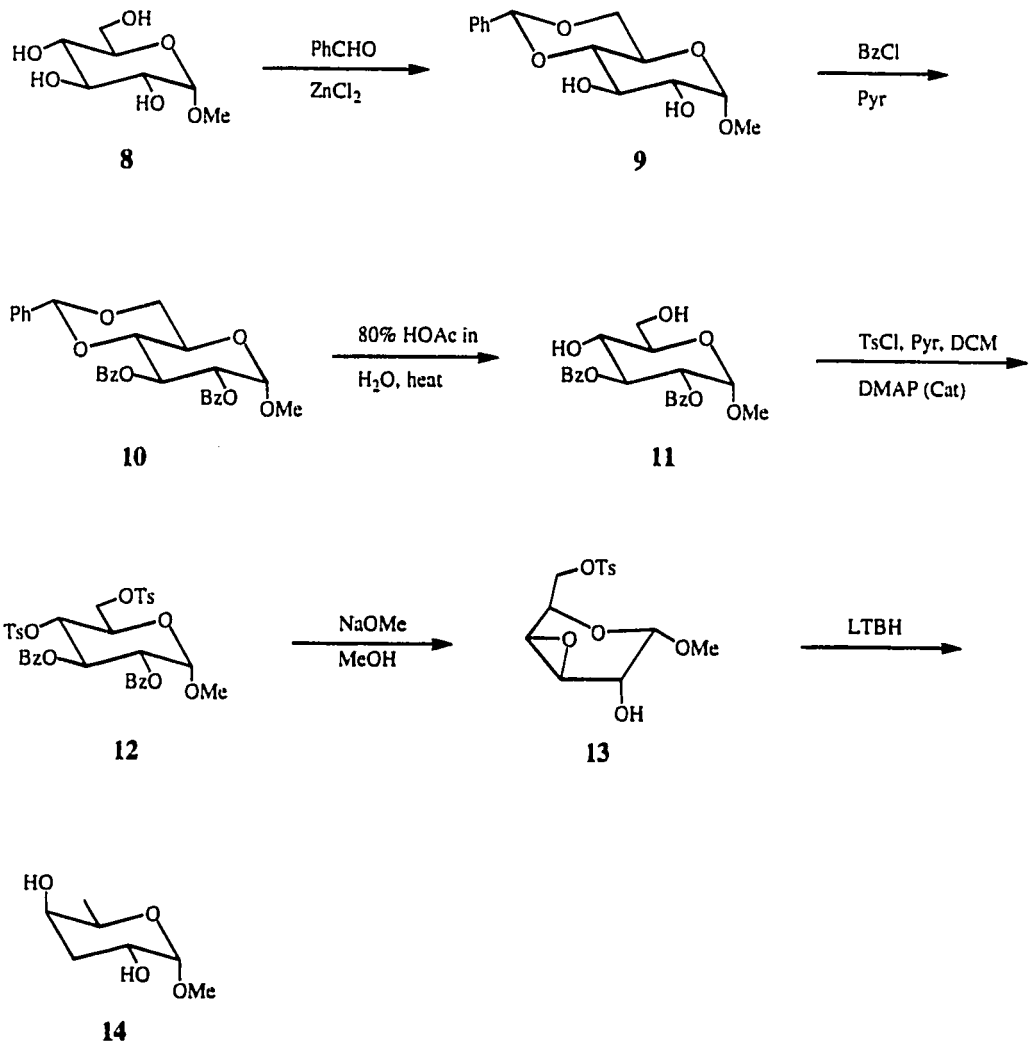

Fig 40. Synthesis of methyl 3,6-dideoxy-α-D-*xylo*hexopyranoside.

Several potential glycosyl donors were synthesized from glycoside **14**. Some gave the wrong product while others gave low yields.

The first donor was the 2,4-diacetyl abequosyl chloride **16**. Acetylation of **14** in acetic anhydride and pyridine followed by treatment with dichloromethyl methyl

ether[96] gave the glycosyl chloride **16** in 75% yield (Fig 41). The glycosyl halide **16** was used to glycosylate[97] the alcohol **7** to give **17** using silver triflate as the promoter and collidine as base (Fig 42). Unfortunately the yield was very low (10-20%).

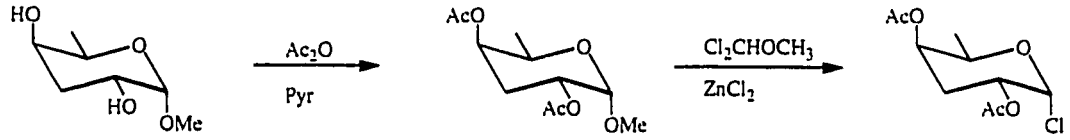

14 **15** **16**

Fig 41. Synthesis of the glycosyl chloride donor.

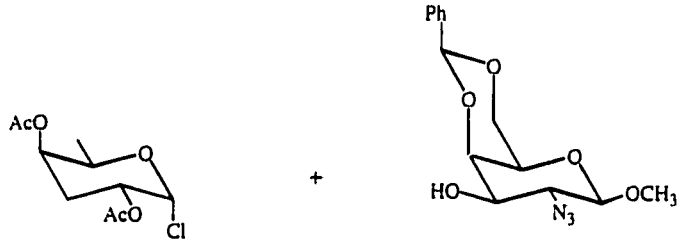

16 **7**

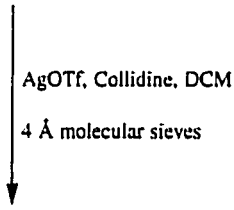

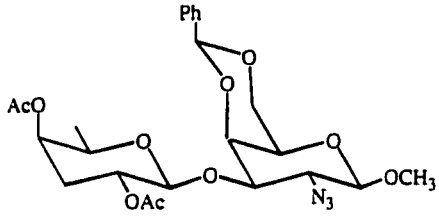

17

Fig 42. Coupling of **16** and **7**.

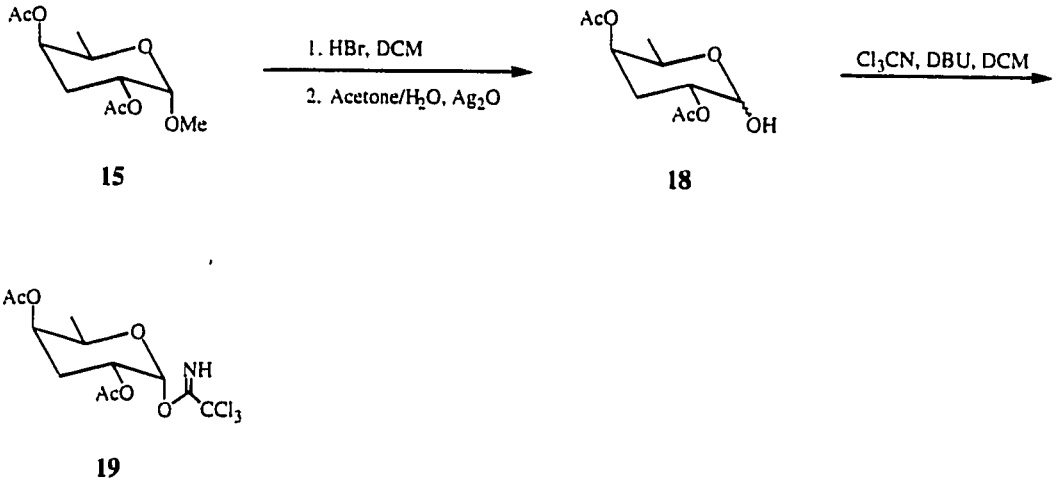

15 18 19

Fig 43. Synthesis of the imidate donor **19**.

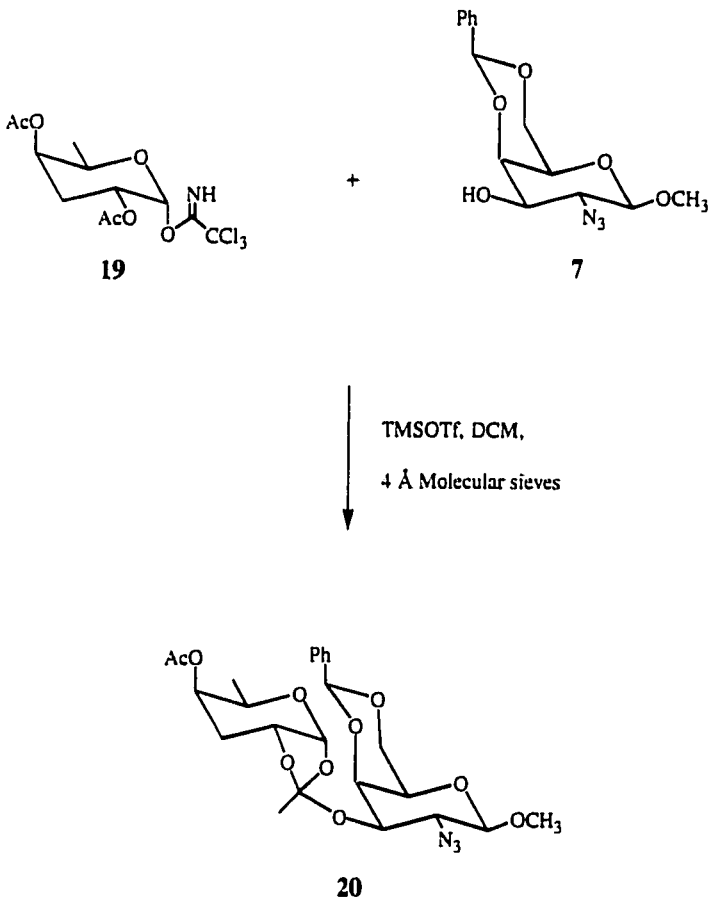

19 7 20

Fig 44. Formation of the orthoester.

An imidate donor was synthesized next using Schmidt's method[98] (Fig 43). The methyl diacetyl abequoside, **15** was first converted to the hemiacetal **18** (96%) by the formation of glycosyl bromide with HBr (33% v/v in acetic acid) in dichloromethane, followed by hydrolysis in wet acetone in the presence of a base, silver oxide, to neutralize any acid. The reaction of **18** with trichloroacetonitrile and DBU in dichloromethane formed the imidate in 65% yield after chromatography. Coupling of imidate **19** with **7** using TMS triflate as the promoter gave the orthoester **20** in 79% yield (Fig 44). The structure of the orthoester was determined using ^{1}H NMR δ 5.38 (d, 1H, $J_{1',2'}$ 3.4 Hz, H-1') 1.44 (s, 3H, $C\underline{H}_3CO_3$).

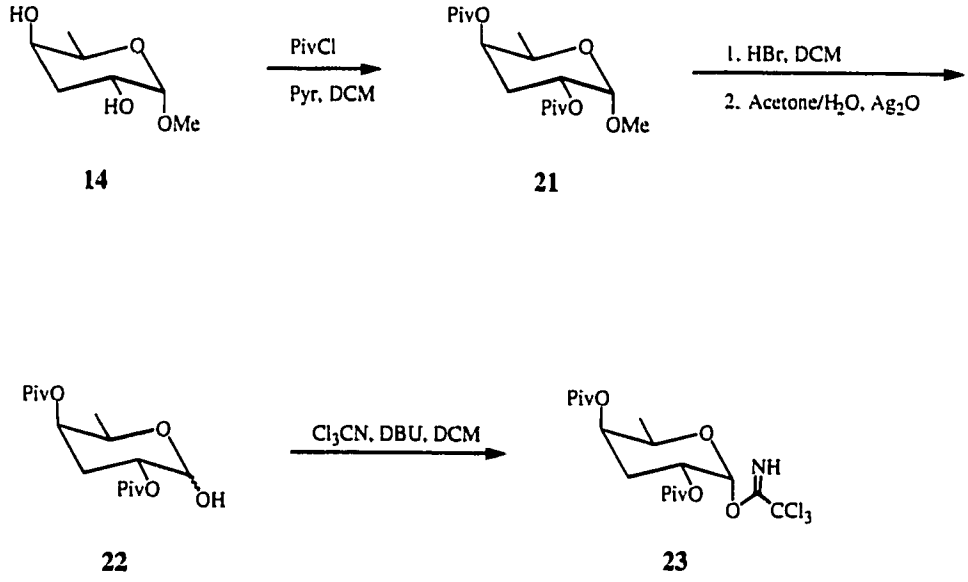

14 **21** **22** **23**

Fig 45. Synthesis of the imidate **23**.

The same synthetic route was attempted again, using pivaloates as the protecting group for the glycosyl donor (Fig 45). Since steric bulk about the quaternary carbon on the pivaloate discourages attack by the acceptor, orthoester formation should be prevented. Methyl abequoside **14** was protected in high yield

using pivaloyl chloride in a mixture of pyridine and dichloromethane. The synthetic route to the dipivalyol hemiacetal **22** and the trichloroacetimidate **23** were similar to those described for **18** and **19**.

Once again the glycosylation was disappointing. The reaction between **23** and **7** gave a low yield (27%) of the desired disaccharide, accompanied by several decomposition and side products (Fig 46).

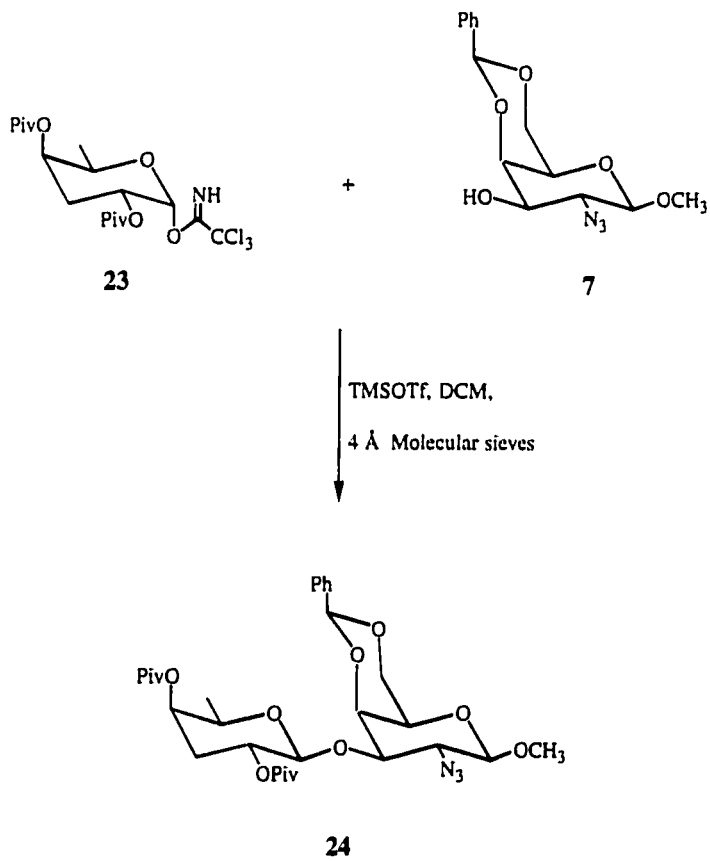

Fig 46. Synthesis of the disaccharide **24**.

A thiol donor was synthesized next (Fig 47) via the acetylation of the hemiacetal **22** to give 1-*O*-acetyl-2,4-di-*O*-pivaloyl-*xylo*-hexopyranose **25** in quantitative yield. Activation with boron trifluoride etherate in the presence of

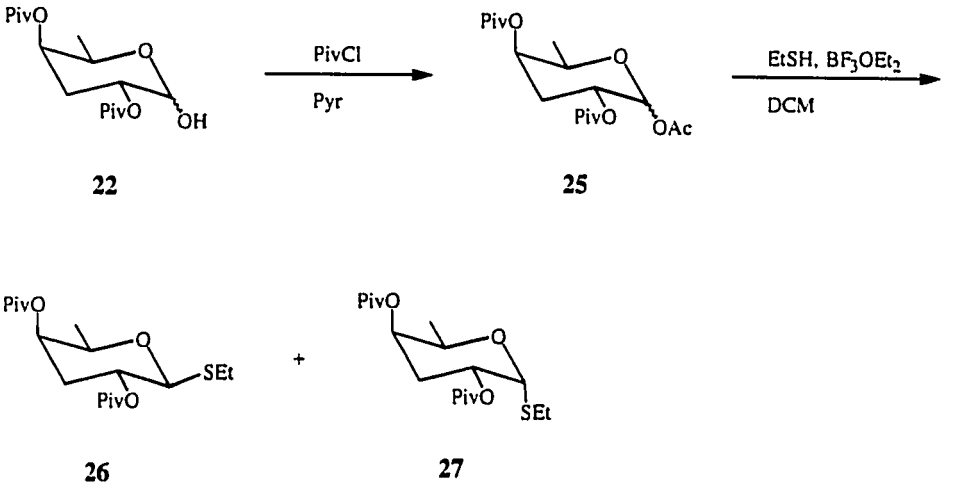

Fig 47. Formation of the abequose thioglycoside protected with pivaloates.

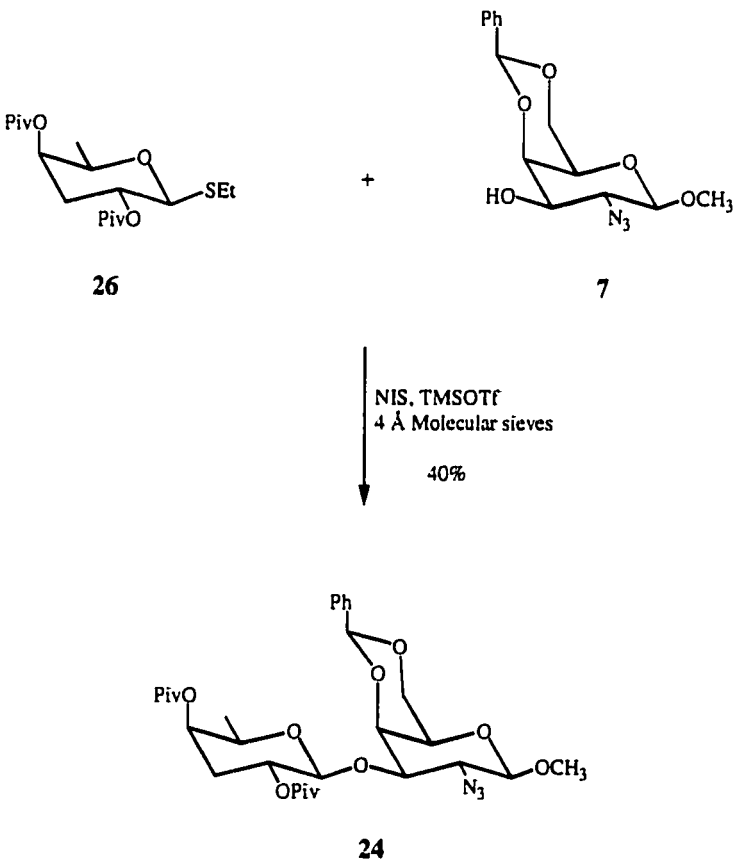

Fig 48. Coupling of **26** with **7**.

ethanethiol gave the thiol donor **26** (41%, ^{1}H, δ 4.45, $J_{1,2}$ 9.9 Hz for H-1) and its α anomer **27** (38%, ^{1}H, δ 5.54, $J_{1,2}$ 5.2 Hz for H-1). The coupling reaction (Fig 48) of **26** and **7** with NIS and TMS triflate gave a major product **24**. The yield however was again low (40%).

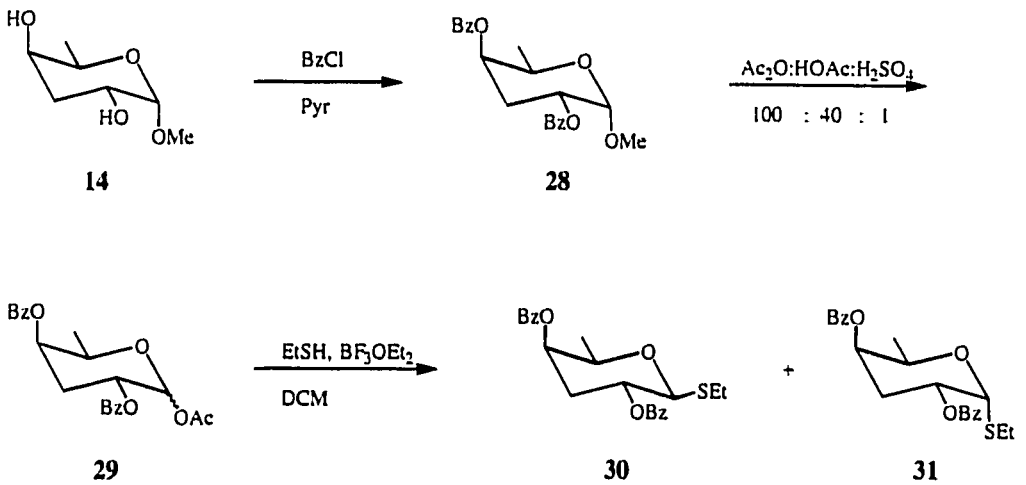

14 **28** **29** **30** **31**

Fig 49. Formation of benzoylated thioethyl glycoside.

A benzoate protecting group[99] was the next choice, which turned out to be the best glycosyl donor (Fig 49). Methyl glycoside **14** was treated with benzoyl chloride and pyridine to give the methyl dibenzoyl abequoside **28** (87%). An acetolysis mixture of acetic anhydride, acetic acid and sulfuric acid was used to convert the methyl glycoside to the glycosyl acetates in 94% yield. The thiol group was then introduced to the anomeric centre of the acetates **29** by activation with boron trifluoride etherate in the presence of ethanethiol to give the 2,4-dibenzoyl thiol donor **30** (43%) and the α-anomer **31**. The coupling reaction of **30** and **7** was performed as described for **26** (Fig 50), to give **32** in 78% yield.

The benzoates of disaccharide **32** were removed by transesterification using

sodium methoxide in methanol to give **33** (86%) over 4 days. The removal of the benzylidene acetal and reduction of the azide were performed in one step by hydrogenolysis in ethanol using Pd-$(OH)_2$ as the catalyst. The free amine was immediately converted to the acetamido group, using acetic anhydride in methanol to yield the final disaccharide **2** (88%).

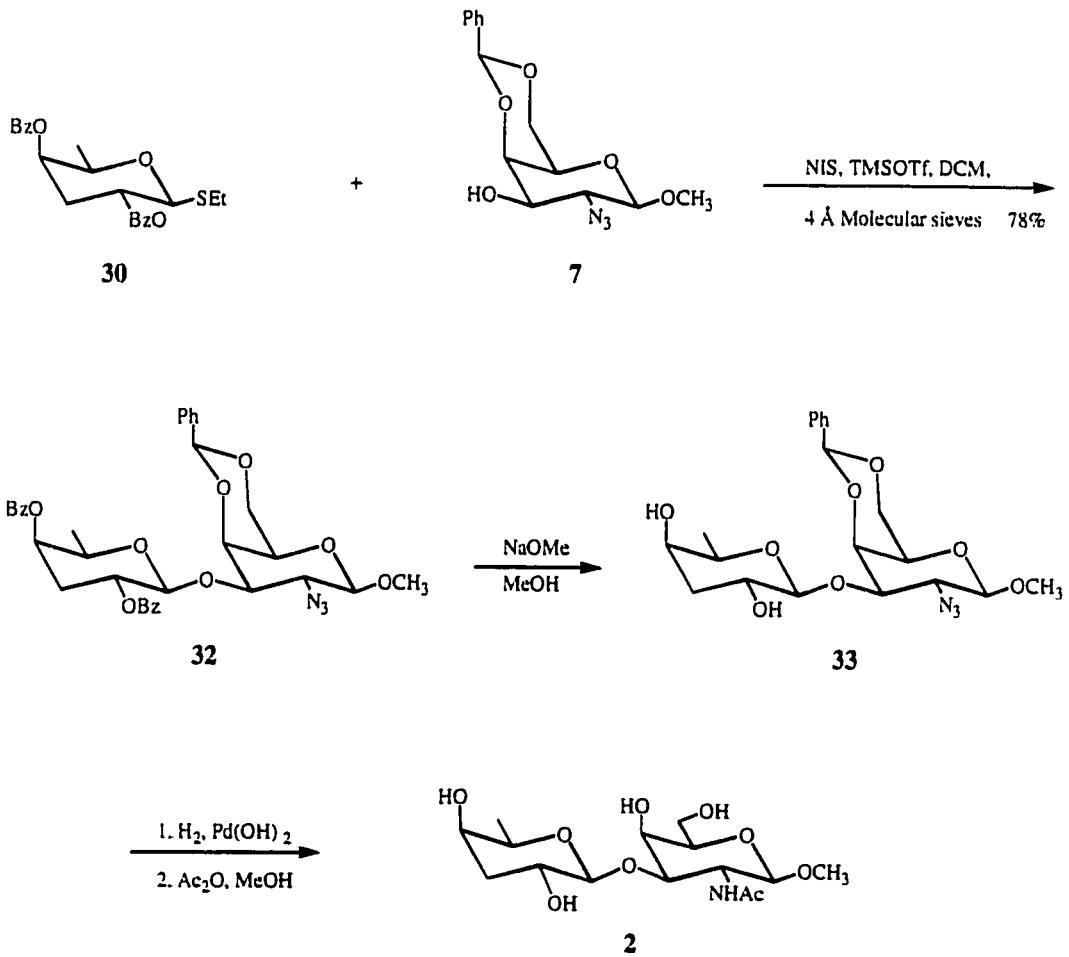

Fig 50. Synthesis of the desired disaccharide **2**.

4.3.3 Par-GalNAc disaccharide

The synthesis of paratose was performed according to Bundle[100] (Fig 51). The

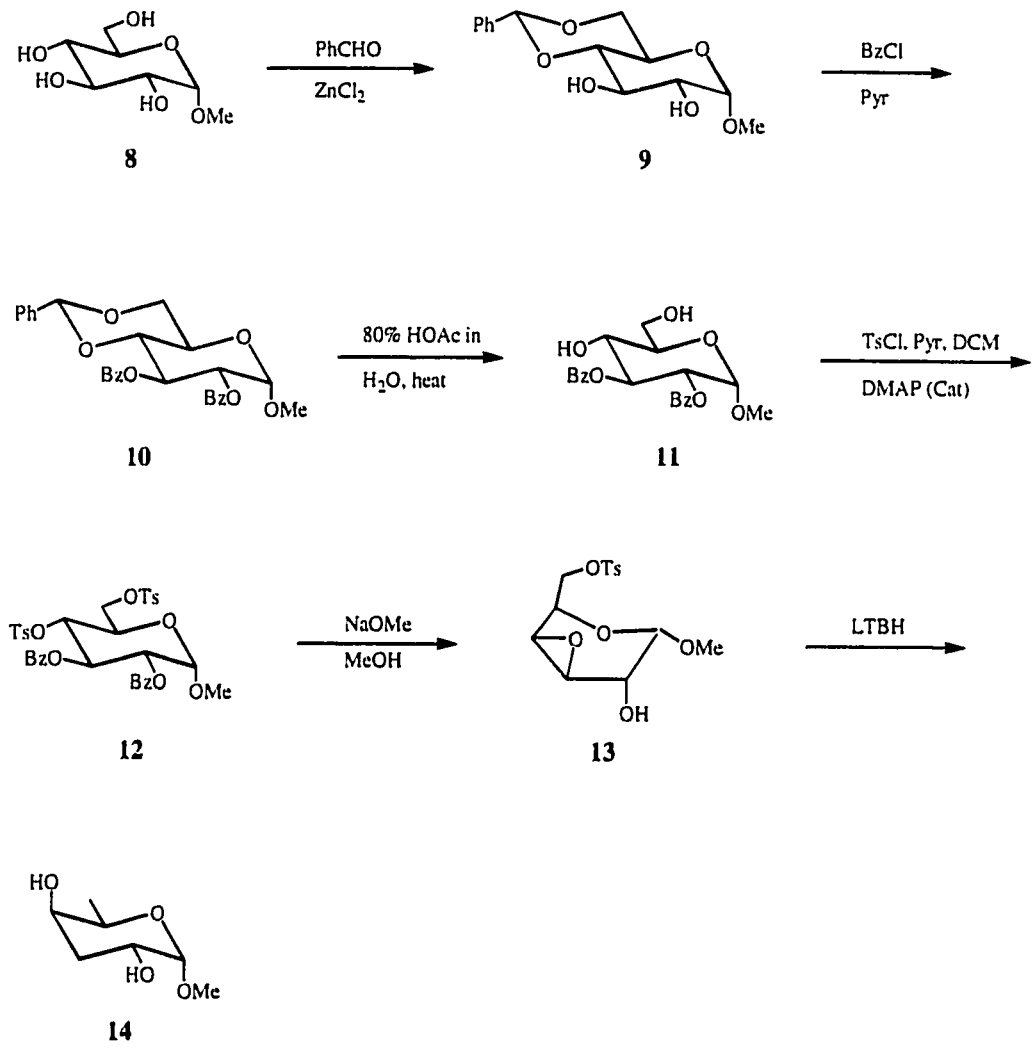

Fig 51. Synthesis of methyl paratoside.

commercially available methyl β-D-glucopyranoside **34** (Glycon Biochemicals, Germany) was protected as its benzylidene acetal by reaction with benzaldehyde to give **35** in 95% yield. Inversion of configuration using a powerful leaving group that also gives highly crystalline intermediates was utilized in the synthesis of **38**. The chlorosulfate **36** was formed using sulphuryl chloride in the presence of pyridine at low temperature. Tetraethylammonium bromide was then introduced to selectively displace the 3-*O*-chlorosulphate to give the 3-bromo-3-deoxy-β-D-allopyranoside **37**.

Potassium iodide was used to remove the 2-chlorosulfate to give **38**. The 3 steps from **35** to **38** were carried out in 1 day without purification to give an overall yield of 57%.

Hydrogenation, catalyzed by 5% Pd/C, reduced the bromide **38** to the 4,6-*O*-benzylidene-3-deoxy-β-D-*ribo*-hexopyranoside **39** in 93% yield after crystallization. NBS was then used to coordinate the free radical ring opening of the benzylidene in carbon tetrachloride to give the 6-bromo derivative **40** (63%), followed by hydrogenation to give the final product, methyl 4-benzoyl paratoside **41** (87%).

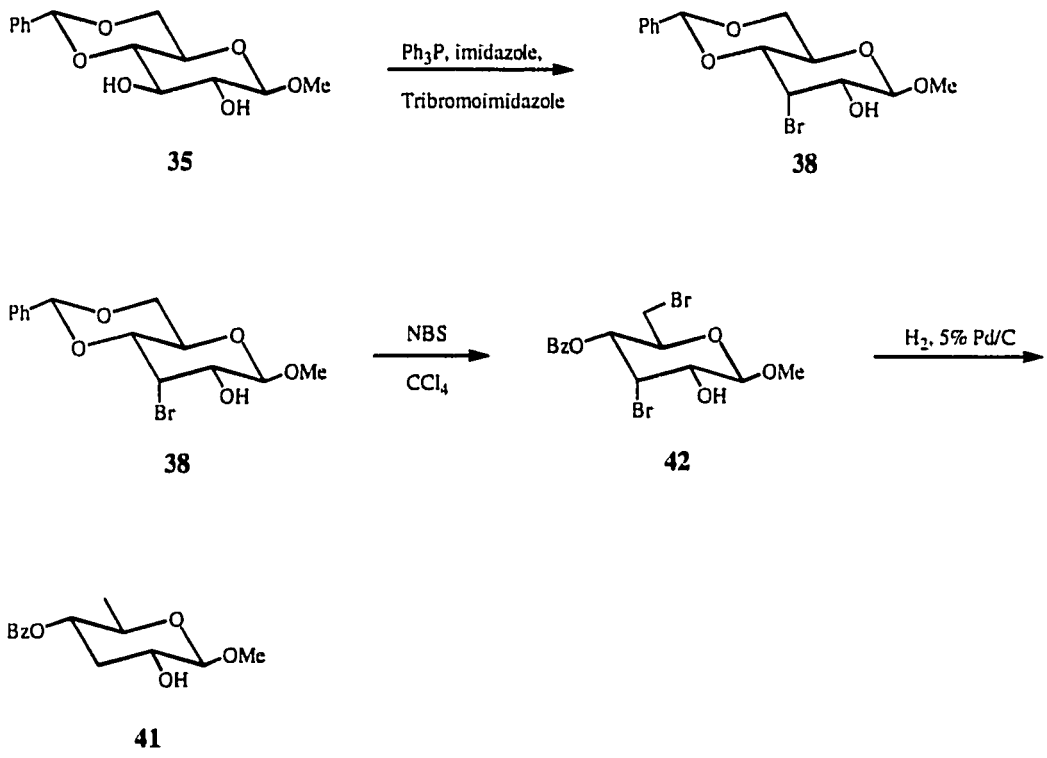

Fig 52. Short cut to the synthesis of **38** and **41**.

Two short cuts for the synthesis of **41** have been developed (Fig 52). One of them is to synthesize **38** directly from **35** using triphenylphosphine,

tribromoimidazole, and imidazole in toluene[101]. The drawback to this procedure is a very tedious workup and the chromatography is laborious and the product not easily cleaned up. By comparison, the 3 step reaction discussed above gives better yields in a shorter time.

The second short cut is to synthesize the dibromo derivative **42** from **38**[100], followed by hydrogenation to give **41**. However, low yields (~40%) result from the benzylidene ring opening with NBS and make it unattractive, even with the elimination of a hydrogenation step.

Synthesis of a 3,6-dideoxy-*ribo*-hexose glycosyl donor (Fig 53) started with pivaloate as the participating group at C-2 of paratose in order to avoid any formation of orthoesters. The pivaloyl group was introduced to **41** according to Becker and Galili[102], using pivaloyl chloride and pyridine in dichloromethane to give **43** in almost quantitative yield (98%). The acylated methyl glycoside **43** was then treated with hydrogen bromide in dichloromethane to give the glycosyl bromide donor **44** (86%).

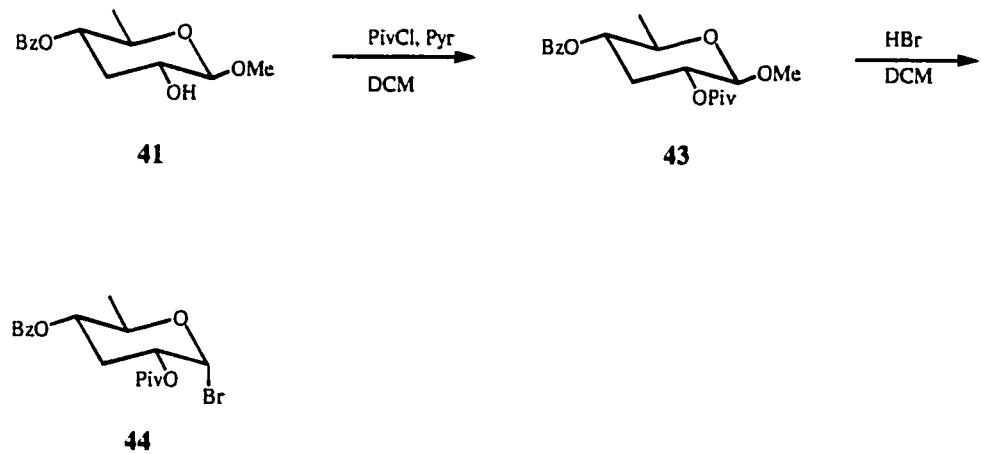

41 **43** **44**

Fig 53. Synthesis of the glycosyl donor **44**.

The glycosyl donor was coupled immediately to **7** (Fig 54), using silver triflate as an activator and tetramethylurea as the acid scavenger to give **45** in 69% yield. When collidine was used instead of tetramethylurea, very little disaccharide formation was observed (~5%).

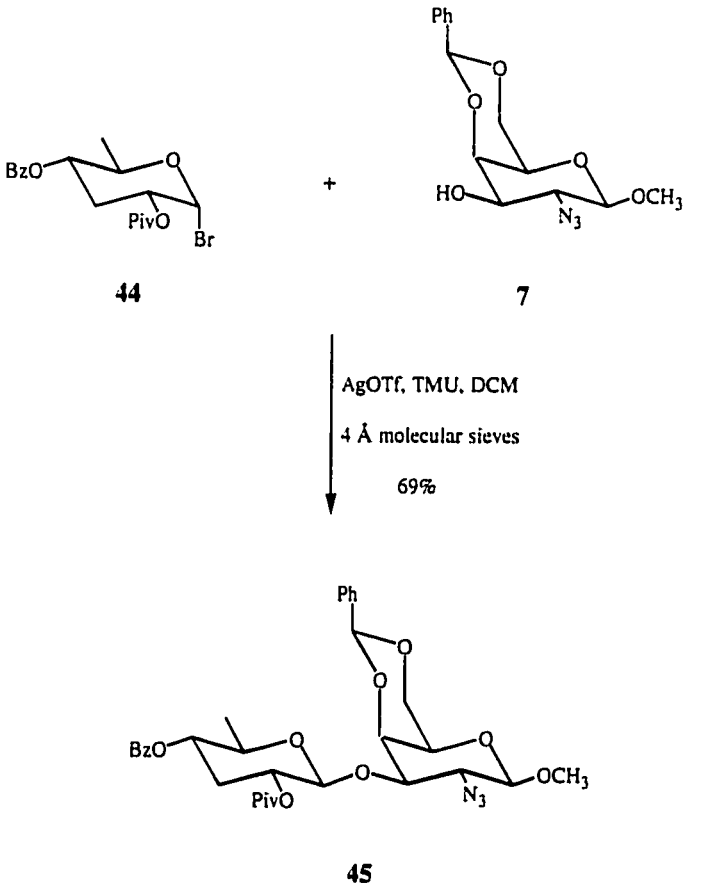

44 **7** **45**

Fig 54. Coupling reaction for **45**.

The ester groups of disaccharide **45** were transesterified by sodium methoxide in methanol to give **46** (86%). Hydrogenolysis was used to remove the benzylidene acetal and to convert the azide to the free amine. Finally acetylation in methanol gave the acetamido product **1** in 86% yield (Fig 55).

The β-configuration of the newly formed linkages of the two target

disaccharides are established by the homonuclear $^{3}J_{1,2}$ coupling constants ($J_{1',2'}$ 8.6 Hz) for **2** and ^{1}H ($J_{1',2'}$ 7.7 Hz) for **1** and by heteronuclear $^{1}J_{C,H}$ coupling constants ($J_{1H,13C}$ 161.5 Hz) for **2** and ($J_{1H,13C}$ 161.4 Hz) for **1**. One bond coupling constants are typically 170 Hz for α anomers and 160 Hz for β anomers[103].

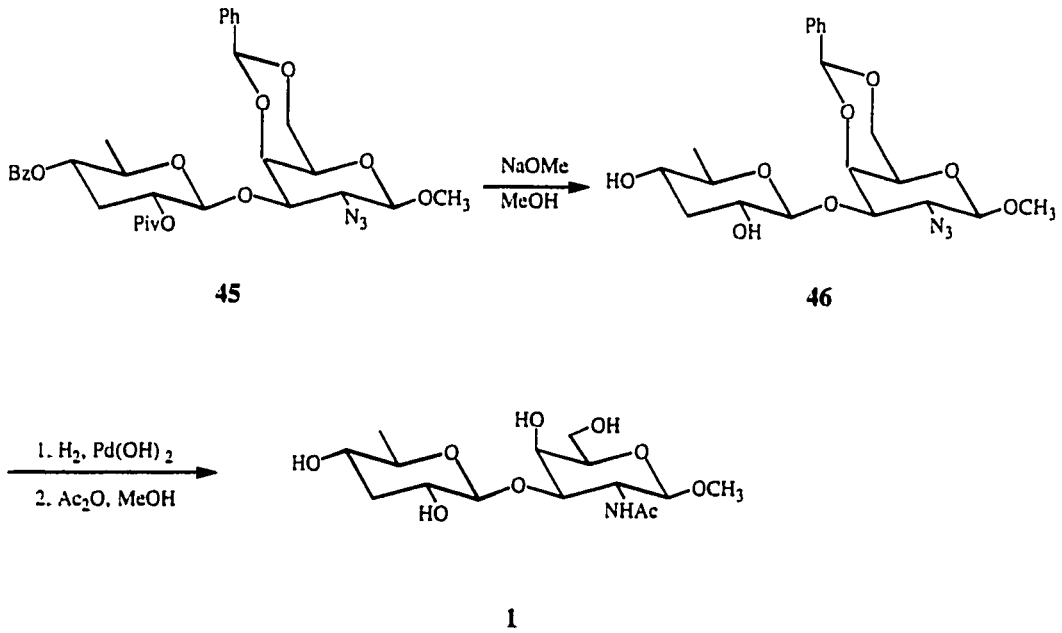

45 **46**

1

Fig 55. Deprotection of **1**.

Thus the NMR data confirm the structures of disaccharides **1** and **2** and these will be tested against the panel of monoclonal antibodies against the *Trichinella* TSL-1 antigens.

4.4 Experimental Procedure

4.4.1 General methods

Analytical TLC was performed on Silica Gel 60-F254 (E. Merck, Darmstadt), and compounds were detected by quenching of fluorescence and/or by charring with sulfuric acid. Column chromatography was performed on either Silica Gel 60 (E. Merck, Darmstadt), or Iatrobeads (Iatron Laboratories, Inc. Tokyo, Japan). Commercial reagents were used as supplied and chromatography solvents were distilled before used.

Solvents used for anhydrous reactions were dried according to literature procedures[104]. Dichloromethane and pyridine were distilled over calcium hydride; methanol was distilled from magnesium and a catalytic amount of iodine.

A Perkin Elmer 241 polarimeter was used to measure the optical rotations at 22 ± 2 °C. Microanalyses were carried out by a Carlo Erba 1108 analyzer by the analytical services group at this Department. All samples submitted to elemental analyses were vacuum dried over phosphorous pentoxide at 56 °C (refluxing acetone). Positive mode electrospray ionization mass spectra were performed on a Micromass ZabSpec Hybrid Sector-TOF mass spectrometer using either a 1% solution of acetic acid in 1:1 water : methanol, or 1:3 toluene : methanol as the liquid carrier and nitrogen as the spray pneumatic aid.

^{1}H NMR spectra were recorded at 360 MHz (Bruker WM-360 spectrometer), 500 MHz (Unity 500-Varian spectrometer) or 600 MHz (Inova 600-Varian spectrometer) as indicated. The residual solvent proton peak of $CDCl_3$ (δ 7.24) was used as the internal reference and for spectra recorded in D_2O the internal reference

was 1% acetone (v/v) (δ 2.225). ^{13}C NMR spectra were recorded at 75 MHz (Bruker AM-300) and referred to the ^{13}C resonance of the $CDCl_3$ solvent. Except where confirmed by two dimensional NMR, the assignment of carbon resonances are tentative and are based on related compounds in the literature.

GCOSY and HMQC experiments were performed on all disaccharides at either 500 or 600 MHz. A single transient per t_1 increment and a 1.2 s relaxation delay (experimental time 34 min.) were used for GCOSY experiments. Both gradients were rectangular in shape, applied in the z direction, of strength 0.6 G/cm and 10 ms duration, with gradient rise and fall times of 10 μs. The RF pulses were calibrated 90° pulses of 7.5 μs duration. Two-dimensional spectra were recorded nonspinning in absolute-value mode with a sweep width of 2500 Hz in both dimensions and 4K data points in F_2 (zero-filled to 8K) and 1K (zero-filled to 2K) data points in F_1, resulting in digital resolutions of 0.6 and 2.4 Hz/pt, respectively. Prior to Fourier transformation, the FIDs were multiplied by unshifted sine-bell squared functions of width $t_2/2$ and $t_1/2$ [105]. Proton coupled HMQC spectra were acquired with quadrature detection in F_1 and a total of $512t_1$ increments of 320 scans each were recorded for a spectral width in F_2 of 7800 Hz and 1500 Hz in F_1[106]. Data were processed to give after zero-filling a matrix (t_1 x t_2) of 512 x 8192 points, and following resolution enhancement as previously described, double transformation gave power spectra. Fixed delays of τ_1 = 3.4 ms and τ_2 = 1.7 ms were employed to select all multiplicities, and a recycle delay of ca. 1 s (~ one proton T_1) was used.

4.4.2 Synthesis

3, 4, 6-tri-O-acetyl-2-azido-2-deoxy-α-D-galactopyranosyl chloride (**4**)

An α/β mixture of tetra-*O*-acetyl 2-azido-2-deoxy D-galactopyranose (**3**) (Toronto Research Chemicals) (2.5 g, 6.7 mmol) was dissolved in dichloromethyl methyl ether (10 ml). Powdered, freshly fused $ZnCl_2$ (1 g), was added to the mixture and the solution was heated to 90 °C. After 30 minutes, the reaction was complete as judged by TLC. The mixture was diluted with dichloromethane (100 ml) and washed with saturated sodium bicarbonate (2x100 ml) and then water (100 ml). The solvent was removed after drying with $MgSO_4$ to give **4** (2.14 g, 91.5%), which was sufficiently pure to perform the next step without chromatography. R_f 0.57 (hexane : ethyl acetate, 2:1). $[\alpha]_D$ +162.2° (*c* 0.6, $CHCl_3$), Lit[92], +145° (*c* 1, $CHCl_3$). ^1H NMR (360 MHz, $CDCl_3$) δ 6.14 (d, 1H, $J_{1,2}$ 3.8 Hz, H-1), 5.48 (dd, 1H, $J_{3,4}$ 3.3 Hz, $J_{4,5}$ 1.4 Hz, H-4), 5.38 (dd, 1H, $J_{2,3}$ 10.9 Hz H-3), 4.49 (dt, 1H, $J_{5,6a} \sim J_{5,6b}$ 6.5 Hz, H-5), 4.16-4.04 (m, 3H, H2, H6a, H6b), 2.13, 2.03 (3x s, 9H, OAc).

^{13}C NMR (300 MHz, $CDCl_3$) δ 92.6 (C-1), 69.7 (C-5), 68.7 (C-3), 66.8 (C-4), 60.9 (C-6), 58.6 (C-2), 20.6 ($3xCH_3$, OAc).

ESMS (high res) m/z = 372.057650 $[M+Na]^+$ (Calcd 372.057448 for $C_{12}H_{16}N_3O_7NaCl$).

Methyl 3, 4, 6-tri-O-acetyl-2-azido-2-deoxy-β-D-galactopyranoside (**5**)

Methanol (5 ml), dichloromethane (50 ml), silver triflate (1.91, 7.45 mmol), and collidine (0.93 ml, 7.06 mmol) were stirred with 3 Å molecular sieves (1 g), for 10 minutes at -78 °C. The galactopyranosyl chloride **4** (1.89 g, 5.40 mmol) was

dissolved in dichloromethane (10 ml), and added dropwise to the cold solution. The mixture was left at room temperature overnight. Then it was filtered through celite, washed with 3% HCl (50 ml), saturated bicarbonate (50 ml), and water (50 ml). After solvent removal, the product was subjected to chromatography (hexane : ethyl acetate, 4:1) to give pure **5** (1.50 g, 80.4%). R_f 0.46 (hexane : ethyl acetate, 2:1). $[\alpha]_D$ -14° (*c* 0.4, $CHCl_3$,), Lit[90] -18° (*c* 0.3, $CHCl_3$). ^1H NMR (360 MHz, $CDCl_3$) δ 5.31 (dd, 1H, $J_{3,4}$ 3.3 Hz, $J_{4,5}$ 1.1 Hz, H-4), 4.77 (dd, 1H, $J_{2,3}$ 10.9 Hz, H-3), 4.25 (d, 1H, $J_{1,2}$ 8.0 Hz, H-1), 4.16 (dd, 1H, $J_{6a,6b}$ 11.2 Hz, $J_{5,6a}$ 6.7 Hz, H-6a), 4.09 (dd, 1H, $J_{5,6b}$ 6.7 Hz, H-6b), 3.83 (dt, 1H, H-5), 3.63 (dd, 1H, H-2), 3.58 (s, 3H, $OC\underline{H}_3$), 2.12, 2.02 (3x s, 9H, OAc)

^{13}C NMR (300 MHz, $CDCl_3$) δ 103.2 (C-1), 71.2 (C-5), 70.7 (C-3), 66.4 (C-4), 61.3 (C-6), 60.9 (C-2), 57.4 (CH_3), 20.6 ($3XCH_3$, OAc)

Anal. Calcd for $C_{13}H_{19}O_3N_3$ (345.35): C, 45.21; H, 5.56; N, 12.17. Found: C, 44.93; H, 5.58; N; 12.05.

Methyl 2-azido-2-deoxy-β-D-galactopyranoside (**6**)

The triacetate (**5**) (1.14 g, 3.30 mmol), was dissolved in dry methanol (38 ml) and a catalytic amount of sodium was added. The reaction was left at room temperature for 1 hr before Rexyn H^+ resin was added to neutralize the solution. The resin was filtered off, and the solvent was removed to give **6** in quantitative yield. R_f 0.54 (ethyl acetate : methanol, 9:1). $[\alpha]_D$ +30.6° (*c* 0.1, MeOH), Lit[90] -72°, (*c* 1, MeOH). ^1H NMR (360 MHz, $CDCl_3$) δ 4.39 (d, 1H, $J_{1,2}$ 8.2 Hz, H-1), 3.92 (m, 1H, $J_{4,5}$ 3.3 Hz, H-4), 3.79 (m, 2H, H-2, H-3), 3.69 (m, 2H, H-6a, H-6b), 3.62 (s, 3H,

$OC\underline{H}_3$), 3.49 (m, 1H, H-5).

The observed optical rotation was significantly different than those reported. However, the observed value was comparable to the value of a related compound, allyl 2-azido-2-deoxy-β-D-galactopyranoside, reported by Sabesan and Lemieux[92]. $[\alpha]_D$ +13.9°, (*c* 0.98, MeOH).

^{13}C NMR (300 MHz, $CDCl_3$) δ 103.4 (C-1), 76.0 (C-5), 72.5 (C-3), 68.8 (C-4), 64.1 (C-2), 61.8 (C-6), 58.0 (CH_3).

ESMS (high res) m/z = 242.075700 (Calcd 242.075290 for $C_7H_{13}N_3O_5Na$).

Methyl 2-azido-4,6-O-benzylidene-2-deoxy-β-D-galactopyranoside (**7**)

Methyl glycoside **6** (100 mg, 0.46 mmol) was suspended in benzaldehyde (5 ml) and formic acid (1.3 ml) was added dropwise. The reaction was left at room temperature for 1 hour before it was neutralized with triethylamine. Evaporation of solvent followed by chromatography (toluene : ethyl acetate, 3:1) gave **7** (125 mg, 89.2%). R_f 0.44 (toluene : ethyl acetate, 1:1). $[\alpha]_D$ -9.1° (*c* 0.5, MeOH), Lit[90] -14° (*c* 0.1, MeOH). ^1H NMR (360 MHz, $CDCl_3$) δ 7.55-7.31 (m, 5H, aromatic), 5.56 (s, 1H, PhC<u>H</u>), 4.35 (dd, 1H, $J_{5,6a}$ 1.5 Hz, $J_{6a,6b}$ 12.5 Hz, H-6a), 4.19 (d, 1H, $J_{1,2}$ 7.8 Hz, H-1), 4.17 (m, 1H, H-4), 4.07 (dd, 1H, $J_{5,6b}$ 1.9 Hz, H-6b) 3.58 (m, 5H, H-2, H-3, $OC\underline{H}_3$), 3.44 (q, 1H, $J_{4,5}$ 1.5 Hz, H-5).

^{13}C NMR (300 MHz, $CDCl_3$) δ 103.02 (C-1), 101.56 (Ph<u>C</u>H), 74.63 (C-3), 71.76 (C-4), 69.09 (C-6), 66.64 (C-5), 64.14 (C-2), 57.20 (CH_3).

Anal. Calcd for $C_{14}H_{17}O_5N_3$ (307.34): C, 54.70; H, 5.59; N, 13.67. Found: C, 54.75; H, 5.55; N, 13.52.

*Methyl 2, 4-di-O-benzoyl-3,6-dideoxy-α-D-*xylo*-hexopyranoside* (**28**)

Methyl abequoside **14** (300 mg, 1.85 mmol) was dissolved in pyridine (10 ml) and cooled to 0 °C. A solution of benzoyl chloride (1 ml, 8.61 mmol) in pyridine (3 ml) was added dropwise to the stirred solution and the reaction mixture was allowed to warm up to room temperature during 2 hours. The solution was diluted with dichloromethane (50 ml), washed with ice-cold 10% hydrochloric acid (50 ml), water (50 ml), and dried over $MgSO_4$. Removal of solvent gave a syrup that was chromatographed on silica gel (hexane : ethyl acetate, 6:1) to give pure **28** (594 mg, 86.7%). R_f 0.54 (hexane : ethyl acetate, 4:1). $[\alpha]_D$ +130.4° (*c* 1.7, $CHCl_3$). ^1H NMR (360 MHz, $CDCl_3$) δ 8.20-7.39 (m, 10H, aromatic), 5.38 (ddd, 1H, $J_{1,2}$ 3.4 Hz, $J_{2,3a}$ 12.4 Hz, $J_{2,3e}$ 5.0 Hz, H-2), 5.31 (m, 1H, H-4), 5.05 (d, 1H, H-1), 4.18 (dq, 1H, $J_{4,5}$ 1.4 Hz, $J_{5,6}$ 6.6 Hz, H-5), 3.47 (s, 3H, $OC\underline{H}_3$), 2.42 (dt, 1H, $J_{3a,3e}$ 13.4 Hz, $J_{3a,4}$ 3.1 Hz, H-3a), 2.26 (dt, 1H, $J_{3e,4}$ 3.9 Hz, H-3e), 1.22 (d, 3H, H-6).

^{13}C NMR (300 MHz, $CDCl_3$) δ 166.11, 166.06 (C=O), 97.05 (C-1), 71.43 (C-4), 67.41 (C-2), 64.91 (C-5), 55.43 ($O\underline{C}H_3$), 28.86 (C-3), 16.41 (C-6).

Anal. Calcd for $C_{21}H_{22}O_6$ (370.43): C, 68.09; H, 6.00. Found: C, 68.02; H, 6.08.

*1-O-acetyl 2-4-di-O-benzoyl-3,6-dideoxy-α/β-D-*xylo*-hexopyranose* (**29**)

The benzoylated glycoside **28** (130 mg, 0.35 mmol) was dissolved in Ac_2O : HOAc : H_2SO_4-100:40:1 (v/v 10 ml) mixture and stirred for 30 minutes at room temperature. It was then poured slowly into a 10% K_2CO_3 (30 ml) solution with stirring. After 30 minutes, the aqueous mixture was extracted with dichloromethane (3x50 ml). The combined organic layers were dried over $MgSO_4$ and evaporated to

give a 1:1 α/β anomeric mixture (116 mg, 83%). ^{1}H NMR (360 MHz, $CDCl_3$) δ 6.47 (d, 1H, $J_{1,2}$ 3.5 Hz, H-1α), 5.97 (d, 1H, $J_{1,2}$ 8.3 Hz, H-1β), 1.29 (d, 3H, $J_{5,6}$ 6.4 Hz, H-6β), 1.22 (d, 3H, $J_{5,6}$ 6.6 Hz, H-6α).

ESMS (high res) m/z = 421.126180 (Calcd 421.126323 for $C_{22}H_{22}O_7Na$).

Ethyl 2, 4-di-O-benzoyl-3,6-dideoxy-1-thio-β-D-xylo-*hexopyranoside* (**30**)

The α/β mixture of 1-*O*-acetyl-2,4-di-*O*-benzyoyl glycoside **29** (100 mg, 0.25 mmol) mixed with EtSH (43 μl, 0.57 mmol) and 4 Å molecular sieves (1 g) in dichloromethane (10 ml) was stirred for 10 minutes at -78 °C. Boron trifluoride etherate (270 μl, 2.2 mmol) was added dropwise at which point the reaction was allowed to warm to room temperature, and the mixture was stirred for another hour. The reaction was terminated by the careful addition of NH_3 (0.5 ml). The concentrated syrup was chromatographed (hexane : ethyl acetate, 4:1) to give the desired β-anomer **30** (43 mg, 43%). R_f 0.72 (hexane : ethyl acetate, 4:1). $[\alpha]_D$ +14.3° (*c* 7.2, $CHCl_3$). ^{1}H NMR (360 MHz, $CDCl_3$) δ 8.20-7.39 (m, 10H, aromatic), 5.40-5.26 (m, 2H, H-2, H-4), 4.71 (d, 1H, $J_{1,2}$ 9.9 Hz, H-1), 3.92 (dq, 1H, $J_{4,5}$ 1.2 Hz, $J_{5,6}$ 6.4 Hz, H-5), 2.85-2.70 (m, 2H, $SC\underline{H}_2CH_3$), 2.64 (ddd, 1H, $J_{2,3e}$ 4.9 Hz, $J_{3a,3e}$ 13.9 Hz, $J_{3e,4}$ 3.2 Hz, H-3e), 2.02 (ddd, 1H, $J_{2,3a}$ 12.6 Hz, $J_{3a,4}$ 3.1 Hz, H-3a), 1.29 (m, 6H, H-6, $SCH_2C\underline{H}_3$).

^{13}C NMR (300 MHz, $CDCl_3$) δ 165.95, 165.36 (C=O), 85.14 (C-1), 75.70 (C-4), 70.70 (C-2), 66.82 (C-5), 35.10 (C-3), 23.83 ($S\underline{C}H_2CH_3$), 16.99 (C-6), 14.98 ($SCH_2\underline{C}H_3$).

ESMS (high res) m/z = 423.12405 $[M+Na]^+$ (Calcd 423.124216 for $C_{22}H_{24}O_5NaS$).

*Methyl 2-azido-3-O-(2,4-di-O-benzoyl-3,6-dideoxy-β-D-*xylo*-hexopyranosyl)-4,6-benzylidene-2-deoxy-β-D-galactopyranoside* (**32**)

The thioglycoside **30** (100 mg, 0.25 mmol), the selectively protected azido sugar glycoside **7** (51 mg, 0.17 mmol), *N*-iodosuccinimide (67 mg, 0.30 mmol) and 4 Å molecular sieves (1 g) were dissolved in dichloromethane (10 ml), and stirred for 30 minutes in the dark at room temperature. The mixture was then cooled to -78 °C and TMS triflate (15 µl, 0.08 mmol) was added dropwise. The reaction was allowed to warm to room temperature and monitored by TLC. NH_3 (0.5 ml) was added to terminate the reaction. The concentrated syrup was chromatographed (hexane : ethyl acetate, 4:1) to give a white solid mass (84 mg, 78% yield). R_f 0.26 (hexane : ethyl acetate, 3:2). $[\alpha]_D$ +19.07° (*c* 1.5, $CHCl_3$). ^1H NMR (600 MHz, $CDCl_3$) δ 8.13-7.29 (m, 15H, aromatic), 5.54 (s, 1H, PhC<u>H</u>), 5.29-5.23 (m, 2H, H-2', H-4'), 5.01 (d, 1H, $J_{1',2'}$ 7.9 Hz, $J_{^1H,\ ^{13}C}$ 160.5 Hz, H-1'), 4.32 (m, 2H, H-4, H-6a), 4.22 (d, 1H, $J_{1,2}$ 8.1 Hz, $J_{^1H,\ ^{13}C}$ 158.5 Hz, H-1), 4.06 (dd, 1H, $J_{5,6b}$ 1.7 Hz, $J_{6a,6b}$ 12.5 Hz, H-6b), 3.96 (dq, 1H, $J_{4',5'}$ 1.5 Hz, $J_{5',6'}$ 6.4 Hz, H-5'), 3.79 (dd, 1H, $J_{2,3}$ 10.6 Hz, H-2), 3.58 (dd, 1H, $J_{3,4}$ 3.5 Hz, H-3), 3.56 (s, 3H, OC<u>H</u>3), 3.40 (m, 1H, H-5), 2.65 (ddd, 1H, $J_{2',3'e}$ 5.1 Hz, $J_{3'a,3'e}$ 14.1 Hz, $J_{3'e,4'}$ 3.3 Hz, H-3'e), 1.95 (ddd, 1H, $J_{2',3'a}$ 11.5 Hz, $J_{3'a,4'}$ 3.3 Hz, H-3'a), 1.27 (d, 3H, H-6').

^{13}C NMR (600 MHz, $CDCl_3$) δ 103.4 (C-1), 103.3 (C-1'), 100.7 (Ph<u>C</u>H), 77.5 (C-3), 75.1 (C-4), 72.6 (C-5'), 69.8 (C-4'), 68.8 (C-6), 68.2 (C-2'), 66.5 (C-5), 61.9 (C-2), 56.7 (O<u>C</u>H3), 32.9 (C-3'), 16.5 (C-6').

ESMS (high res) m/z = 668.221550 $[M+Na]^+$ (Calcd 668.222015 for $C_{34}H_{35}O_{10}N_3Na$).

*Methyl 2-azido-2-deoxy-3-O-(3,6-dideoxy-β-D-*xylo*-hexopyranosyl)-4,6-O-benzylidene-β-D-galactopyranoside* (**33**)

The protected disaccharide glycoside **32** (50 mg, 0.077 mmol) was dissolved in dry methanol (10 ml) and a catalytic amount of Na was added. The solution was left to stir at room temperature for 4 days and the solution was then neutralized with Rexyn H^+ resin. Solvent removal gave a syrup that was chromatographed on silica gel (hexane : ethyl acetate, 1:1) to give a clear product (26 mg, 86% yield). R_f 0.33 (ethyl acetate). $[\alpha]_D$ -7.5° (*c* 1, $CHCl_3$). ^1H NMR (600 MHz, $CDCl_3$) δ 7.53-7.30 (m, 5H, aromatic), 5.52 (s, 1H, PhC<u>H</u>), 4.45 (d, 1H, $J_{1',2'}$ 7.7 Hz, $J_{1H,\ 13C}$160.3 Hz, H-1'), 4.31 (dd, 1H, $J_{5,6a}$ 1.7 Hz, $J_{6a,6b}$ 12.3 Hz, H-6a), 4.25 (m, 1H, H-4), 4.22 (d, 1H, $J_{1,2}$ 7.9 Hz, $J_{1H,\ 13C}$ 158.8 Hz, H-1), 4.04 (dd, 1H, $J_{5,6b}$ 1.7 Hz, H-6b), 3.86 (dd, 1H, $J_{2,3}$ 10.6 Hz, H-2), 3.74 (ddd, 1H, $J_{2',3'e}$ 5.3 Hz, $J_{2',3'e}$ 11.9 Hz, H-2'), 3.65 (m, 2H, H-4', H-5'), 3.58 (s, 3H, OC<u>H</u>3), 3.55 (dd, 1H, $J_{3,4}$ 3.5 Hz, H-3), 3.40 (m, 1H, H-5), 2.28 (ddd, 1H, $J_{3'a,3'e}$ 13.7 Hz, $J_{3'e,4'}$ 2.9 Hz, H-3'e), 1.59 (ddd, 1H, $J_{3'a,4'}$ 2.9 Hz, H-3'a), 1.25 (d, 1H, $J_{5',6'}$ 6.4 Hz, H-6').

^{13}C NMR (600 MHz, $CDCl_3$) δ 106.9 (C-1'), 103.8 (C-1), 101.2 (Ph<u>C</u>H), 75.7 (C-3), 75.2 (C-4), 73.7 (C-5'), 68.7 (C-6), 68.6 (C-4'), 66.2 (C-5), 65.4 (C-2'), 61.8 (C-2), 57.0 (O<u>C</u>H3), 36.9 (C-3'), 15.1 (C-6').

ESMS (high res) m/z = 460.170420 $[M+Na]^+$ (Calcd 460.169585 for $C_{20}H_{27}N_3O_8Na$).

*Methyl 2-acetamido-2-deoxy-3-O-(3,6-dideoxy-β-D-*xylo*-hexopyranosyl)-β-D-galactopyranoside* (**2**)

The azido derivative **33** (27 mg, 0.062 mmol) was dissolved in ethanol (20

ml), then 20% $Pd(OH)_2$ (20 mg) was added. The suspension was stirred under a constant flow of H_2 at 1 atmosphere for 3 hours. After filtration and solvent removal, the residue was dissolved in methanol (5 ml) and acetic anhydride (2 ml) and stirred overnight before co-concentration with toluene. Chromatography on Iatrobeads (ethyl acetate : methanol, 9:1) and freeze drying gave **2** as a white solid product (19 mg, 88% yield). R_f 0.33 (ethyl acetate : methanol, 7:3). $[\alpha]_D$ -12.0° (*c* 1.2, D_2O). ^1H NMR (600 MHz, $CDCl_3$) δ 4.45 (d, 1H, $J_{1,2}$ 8.6 Hz, $J_{^1H,\ ^{13}C}$ 161.5 Hz, H-1), 4.42 (d, 1H, $J_{1',2'}$ 7.9 Hz, $J_{^1H,\ ^{13}C}$ 160.8 Hz, H-1'), 4.15 (m, 1H, H-4), 4.00 (dd, 1H, $J_{2,3}$ 11.0 Hz, H-2), 3.86 (dd, 1H, $J_{3,4}$ 3.3 Hz, H-3), 3.83 (dd, 1H, $J_{5,6a}$ 7.9 Hz, $J_{6a,6b}$ 11.7 Hz, H-6a), 3.80-3.74 (m, 3H, H-4', H-5', H-6b), 3.71 (dd, 1H, $J_{4,5}$ 4.2 Hz, H-5), 3.66 (ddd, 1H, $J_{2',3a'}$ 12.9 Hz, $J_{2',3'e}$ 5.1 Hz, H-2'), 3.52 (s, 3H, OC<u>H</u>3), 2.17 (ddd, 1H, $J_{3'a,3'e}$ 13.7 Hz, $J_{3'e,4'}$ 3.1 Hz, H-3'e), 2.01 (s, 3H, OAc), 1.69 (ddd, $J_{3'a,4}$ 3.1 Hz, H-3'a), 1.18 (d, $J_{5',6'}$ 6.41 Hz, H-6').

^{13}C NMR (600 MHz, $CDCl_3$) δ 107.7 (C-1'), 103.1 (C-1), 80.5 (C-3), 75.6 (C-5), 74.9 (C-5'), 69.3 (C-4), 69.0 (C-4'), 65.7 (C-2'), 62.0 (C-6), 57.8 (O<u>C</u>H_3), 51.9 (C-2), 37.4 (C-3'), 23.0 (OC(O)<u>C</u>H_3), 16.5 (C-6').

ESMS (high res) m/z 388.158550 $[M+Na]^+$, (Calcd 388.158352 for $C_{15}H_{27}NO_9Na$), 366.1755 $[M+H]^+$ ($C_{15}H_{27}NO_9$ requires m/z = 365.43).

*Methyl 4-O-benzoyl-3,6-dideoxy-2-O-pivaloyl-β-D-*ribo*-hexopyranoside* (**43**)

Methyl 4-*O*-benzoyl 3,6-dideoxy-β-D-*ribo*hexopyranoside **41** (1 g, 3.75 mmol) was dissolved in a mixture of dichloromethane (3 ml) dry pyridine (2.5 ml). The mixture was stirred under argon for 5 minutes at room temperature and pivaloyl

chloride (2.3 ml, 18.7 mmol) was added dropwise. After 2.5 hours, TLC showed that the starting material had been consumed. The solvent was evaporated under reduced pressure and the residue was dissolved in ether (100 ml). The solution was washed with 10% H_2SO_4 (50 ml), 10% $CuSO_4$ (50 ml), saturated $NaHCO_3$ (50 ml) and water (50 ml). The organic layer was dried over $MgSO_4$ and the solvent was removed under reduced pressure. The crude product was used without chromatography (1.47 g, 98%). R_f 0.61 (hexane : ethyl acetate, 6:1). $[\alpha]_D$ -41.69° (*c* 0.6, $CHCl_3$). ^1H NMR (360 MHz, $CDCl_3$) δ 8.15-7.35 (m, 5H, aromatic), 4.80 (m, 2H, H-2, H-4), 4.39 (d, 1H, $J_{1,2}$ 7.8 Hz, H-1), 3.70 (dq, 1H, $J_{4,5}$ 9.2 Hz, $J_{5,6}$ 6.1 Hz, H-5), 3.48 (s, 3H, $OC\underline{H}_3$), 2.57 (dt, 1H, $J_{2,3e} \sim J_{3e,4}$ 5.2 Hz, $J_{3a,3e}$ 11.8 Hz, H-3e), 1.65 (q, 1H, $J_{2,3a} \sim J_{3a,4}$ 11.8 Hz, H-3a), 1.28 (d, 3H, H-6), 1.15 (s, 9H, H-C($C\underline{H}_3$)$_3$). ^{13}C NMR (300 MHz, $CDCl_3$) δ 176.96, 165.32 (C=O), 133.25, 129.86, 129.61, 128.45 (aromatic), 103.49 (C-1), 73.58 (C-5), 71.69 (C-4), 68.60 (C-2), 56.70 ($O\underline{C}H_3$), 38.69 ($\underline{C}(CH_3)_3$), 33.45 (C-3), 27.02 ($C(\underline{C}H_3)_3$), 17.78 (C-6).

Anal. Calcd for $C_{19}H_{26}O_6$ (350.45): C, 65.11; H, 7.49. Found: C, 64.79; H, 7.58.

4-O-Benzoyl-3,6-dideoxy-2-O-pivaloyl-β-D-ribo-*hexopyranosyl bromide* (**44**)

The pivaloylate **43** (100 mg, 0.29 mmol) was dissolved in dichloromethane (20 ml) and cooled to 0 °C. A solution of HBr in HOAc (33% w/v) (2 ml) was added dropwise to the reaction before it was allowed to warm to room temperature. After 3 hours, the reaction was complete as judged by TLC. The reaction mixture was diluted with cold dichloromethane (50 ml) and washed with saturated $NaHCO_3$ (50 ml) and water (50 ml). The solvent was removed after drying with $MgSO_4$. The crude product

was left on the pump for 1 hour before using in the next step. R_f 0.62 (hexane : ethyl acetate, 6:1). ^{1}H NMR (360 MHz, $CDCl_3$) δ 8.10-7.10 (m, 5H, aromatic), 6.65 (d, 1H, $J_{1,2}$ 3.6 Hz, H-1), 4.84 (ddd, 1H, $J_{3a,4}$ 11.4 Hz, $J_{3e,4}$ 4.7 Hz, $J_{4,5}$ 9.9 Hz, H-4), 4.77 (ddd, 1H, $J_{2,3a}$ 12.0 Hz, $J_{2,3e}$ 4.6 Hz, H-2), 4.18 (dq, 1H, $J_{5,6}$ 6.2 Hz, H-5), 2.35 (ddd, 1H, $J_{3a,3e}$ 11.8 Hz, H-3e), 2.20 (q, 1H, H-3a), 1.29 (d, 3H, H-6), 1.19 (s, 9H, H-$C(C\underline{H}_3)_3$).

*Methyl 2-azido-3-O-(4-O-benzoyl-3,6-dideoxy-2-O-pivaloyl-β-D-*ribo*-hexopyranosyl) -4,6-O-benzylidene-2-deoxy-β-D-galactopyranoside* (**45**)

The selectively protected alcohol **7** (59 mg, 0.19 mmol), 4 Å molecular sieves (1 g), silver triflate (103 mg, 0.4 mmol), and tetramethylurea (240 μl, 2 mmol) were dissolved in dry dichloromethane (10 ml) and stirred for 30 minutes at -78 °C in the dark. The glycosyl bromide **44** (114 mg, 0.28 mmol), dissolved in dichloromethane (5 ml), was added dropwise to the solution containing the acceptor. The reaction was allowed to warm to room temperature and stirred overnight. After filtration through celite, the filtrate was washed with saturated sodium bicarbonate and the concentrated syrup was purified on a silica gel column (hexane : ethyl acetate, 5:1) to give pure disaccharide **45** (82 mg, 69%). R_f 0.61 (hexane : ethyl acetate, 3:2). $[\alpha]_D$ -6.8° (*c* 2.5, $CHCl_3$). ^{1}H NMR (600 MHz, $CDCl_3$) δ 7.98-7.29 (m, 5H, aromatic), 5.54 (s, 1H, PhC$\underline{H}$), 4.95 (d, 1H, $J_{1',2'}$ 7.7 Hz, $J_{1H,13C}$ 163.5 Hz, H-1'), 4.84 (m, 2H, H-2', H-4'), 4.32 (dd, 1H, $J_{5,6a}$ 1.5 Hz, $J_{6a,6b}$ 12.5 Hz, H-6a), 4.24 (d, 1H, $J_{1,2}$ 8.1 Hz, $J_{1H,13C}$ 159.0 Hz, H-1), 4.22 (m, 1H, H-4), 4.05 (dd, 1H, $J_{5,6b}$ 1.5 Hz, H-6b), 3.80 (dd, 1H, $J_{2,3}$ 10.4 Hz, H-2), 3.72 (dq, $J_{4',5'}$ 9.2 Hz, $J_{5',6'}$ 6.1 Hz, H-5'), 3.58 (s, 3H, OC$\underline{H}_3$), 3.55 (dd, 1H,

$J_{3,4}$ 3.5, H-3), 3.40 (m, 1H, H-5), 2.63 (dt, 1H, $J_{2',3'e} \sim J_{3'e,4'}$ 5.1 Hz, $J_{3'a,3'e}$ 11.7 Hz, H-3'e), 1.65 (q, 1H, H-3'a), 1.28 (d, 1H, H-6'), 1.17 (s, 9H, $HC(C\underline{H}_3)_3$).

^{13}C NMR (600 MHz, $CDCl_3$) δ 132.9, 129.4, 128.1, 125.9 (aromatic), 103.3 (C-1), 102.2 (C-1'), 100.5 (Ph$\underline{C}$H), 75.8 (C-3), 75.0 (C-4), 73.3 (C-5'), 71.1 (C-4'), 68.5 (C-2'), 68.4 (C-6), 65.6 (C-5), 61.9 (C-2), 56.7 ($O\underline{C}H_3$), 33.0 (C-3'), 17.4 (C-6).

Anal. Calcd for $C_{32}H_{39}N_3O_{10}$ (625.14): C, 61.42; H, 6.30; N, 6.72. Found: C, 61.40; H, 6.30; N, 6.54.

*Methyl 2-azido-4,6-O-benzylidene-2-deoxy-3-O-(3,6-dideoxy-β-D-*ribo*-hexopyranosyl)-β-D-galactopyranoside* (**46**)

The fully protected disaccharide glycoside **45** (50 mg, 0.08 mmol) was transesterified in a similar manner to that described for compound **32** to give the partial deprotected disaccharide **46** (30 mg, 86% yield). R_f 0.41 (ethyl acetate). $[\alpha]_D$ -1.74° (*c* 0.5, $CHCl_3$). ^1H NMR (600 MHz, $CDCl_3$) δ 7.60-7.28 (aromatic), 5.57 (s, 1H, PhC$\underline{H}$), 4.43 (d, 1H, $J_{1',2'}$ 7.33 Hz, $J_{1H,13C}$ 160.3 Hz, H-1'), 4.31 (dd, 1H, $J_{5,6a}$ 1.53 Hz, $J_{6a,6b}$ 12.36 Hz, H-6a), 4.24 (m, 1H, H-4), 4.23 (d, 1H, $J_{1,2}$ 7.94 Hz, $J_{1H,13C}$ 158.4 Hz, H-1), 4.05 (dd, 1H, $J_{5,6b}$ 1.58 Hz, H-6b), 3.85 (dd, 1H, $J_{2,3}$ 10.53 Hz, H-2), 3.58 (s, 1H, $OC\underline{H}_3$), 3.53 (dd, 1H, $J_{2,3}$ 10.53 Hz, $J_{3,4}$ 3.20 Hz, H-3), 3.52 (m, 1H, H-2'), 3.40 (d, 1H, $J_{5,6b}$ 1.07 Hz, H-6b), 3.30 (m, 2H, H-4', H-5'), 2.31 (dt, 1H, $J_{2',3'e} \sim J_{3'e,4'}$ 4.58 Hz, $J_{3'a,3'e}$ 11.75 Hz, H-3'e), 1.47 (q, 1H, H-3'a), 1.28 (d, 3H, $J_{5',6'}$ 5.65 Hz, H-6').

^{13}C NMR (600 MHz, $CDCl_3$) δ 128.8, 127.9, 126.2 (aromatic), 106.5 (C-1'), 103.1 (C-1), 101.2 (Ph$\underline{C}$H), 78.2 (C-3), 75.7 (C-5'), 75.2 (C-4), 70.1 (C-4'), 68.7 (C-6), 67.8 (C-2'), 66.1 (C-5), 61.6 (C-2), 56.6 (O$\underline{C}$H3), 37.8 (C-3'), 17.3 (C-6').

ESMS (high res) m/z = 460.169430 $[M+Na]^+$ (Calcd 460.169585 for $C_{20}H_{27}N_3O_8Na$).

*Methyl 2-acetamido-2-deoxy-3-O-(3,6-dideoxy-β-D-*ribo-*hexopyranosyl)-β-D-galactopyranoside* (**1**)

The procedure for the conversion of **46** to **1** was performed the same way as for **2**. The partially protected azido derivative **46** (21 mg, 0.048 mmol) was dissolved in ethanol (20 ml), then 20% $Pd(OH)_2$ (20 mg) was added. The suspension was stirred under a constant flow of H_2 at 1 atmosphere for 3 hours. After filtration and solvent removal, the residue was dissolved in methanol (5 ml) and acetic anhydride (2 ml) and stirred overnight before co-concentration with toluene. Chromatography using ethyl acetate : methanol, 9:1 on Iatrobeads gave **1** (15 mg, 86%). R_f 0.40 (ethyl acetate : methanol, 7:3). $[\alpha]_D$ -36.3° (*c* 0.5, D_2O). ^1H NMR (600 MHz, $CDCl_3$) δ4.44 (d, 1H, $J_{1,2}$ 8.4 Hz, $J_{1H,\ 13C}$ 161.1 Hz, H-1), 4.42 (d, 1H, $J_{1',2'}$ 7.7 Hz, $J_{1H,\ 13C}$ 161.4 Hz, H-1'), 4.11 (m, 1H, H-4), 4.01 (dd, 1H, $J_{2,3}$10.9 Hz, H-2), 3.87 (dd, 1H, $J_{3,4}$ 3.3 Hz, H-3), 3.82 (dd, 1H, $J_{5,6a}$ 7.9 Hz, $J_{6a,6b}$ 11.7 Hz, H-6a), 3.76 (dd, 1H, $J_{5,6b}$ 4.3 Hz, H-6b), 3.70 (m, 1H, H-5), 3.52 (s, 3H, $OC\underline{H}_3$), 3.50 (m, 1H, H-2'), 3.42 (dd, 1H, $J_{4',5'}$ 9.3 Hz, $J_{5',6'}$ 6.0 Hz, H-5'), 3.42 (m, 1H, H-4'), 2.32 (dt, 1H, $J_{2',3'e} \sim J_{3'e,4'}$ 4.8 Hz, $J_{3'a,3'e}$ 12.1 Hz, H-3'e), 2.01 (s, 3H, OAc), 1.46 (q, 1H, $J_{2',3'a} \sim J_{3'a,4'}$ 11.7 Hz, H-3'a), 1.26 (d, 1H, H-6').

^{13}C NMR (600 MHz, $CDCl_3$) δ107.3 (C-1'), 102.9 (C-1), 80.3 (C-3), 76.7 (C-5'), 75.6 (C-5), 70.8 (C-4'), 69.1 (C-4), 68.5 (C-2'), 61.9 (C-6), 57.8 (OCH3), 52.1 (C-2), 38.6 (C-3'), 22.9 ($OC(O)\underline{C}H_3$), 19.3 (C-6').

ESMS (high res) m/z = 388.158990 $[M+Na]^+$ (Calcd 388.158352 for $C_{15}H_{27}NO_9Na$).

Chapter V Conclusion

Four goals have been accomplished in this thesis. 1) A protocol was developed for the purification of rat monoclonal antibodies 9D, 9E and 18H IgG molecules[34,40]. 2) The conditions of proteolysis for IgG leading to Fab fragments of the three antibodies were established. The 18H Fab material has yielded crystals in Dr. Cygler's laboratory (NRC, Montreal). 3) Partial amino acid sequences of the 18H heavy and light chains were obtained to aid in the interpretation of the elution diffraction data. 4) Two disaccharide analogues of Tyv-GalNAc were synthesized for use in chemical mapping studies.

This thesis work marks the beginning of an investigation into the *Trichinella spiralis* antigen-antibody interactions. Much work remains to be done in probing the system. For example, the peptide sequencing of the 18H heavy and light chains should be completed by further investigation of the tryptic digestion mixture. The sequencing information should also be verified by obtaining the mass spectrometry data of proteolytic fragments prepared from the two chains with other enzymes, in order to create overlapping sequences. One of the most burning questions, however is, how well will the disaccharide analogues Par-GalNAc and Abe-GalNAc bind to the *T. spiralis* antibodies.

An EIA inhibition study should be set up for the binding analysis (Fig 56). Purified monoclonal antibodies will be coated onto an EIA plate[107,108]. The disaccharide methyl glycosides should compete with a Tyv-GalNAc-BSA conjugate for binding to the monoclonal antibodies. The protein conjugate will be labeled with biotin at the BSA end, since biotin binds specifically to streptavidin with a high

affinity. Horse radish peroxidase, the enzyme of choice as an immunoassay marker, is covalently linked to the Streptavidin and in the presence of a TMB peroxidase substrate, absorbance readings on the plate are measured. The O.D. values should be monitored and the substrate stopped with phosphoric acid before positive wells are no longer recordable (absorbance of 1.5-2.0 O.D). As inhibition power increases, less conjugate binds to the antibody and the observed EIA signal decreases.

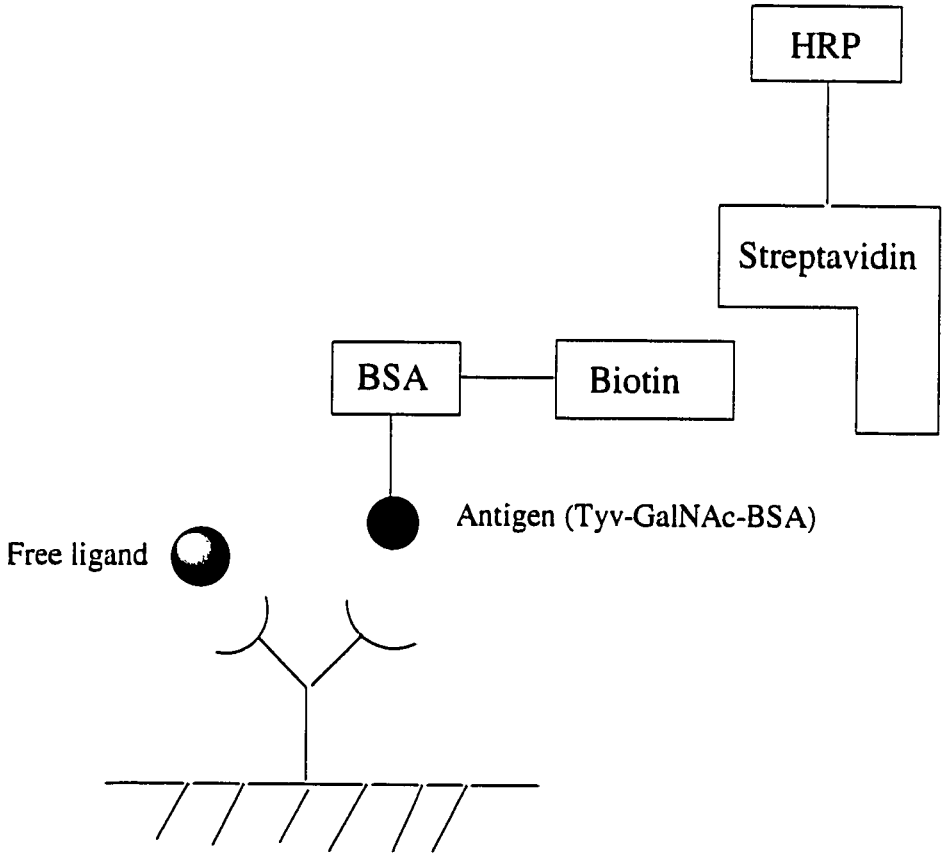

Fig 56. A possible EIA set up for testing the affinity of the disaccharide analogues.

A graph of absorbance versus inhibitor concentration or percentage inhibition versus inhibitor concentration can be plotted to show whether the disaccharides exhibit better binding than the native disaccharide Tyv-GalNAc. The synthetic

disaccharides could show other possible results such as, partial binding, or no binding at all to the antibodies of interest. It is highly unlikely that the analogues will form tighter complexes with the antibodies than the natural antigenic determinant. The other two possibilities offer detailed information on the importance to binding of the C-2 and C-4 hydroxyl groups of tyvelose. If partial binding is observed between Par-GalNAc and the antibody, we might conclude that the C-2 hydroxyl group on the tyvelose of the *T. spiralis* antigen is not completely buried in the binding site. By sitting close to or partially inside the binding pocket, the properly oriented C-4 OH group may still be engaged in the binding between the ligand and the protein. In this case, substitution of a C-2 axial hydroxyl group by an equatorial OH has resulted in a lower binding affinity for the substrate. If Par-GalNAc does not bind at all to the antibodies, then we would know that it is very probable that the C-2 axial hydroxyl plays an essential role in the binding and that it is very likely that the 2-OH is buried inside the binding pocket.

Depending on the activity profile, related conclusions could also be drawn for C-4 hydroxyl group of the Abe-GalNAc complex. Of course, the fact that an equatorial C-2 OH is also present on abequose should be taken into consideration as well. In this respect, the Abe-GalNAc disaccharide holds less similarity to the Tyv-GalNAc structure.

The EIA studies should give us a good indication of the binding involvement of the hydroxyl groups present in the 3,6-dideoxy sugar of the antigenic determinant. The results are based on the assumption that the three disaccharides, Tyv-GalNAc, Par-GalNAc and Abe-GalNAc have similar conformations. NOE studies should be

carried out to verify this hypothesis by measuring the distances between the hydrogen atoms attached to the C-1' and C-3 carbon atoms. The torsional angles Φ and Ψ (Fig 57) may also be estimated by measuring $^{3}J_{C,H}$ coupling constants. These heteronuclear coupling constants follow a Karplus type relationship[109-111].

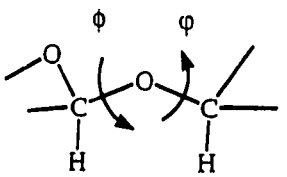

Fig 57. Torsional angles on the coupled disaccharides.

Combined with titration microcalorimetry analysis and X-ray crystallographic studies, inhibition data can eventually lead to an in-depth understanding of the *T. spiralis* antigen-antibody system.

Bibliography

1. S. Hakomori, *Cancer Res*, 45 (1985), 2405-2414.

2. J. Kellermann, F. Lottspeich, A. Henschen and W. Muller-Esterl, *Eur. J. Biochem.*, 154 (1986), 471-478.

3. J. Montreuil, *Adv. Carbohydr. Chem. Biochem.*, 37 (1980), 157-223.

4. N. Sharon, *Trends Biochem. Sci.*, 9 (1984), 198.

5. S. Hakomori and A. Kombata, *The antigens*, ed, M. Sela, 1974, vol II, 79.

6. G. D. MacLean and B. M. Longeneckeer, *Can. J. Oncol.*, 4 (1994), 249-254.

7. D. M. Pardoll, *Trends Pharmacol. Sci.*, 14 (1993), 202-208.

8. T. Toyokuni and A. K. Singhal, *Chem. Soc. Rev.*, 23 (1995), 231-242.

9. Y. Ogawa, P-S. Lei, and P. Kovac, *Bioorg. Med. Chem. Lett.*, 5 (1995), 2283-2286.

10. A. Arancibia-Mohar, O. Madrazo-Alonso, A. Ariosa-Alvarez, J. Sarracent Perez, M. Alfonso, J. L. Perez, M. Ramirez, R. Montes and V. Verez-Bencomo, *Carbohydr. Lett.*, 1 (1995), 173-178.

11. A. G. C. Renwick, *Glycoproteins, Secretors*, in *Molecular biology and biotechnology*, Ed R. A. Meyers, VCH Publishers Inc, New York, NY, USA, 1995.

12. A. Kobata, *Glycobiology*, in Molecular *biology and biotechnology*, Ed R. A. Meyers, VCH Publishers Inc, New York, NY, USA, 1995.

13. B. C. O'Connell, F. K. Hagen, and L. A. Tabak, *J. Biol. Chem.*, 267 (1992), 25010-25018.

14. I. B. H. Wilson, Y. Gavel, and G. Von Heijne, *Biochem. J.*, 275 (1991), 529-534.

15. R. C. Hughes, A. F. Bradbury, and D. G. Smyth, *Carbohydr. Res.*, 178 (1988), 259-269.

16. J. P. Briand, S. P. Andrews, Jr., E. Cahill, N. A. Conway, and J. D. Young, *J. Biol. Chem.*, 256 (1981), 12205-12207.

17. B. W. Sigurskjold and D. R. Bundle, *J. Biol. Chem.*, 267 (1992), 8371-8376.

18. D. R. Bundle, E. Eichler, M. A. J. Gidney, M. Meldal, A. Ragauskas, B. W. Sigurskjold, B. Sinnott, D. C. Watson, M. Yaguchi and N. M. Young, *Biochemistry*, 33 (1994), 5172-5182

19. D. R. Bundle, H. Baumann, J. R. Brisson, S. M. Gagne, A. Zdanov and M. Cygler, *Biochemistry*, 33 (1994), 5183-5192.

20. D. R. Bundle and E. Eichler, *Bioorg. Med. Chem.*, 2 (1994), 1221-1229.

21. D. Solis and T. Diaz-Maurino, *Analysis of protein-carbohydrate interaction using engineered ligands*, *Glycosciences*, ed H-J and S. Gabius, Chapman and Hall, 1997.

22. L. Pauling, *The nature of the chemical bond*, 3rd ed. Ithaca NY: Cornell University press, 1980.

23. I. P. Street, C. R. Armstrong and S. G. Withers, *Biochemistry*, 25 (1986), 6021-6027.

24. P. V. Nikrad, H. Beierbeck, and R. U. Lemieux, *Can. J. Chem*, 70 (1992), 241-253.

25. T. Peters and B. M. Pinto, *Curr*, 6 (1996), 710-720.

26. D. R. Bundle and B. W. Sigurskjold, *Meth. Enzymol.*, 242 (1994), 288-305

27. E. J. Toone, *Curr. Opin. Struct. Biol.*, 4 (1994), 719-728.

28. W. C. Campbell, *Trichinella and Trichinosis*, New york/London, 1983, 425-444

29.. S. E. Gould, *Trichinosis*, Charles C. Thomas, Springfield, Illinois, USA, 1945.

30. S. E. Gould, *Trichinosis in man and animals*, Charles C. Thomas, Springfield, Illinois, USA, 1970.

31. N. B. Millet, G. D. Hart, T. A. Reyman, M. R. Zimmermann and P. K. Lewin, *Mummies, Disease and Ancient Cultures*, 1980, 71-84.

32. *5th international conference on trichinellosis*, ed C. W. Kim, E. J. Ruitenberg, J. S. Teppema, Reedbooks Ltd, Chertsey, Surrey, England, 1981.

33. R. Ducas, *Thesis*, Faculty of Medicine of Paris, Jouve, Paris, 1921, 47.

34. J. A. Appleton and D. D. McGregor, *Science*, 226 (1984), 70-72.

35. M. S. Carlisle, D. D. McGregor and J. A. Appleton, *Immunology*, 70 (1990), 126-132.

36. E. Y. Denkers, D. L. Wassom, and C. E. Hayes, *Mol. Biochem. Parasitol.*, 41 (1990), 241-250.

37. D. S. Silberstein, D. D. Despommier, *J. Immunol.*, 132 (1984), 898-904.

38. A. M. Gold, D. D. Despommier and S. W. Buck, *Mol. Biochem. Parasitol.*, 41 (1990), 187-196.

39. J. A. Appleton, L. R. Schain and D. D. McGregor, *Immunology*, 65 (1988), 487-492.

40. L. A. Ellis, A. J. Reason, H. R. Morris, A. Dell, R. Iglesias, F. M. Ubeira and J. A. appleton, *Glycobiology*, 4 (1994), 585-592.

41. E. Y. Denkers, C. E. Hayes and D. L. Wassom, *Exp. Parasitol.*, 72 (1991), 403-410.

42. N. Wisnewski, M. McNeil, R. B. Grieve, and D. L. Wassom, *Mol. Biochem. Parasitol.*, 61 (1993), 25-36.

43.. A. J. Reason, L. A. Ellis, J. A. Appleton, N. Wisnewski, R. B. Grieve, M. McNeil, D. L. Wassom, H. R. Morris and A. Dell, *Glycobiology*, 4 (1994), 593-603.

44. M. A. Probert, J. Zhang, and D. R. Bundle, *Carbohydr. Res.*, 296 (1996), 149-170

45. J. Zhang, A. Otter, and D. R. Bundle, *Bioorg. & Medical Chem.*, 4 (1996), 1989-2001.

46. C. J. Edge, T. W. Wormald, M. R. Parekh, R. B. Butters, D. R. Wing and R. A. Dwek. *Proc. Natl. Acad. Sci. USA*, 89 (1992), 6338-6342.

47. T. Patel, J. Bruce, A. Merry, C. Bigge, M. Wormald, A. R. Jaques and R. Parekh, *Biochemistry*, 32 (1993) 679-693.

48. D. R. Bundle and R. U. Lemieux, *Meth. Carbohydr. Chem.*, 7 (1976), 79-86.

49. H. Van Halbeek, *Methods in Enzymology*, 230 (1994), 132-168.

50. L. A. Ellis, C. S. McVay, M. A. Probert, J. Zhang, D. R. Bundle, and J. A.

Appleton, *Glycobiology*, 7 (1997), 383-390.

51. E. A. Peterson, *Cellulosic Ion Exchangers*, North-Holland, Amsterdam, 1970.

52. S. H. Herrmann and M. F. Mescher, *J. biol. Chem.*, 254 (1979), 8713-8716.

53. E. Harlow and D. Lane, *Antibodies. A laboratory manual*, Cold spring harbor, NY, 1988.

54. J. Rousseaux, R. Rousseaux-Prevost and H. Bazin, *J. Immunol. Methods*, 64 (1983), 141-146.

55. R. Aebersold, *Thesis*, Faculty of Science, University of Basel, Basel, 1983.

56. U. K. Laemmli, *Nature*, 227 (1970), 680-685.

57. N. M. Young, D. C. Watson, and P. Thibault, *Glycoconjugate J.*, 13 (1996), 575-582.

58. N. M. Young, D. C. Watson, M. Yaguchi, R. Adar, R. Arango, E. Rodriguez-Arango, N. Sharon, P. Blay, and P. Thibault, *J. Biol. Chem.*, 270 (1995), 2563-2570.

59. K. Biemann and H. A. Scoble, *Science*, 237 (1987), 992-998.

60. K. Biemann, *Methods in Enzymology*, 193 (1990), 351-360.

61. C. G. Edmonds and R. D. Smith, *Methods in Enzymology*, 193 (1990), 412-431.

62. M. Mann, C. K. Meng and J. B. Fenn, *Anal. Chem.*, 61 (1989), 1702-1708.

63. B. B. Reinhold and V. N. Reinhold, *J. Am. Soc. Mass Spectrom.*, 3 (1992), 207-215.

64. M. Mann and M. Wilm, *TIBS*, 20 (1995), 219-224.

65. O. Leger, E. Jackson and C. Dean, *Mol. Immunol.*, 32 (1995), 697-709.

66 M. Bruggemann, *Gene*, 74 (1988), 473-482.

67. J. S. Crowe, M. A. Smith and H. J. Cooper, *Nucl. Acids, Res.*, 17 (1989), 7992.

68. H. W. Sheppard and G. A. Gutman, *Proc. Nat. Acad. Sci. USA*, 78 (1981), 7064-7068.

69. X. J. Tang, P. Thibault, R. K. Boyd, *Anal. Chem.* 65 (1993), 2824-2834.

70. K. P. Bateman, P. Thibault, D. J. Douglas, R. L. White, *J. Chromatogr.A*, 712 (1995), 253-268

71. N. Sharon, *Complex Carbohydrates: Their Chemistry, Biosynthesis and Functions*, Addison Wesley, Reading MA, USA, 1975.

72. H. Paulson, *Angew. Chem. Int. Ed. Engl.*, 21 (1982), 155-173.

73. T. Mukaiyama, Y. Murai and S. Shoda, *Chem. Lett.*, 1981, 431-432.

74. R. R. Schmidt and J. Michel, *Angew. Chem. Int. Ed. Engl.*, 19 (1980), 731-735.

75. R. R. Schmidt, *Pure & Appl. Chem.*, 61 (1989), 1257-1270.

76. B. Wegmann and R. R. Schmidt, *J. Carbohydr. Chem.*, 6 (1987), 357-375.

77. R. Preuss and R. R. Schmidt *Synthesis*, 1988, 694-696.

78. K. Koike, M. Mori, Y. Ito, Y. Nakahara and T. Ogawa, *Glycoconjugate J.*, 4 (1987), 109-116.

79. R. J. Ferrier, R. W. Hay, and N. Vethaviyasar, *Carbohydr. Res.*, 27 (1973), 55-61.

80. Y. Ito and T. Ogawa, *Tet. Lett.*, 28 (1987), 4701-4704.

81. R. U. Lemieux, J. L. Hayimi, *Can. J. Chem.*, 43 (1965), 2162-2173.

82. R. U. Lemieux, K. B. Hendriks, R. V. Stick and K. James, *J. Am. Chem. Soc.*, 97 (1975), 4056-4062.

83. H. Paulsen and O. Lockhoff, *Chem. Ber.*, 114 (1981), 3102-3144.

84. P. J. Garreg, P. Ossowski, *Acta Chem. Scand.* , B 37 (1983), 249-250.

85. F. Barresi and O. Hindsgaul, *J. Am. Chem. Soc.*, 113 (1991), 9376-9377.

86. F. Barresi and O. Hindsgaul, *Synlett.*, 1992, 759-761.

87 . F. Barresi and O. Hindsgaul, *Can. J. Chem.*, 72 (1994), 1447-1465.

88. G. Stork, and G. Kim, *J. Am. Chem. Soc.*, 114 (1992), 1087-1088.

89. M. Nitz, unpublished data.

90. H. Paulsen and M. Paal, *Carbohydr. Res.* 135 (1984), 53-69.

91. R. U. Lemieux and R. M. Ratcliffe, *Can. J. Chem,*. 57 (1979) 1244-1451.

92. S. Sabesan and R. U. Lemieux, *Can. J. Chem*, 62 (1984), 644-654.

93. G. Siewert and O. Westphal, *Justus Liebigs Ann. Chem.* 1968 (720) 161-170.

94. G. Siewert and O. Westphal, *Justus Liebigs Ann. Chem.* 1968 (720) 171-176.

95. H. H. Baer and D. J. Astles, *Carbohydr. Res.* 126 (1984), 343-347.

96. R. Bognar, I. Farkas-Szabo, I. Farkas and H. Gross, *Carbohydr. Res.*, 5 (1967), 241-243.

97. D. R. Bundle and S. Josephson, *Can. J. Chem.*, 57 (1979), 662-668.

98. W. Dullenkopf, J. C. Castro-Palomino, L. Manzoni, R. R. Schmidt, *Carbohydr. Res.*, 296 (1996), 135-147.

99. P. Zhang, unpublished data.

100. D. R. Bundle, *J.C.S. Perkin I,* 1979, 2751-2755

101. B. Classon, P. J. Garegg and B. Samuelsson, *Can. J. Chem.*, 159 (1981), 339-343.

102. Becker and Galili *Carbohydrate Res*, 248 (1993), 129-141.

103. K. Bock and C. Pedersen, *J. Chem. Soc., Perkin Trans.*, 2 (1974), 293-297.

104. D. D. Perrin and W. L. F. Armarego, *Purification of Laboratory Chemicals (third Ed.)*, Oxford; Pergamon Press, New York, NY, USA, 1988.

105. A. Otter and D. R. Bundle, *J. Magn. Res., Ser. B*, 109 (1995), 194-201.

106. A. Bax and S. Subramanian, *J. Magn. Reson.*, 67 (1986), 565-569.

107. P. J. Meikle, N. M. Young and D. R. Bundle, *J. Immunol. Methods*, 132 (1990), 255-261.

108. E. Vorberg and D. R. Bundle, *J. Immunol. Methods*, 132 (1990), 81-89.

109. V. V. Krishnamurthy, *J. Magn. Reson. Ser. A*, 121 (1996), 33-41.

110. I. Tvaroska, M. Hricovini and E. Petrakova, *Carbohydr. Res.*, 189 (1989), 359-362.

111. I. Tvaroska, *Carbohydr. Res.*, 206 (1990), 55-64.

IMAGE EVALUATION TEST TARGET (QA-3)

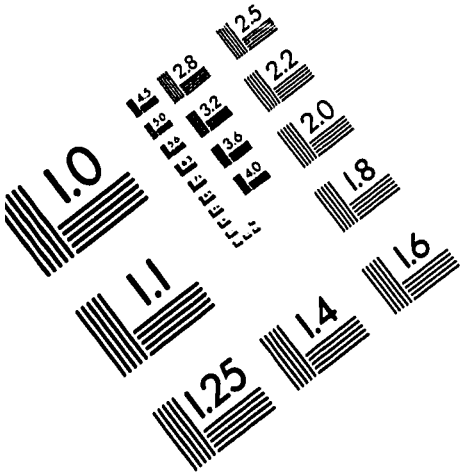

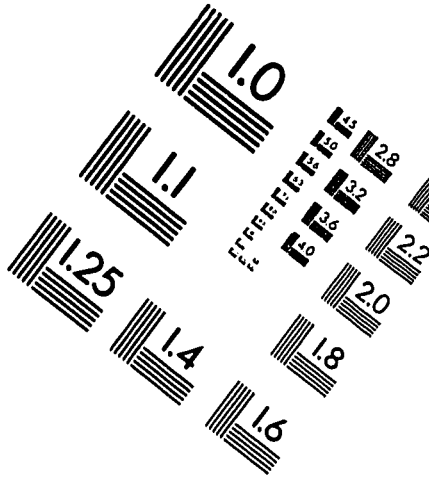

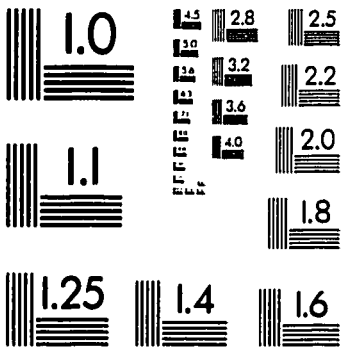

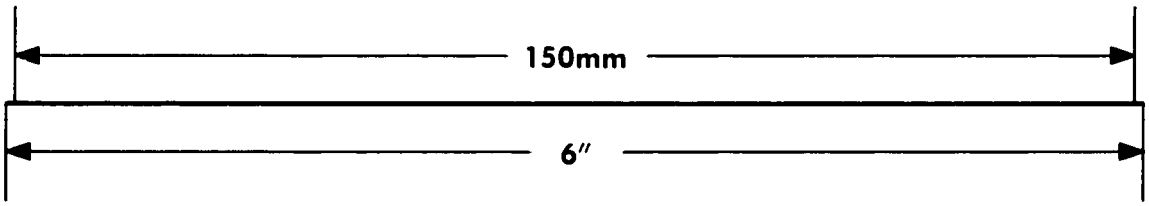

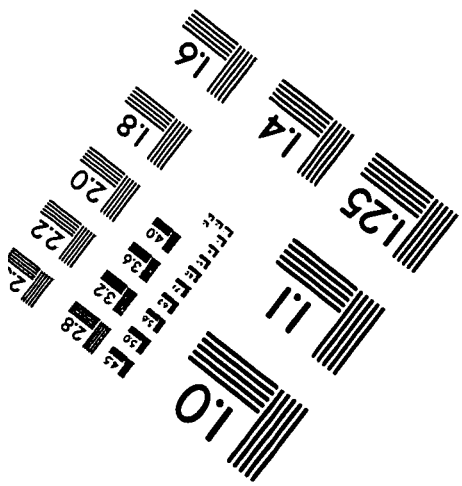

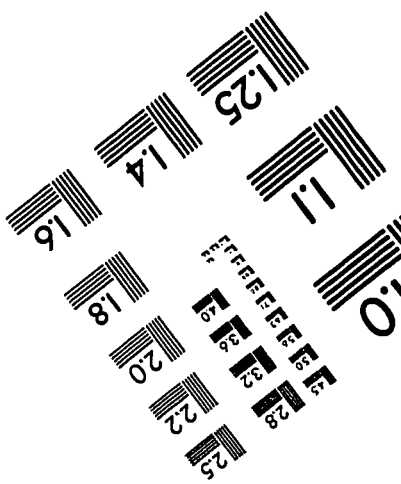

APPLIED IMAGE, Inc
1653 East Main Street
Rochester, NY 14609 USA
Phone: 716/482-0300
Fax: 716/288-5989